

Microbial Biotransformation of Kimberlite Ores

by

Karishma Ramcharan BSc (Hons)

Submitted in partial fulfilment of the requirements for the degree of
Masters of Science in the Department of Microbiology, University of
KwaZulu-Natal, Pietermaritzburg

December 2008

Declaration by supervisor

As the candidate's supervisor, I, _____,
agree/do not agree to the submission of this dissertation.

Signed

Declaration 1 - Plagiarism

I, _____, declare that

1. The research reported in this dissertation, except where otherwise indicated, is my original work.
2. This dissertation has not been submitted for any degree or examination at any other university.
3. This thesis does not contain other persons' data, pictures, graphs or other information, unless specifically acknowledged as being sourced from other persons.
4. This thesis does not contain other persons' writing, unless specifically acknowledged as being sourced from other researchers. Where other written sources have been quoted , then:
 - a. Their words have been re-written but the general information attributed to them has been referenced.
 - b. Where the exact words have been used, then their writing has been placed in italics and inside quotation marks, and referenced.
5. This thesis does not contain text, graphics or tables copied and pasted from the Internet, unless specifically acknowledged, and the source being detailed in the thesis and in the References section.

Signed

Acknowledgements

This dissertation is the result of a research project that emanated and was funded by *Mintek* whose financial support is greatly appreciated. Many individuals have been instrumental in ensuring the successful delivery of this project and I would like to thank the following people:

My supervisor, Mr Charles Hunter. When nothing held together or made the slightest bit of sense, you have always helped restore my inner confidence. Thank you for your advice, support and encouragement.

Mrs Mariekie Gericke from *Mintek* for all her cooperation and assistance in the project.

Professor J. Hughes for his help and expertise in X-Ray Diffraction analyses.

Dr C. Southway for his assistance and expertise in Inductive Coupled Plasma and High Performance Liquid Chromatography analyses.

Members and the laboratorial technicians of the Microbiology Department for their assistance and advice in experimental work.

Finally to my family and friends for their incredible support, understanding, guidance and tolerance throughout the course of this work.

Abstract

Microbial leaching plays a significant role in the natural weathering of silicate-containing ores such as diamond-bearing kimberlite. Harnessing microbial leaching processes to pre-treat mined kimberlite ores has been proposed as a means of improving diamond recovery efficiencies. The biomineralization of kimberlite is rarely studied. Therefore, this study investigated the feasibility of exploiting both chemolithotrophic and heterotrophic leaching processes to accelerate the weathering of kimberlite.

Preliminary investigations using mixed chemolithotrophic leaching cultures were performed on four finely ground kimberlite samples (<100µm) sourced from different mines in South Africa and Canada. Mixed chemolithotrophic cultures were grown in shake flasks containing kimberlite and inorganic basal media supplemented either with iron (Fe^{2+} , 15g/l) or elemental sulfur (10g/l) as energy sources. Weathering due to dissolution was monitored by Inductive Coupled Plasma (ICP) analyses of Si, Fe, K, Mg and Ca in the leach solutions at known pH. Structural alterations of kimberlite after specified treatment times were analyzed by X-ray Powder Diffraction (XRD). The results of the preliminary investigation showed that weathering can be accelerated in the presence of microbial leaching agents but the degree of susceptibility and mineralogical transformation varied between different kimberlite types with different mineralogical characteristics. In general, the results showed that the kimberlite sample from Victor Mine was most prone to weathering while the sample from Gahcho Kue was the most resistant. It was therefore deduced that kimberlite with swelling clays as their major mineral component weathered relatively more easily when compared to kimberlite that consisted of serpentine and phlogopite as their major minerals. Gypsum precipitates were also distinguished indicating that a partial alteration in the kimberlite mineralogical structure occurred. Both energy sources positively influenced the dissolution process, with sulfur producing superior results. This was attributed to the generation of sulfuric acid which promotes cation dissolution and mineral weathering.

Success in the preliminary investigations led to further experimental testing performed to determine the effect of particle size and varying energy source

concentrations on the biotransformation of kimberlite. It was observed that although weathering rates of the larger kimberlite particles (>2mm<5mm) were lower than that of the finer particles, slight changes in their mineralogical structures represented by the XRD analyses were seen. Optimisation studies of energy source concentration concluded that although the highest concentration of elemental sulfur (20% w/w) and ferrous iron (35% w/w) produced the most pronounced changes for each energy source tested, the leaching efficiency at these concentrations were not drastically greater than the leaching efficiency of the lower concentrations, as expected.

Following the success of batch culture shake flasks weathering tests, the effect of continuous chemolithotrophic cultures on the biotransformation of larger kimberlite particles (>5mm<6.7mm) was investigated. A continuous plug-flow bioleach column was used to model the behaviour of chemolithotrophic consortia in a dump- or heap leaching system. Two sequential columns were setup, in which the first consisted of kimberlite mixed with sulfur and the second purely kimberlite. Inorganic growth medium was pumped to the first column at a fixed dilution rate of 0.25h^{-1} and the leachate from the first column dripped into the second. After an 8 week investigation period, the ICP and XRD data showed that weathering did occur. However, the pH results showed that the leaching process is governed by the amount of acid produced by the growth-rate independent chemolithotrophic consortia. Data from pH analyses also showed that the leaching bacteria reached 'steady state' conditions from day 45 onwards. The pH also remained higher in the second column than in the first column highlighting the alkaline nature of the kimberlite ores and its ability to act as a buffering agent and resist weathering. This important factor, as well as further optimisation studies in process operating conditions and efficiency, needs to be considered when establishing heap-leaching technology for these kimberlite ores.

In the preliminary heterotrophic investigation, *Aspergillus niger* was used to produce organic metabolites to enhance kimberlite mineralization. The results demonstrated that the organic acid metabolites generated caused partial solubilization of the kimberlite minerals. However, it was deduced that for more significant changes to be observed higher amounts of organic acids need to be produced and maintained. The results obtained in this study also showed that the type of kimberlite presents a

different susceptibility to the dissolution process and the presence of the fungal cells may improve the leaching efficiency.

The results in this study provided an optimistic base for the use of microbial leaching processes in accelerating the weathering of kimberlite. These findings may also serve to supply data to formulate recommendations for further and future column microbial leach tests as well as validation and simulation purposes.

<i>Contents</i>	<i>Page</i>
Declaration by supervisor	i
Declaration	i
Acknowledgements	ii
Abstract	iii
Contents	vi
List of Figures	xi
List of Tables	xiv
 CHAPTER 1: <i>Microbial biotransformation of kimberlite ores</i>	 1
1.1 Introduction	1
1.2 Microbial role in the natural weathering of rocks and minerals	2
1.2.1 Microorganisms involved in the weathering of rocks and minerals	3
1.2.1.1 Chemolithotrophic microorganisms	3
1.2.1.2 Chemolithotrophic mechanisms of bioleaching	4
1.2.1.3 Chemolithotrophic attachment on mineral/ore surfaces	7
1.2.1.4 Advantages and disadvantages of using chemolithotrophic leaching processes	8
1.2.2.1 Heterotrophic microorganisms	10
1.2.2.2 Heterotrophic mechanisms of bioleaching	10
1.2.2.3 Advantages and disadvantages of using heterotrophic leaching processes	11
1.3 Weathering of minerals	14
1.3.1 Weathering of silicate minerals and rocks	14
1.3.1.1 Weathering of kimberlite	17
1.4 Biohydrometallurgical applications	19
1.4.1 Industrial biohydrometallurgical processes	21
1.4.1.1 Dump leaching	21
1.4.1.2 Heap leaching	22
1.4.1.3 <i>In situ</i> leaching	22
1.4.1.4 Stirred-tank reactor leaching	23
1.4.2 Advantages of biohydrometallurgical processes	24
1.4.3 Possible application of biohydrometallurgical processes to kimberlite	25
1.5 Dissertation overview	26
1.5.1 Aims and objectives	26

	<i>Page</i>
CHAPTER 2: <i>Materials and Methods</i>	27
2.1 Kimberlite	27
2.2 Microorganisms	28
2.2.1 Chemolithotrophic microorganisms	28
2.2.2 Heterotrophic microorganisms	28
2.3 Maintenance and storage of microorganisms	28
2.3.1 Maintenance and storage of chemolithotrophic microorganisms	28
2.3.2 Maintenance and storage of heterotrophic microorganisms	29
2.4 Media	29
2.4.1 Inorganic basal medium	29
2.4.2 Heterotrophic medium	29
2.5 Analyses	30
2.5.1 Inductive coupled plasma-optical emission spectroscopy (ICP-OES)	30
2.5.1.1 Sample preparation	30
2.5.1.2 ICP conditions	30
2.5.1.3 Chemicals and elemental species standard solutions	31
2.5.2 X-Ray diffraction powder analysis (XRD)	32
2.5.2.1 Sample preparation	32
2.5.2.2 XRD conditions	32
CHAPTER 3: <i>Susceptibility of kimberlite ores to microbial weathering using known and enriched natural microbial populations from weathered kimberlite</i>	34
3.1 Introduction	34
3.2 Experimental Procedure	35
3.2.1 Preliminary evaluation of the biotransformation of kimberlite using known chemolithotrophic bioleach cultures	35
3.2.1.1 Kimberlite	35
3.2.1.2 Microorganisms	35
3.2.1.3 Shake flask weathering tests	35
3.2.2 Selective enrichment of microbial communities from naturally weathered kimberlite and investigating their role and efficiency in the mineralization of kimberlite	37
3.2.2.1 Kimberlite	37

	<i>Page</i>
3.2.2.2 Enrichment of leaching microbial populations from naturally weathered kimberlite	37
3.2.2.3 Batch culture shake flask weathering tests using enriched microbial cultures from naturally weathered kimberlite	38
3.2.3 Statistical analyses	39
3.3 Results	39
3.3.1 Preliminary evaluation of the biotransformation of kimberlite using known chemolithotrophic bioleach cultures	39
3.3.1.1 ICP results	40
3.3.1.2 XRD results	44
3.3.2 Selective enrichment of microbial communities from naturally weathered kimberlite and investigating their role and efficiency in the mineralization of kimberlite	49
3.3.2.1 ICP results	49
3.3.2.2 XRD results	51
3.4 Discussion	54
CHAPTER 4: <i>Optimization studies to determine the influence of particle size and energy source concentration on the biotransformation of kimberlite ores</i>	59
4.1 Introduction	59
4.2 Experimental Procedure	60
4.2.1 Evaluation of the effect of kimberlite particle size on biotransformation by a known chemolithotrophic bioleach consortia	60
4.2.1.1 Kimberlite	60
4.2.1.2 Microorganisms	60
4.2.1.3 Shake flask weathering tests	60
4.2.2 Influence of energy source concentration on the biotransformation of kimberlite ores by chemolithotrophic bioleach cultures	60
4.2.2.1 Kimberlite	60
4.2.2.2 Microorganisms	60
4.2.2.3 Energy Sources	61
4.2.2.4 Shake Flask weathering tests	61
4.2.3 Effect of longer treatment time on the biotransformation of kimberlite ores using chemolithotrophic bioleach cultures	61
4.2.3.1 Kimberlite	61
4.2.3.2 Microorganisms	61

	<i>Page</i>
4.2.3.4 Shake Flask weathering tests	61
4.2.3 Statistical analyses	62
4.3 Results	62
4.3.1 Evaluation of the effect of kimberlite particle size on biotransformation by a known chemolithotrophic bioleach consortia	62
4.3.1.1 ICP results	62
4.3.1.2 XRD results	64
4.3.2 Influence of energy source concentration on the biotransformation of kimberlite ores by chemolithotrophic bioleach cultures	67
4.3.2.1 ICP results	68
4.3.2.2 XRD results	70
4.3.3 Effect of increasing treatment time of kimberlite ores during microbial leaching processes	73
4.3.3.1 ICP results	74
4.3.3.2 XRD results	76
4.4 Discussion	77
CHAPTER 5: <i>Evaluation of a continuous flow bioleach column system to determine the influence of chemolithotrophic cultures on the biotransformation of kimberlite ores</i>	80
5.1 Introduction	80
5.2 Experimental Procedure	81
5.2.1 Kimberlite	81
5.2.2 Microorganisms	81
5.2.3 Column weathering test	81
5.3 Results	83
5.3.1 ICP results	83
5.3.2 XRD results	83
5.4 Discussion	87
CHAPTER 6: <i>Susceptibility of kimberlite ores to heterotrophic microbial leaching using Aspergillus niger</i>	90
6.1 Introduction	90
6.2 Experimental Procedure	90
6.2.1 Kimberlite	90
6.2.2 Microorganisms	91

	<i>Page</i>
6.2.3 Shake flask weathering tests	91
6.2.4 Statistical analyses	92
6.3 Results	92
6.3.1 ICP results	93
6.3.2 XRD results	95
6.4 Discussion	97
 CHAPTER 7: <i>Concluding remarks</i>	 100
 References	 103

	<i>List of Figures</i>	<i>Page</i>
Figure 1.1	Picture of a typical kimberlite ore found at Kimberley diamond mines in South Africa. (Re-printed) from www.guilford.edu/geology/imagelibrary/MVC-061F.JPG)	17
Figure 1.2	Flow diagram of kimberlite processing and diamond liberation. (Re-drawn from Morkel, 2007)	19
Figure 1.3	Heap-leaching processing plant of copper operational at Cerro Colorado, Chile. (Re-drawn from Rawlings, 2004)	22
Figure 1.4	Photograph of stirred-tank reactors used in the biooxidation of gold found at Tamboraque gold mine, 90 km east of Lima, Peru. (Re-drawn from Rawlings, 2004)	24
Figure 3.1	Changes in pH over time (days) observed during the chemolithotrophic microbial transformation of kimberlite ores from Victor mine.	39
Figure 3.2	Magnesium ion dissolution trends of four kimberlite ores from different diamond mines subjected to various leaching treatments. (A, B, C, D represents the ICP results for the kimberlite sample from Victor, Premier, Venetia and Gahcho Kue diamond mine, respectively.)	42
Figure 3.3	Magnesium ion dissolution trends illustrating the weathering susceptibility of the treated kimberlite samples from different diamond mines. (Data was obtained from ICP analyses of the leachate solutions of the 'sulfur treatment'.)	43
Figure 3.4	XRD analyses of kimberlite from Victor mine that was subjected to various leaching treatments. [A (negative control), B (positive chemical control), C (chemolithotrophic bacteria in the presence of 1% (w/v) S⁰), D (chemolithotrophic bacteria in the presence of 10% (w/v) Fe²⁺)].	45
Figure 3.5	XRD analyses of kimberlite from Premier mine that was subjected to various leaching treatments. [A (negative control), B (positive chemical control), C (chemolithotrophic bacteria in the presence of 1% (w/v) S⁰), D (chemolithotrophic bacteria in the presence of 10% (w/v) Fe²⁺)].	46
Figure 3.6	XRD analyses of kimberlite from Venetia mine that was subjected to various leaching treatments. [A (negative control), B (positive chemical control), C (chemolithotrophic bacteria in the presence of 1% (w/v) S⁰), D (chemolithotrophic bacteria in the presence of 10% (w/v) Fe²⁺)].	47
Figure 3.7	XRD analyses of kimberlite from Gahcho Kue mine that was subjected to various leaching treatments. [A (negative control), B (positive chemical control), C (chemolithotrophic bacteria in the presence of 1% (w/v) S⁰), D (chemolithotrophic bacteria in the presence of 10% (w/v) Fe²⁺)].	48

Figure 3.8	Magnesium ion dissolution trends illustrating the efficiency of enriched microbial populations from naturally weathered kimberlite in the weathering of two kimberlite ores. (A, B represents the ICP results for the kimberlite sample from Premier and Venetia diamond mine, respectively.)	51
Figure 3.9	XRD analyses of kimberlite from Premier mine that was subjected to leaching treatments with enriched microbial cultures from naturally weathered kimberlite. [A (negative control), B (positive control-known mesophilic chemolithotrophic culture + S ⁰), C (enriched chemolithotrophic culture + 1% (w/v) S ⁰), D (positive control-known mesophilic chemolithotrophic culture + Fe ²⁺), E (enriched chemolithotrophic culture + 10% (w/v) Fe ²⁺)].	52
Figure 3.10	XRD analyses of kimberlite from Venetia mine that was subjected to leaching treatments with enriched microbial cultures from naturally weathered kimberlite. [A (negative control), B (positive control-known mesophilic chemolithotrophic culture + S ⁰), C (enriched chemolithotrophic culture + 1% (w/v) S ⁰), D (positive control-known mesophilic chemolithotrophic culture + Fe ²⁺), E (enriched chemolithotrophic culture + 10% (w/v) Fe ²⁺)].	53
Figure 4.1	Influence of kimberlite ore particle size on magnesium ion dissolution trends. (The larger particles were in size range of >2mm<5mm whilst the finer particles were < 100mm. Data was obtained from ICP analyses of the leachate solutions of the 'sulfur treatment' (Table 4.1) and converted to mg/g).	64
Figure 4.2	XRD analyses of kimberlite of particle size >2mm<5mm from Victor mine that was subjected to various leaching treatments. [A (negative control), B (positive chemical control), C (chemolithotrophic bacteria in the presence of 1% (w/v) S ⁰), D (chemolithotrophic bacteria in the presence of 10% (w/v) Fe ²⁺)].	65
Figure 4.3	XRD analyses of kimberlite of particle size >2mm<5mm from Gahcho Kue mine that was subjected to various leaching treatments. [A (negative control), B (positive chemical control), C (chemolithotrophic bacteria in the presence of 1% (w/v) S ⁰), D (chemolithotrophic bacteria in the presence of 10% (w/v) Fe ²⁺)].	66
Figure 4.4	Changes in pH over time (days) observed during the biotransformation of kimberlite ores from Venetia Mine. Energy source concentrations were varied to determine its influence on kimberlite mineralization. [A (sulfur was used as the energy source), B (ferrous iron was used as the energy source)].	67
Figure 4.5	Magnesium ion dissolution trends illustrating the effect of the different concentrations of energy sources used in the microbial leaching treatments of kimberlite ores from Venetia Mine. [A (sulfur was used as the energy source), B (ferrous iron was used as the energy source). Data was obtained from ICP analyses (Table 4.2)].	70
Figure 4.6	XRD analyses of kimberlite from Venetia mine after treatment with a mixed chemolithotrophic culture in the presence of different concentrations of elemental sulfur. [A (negative control), B (20% (w/w) S ⁰), C (10% (w/w) S ⁰), D (5% (w/w) S ⁰), E (2.5% (w/w) S ⁰)].	71

Figure 4.7	XRD analyses of kimberlite from Venetia mine after treatment with a mixed chemolithotrophic culture in the presence of different concentrations of ferrous iron. [A (negative control), B (35% (w/w) Fe^{2+}), C (18% (w/w) Fe^{2+}), D (9% (w/w) Fe^{2+}), E (4.5% (w/w) Fe^{2+})].	72
Figure 4.8	Changes in pH over time (days) observed during the biotransformation of kimberlite ores from Venetia Mine.	73
Figure 4.9	Magnesium ion dissolution trends illustrating the effect of increasing the microbial leaching time of kimberlite ores from Venetia Mine. [Data was obtained from ICP analyses (Table 4.3)].	74
Figure 4.10	XRD analyses of kimberlite from Venetia mine after extending microbial leaching treatment time of the kimberlite ores from 6 to 8 weeks. [A (negative control), B (positive chemical control), C (chemolithotrophic bacteria in the presence of 1% (w/v) S^0), D (chemolithotrophic bacteria in the presence of 10% (w/v) Fe^{2+})].	76
Figure 5.1	Experimental continuous flow bioleach column setup using a chemolithotrophic mesophilic culture. [A = reservoir of inorganic growth medium, B = peristaltic pump set at a flow rate of 1ml/min, C= column 1 containing kimberlite mixed with S^0 (w/w) as the energy source, D = Column 2 containing kimberlite with no energy source].	82
Figure 5.2	Changes in pH observed in two sequential continuous flow leaching columns. (Column 1 contained kimberlite mixed with S^0 (w/w) as the energy source whilst Column 2 contained kimberlite with no energy source.)	83
Figure 5.3	Magnesium ion dissolution trends illustrating the effectiveness of continuous leaching on kimberlite. [Column 1 was inoculated with a mixed mesophilic chemolithotrophic culture with elemental sulfur (20% w/w) as the energy source. A fixed continuous flow of growth medium was pumped into Column 1. The leachate from Column 1 percolated through to Column 2 which contained no energy source. Data was obtained from ICP analyses of the leachate solutions of Column 1 and 2 represented in Table 5.1.].	84
Figure 5.4	XRD analyses of kimberlite from Venetia Diamond Mine after subjected to continuous column leaching. [A (control), B (Column 1 – kimberlite in the presence of a mixed mesophilic chemolithotrophic culture in a continuous flow bioleach system and elemental sulfur as the energy source), C (Column 2 – leaching of kimberlite with the leachate from column 1, no energy source present)].	86
Figure 6.1	Magnesium ion dissolution trends illustrating the effectiveness of the heterotrophic leaching treatments used in the weathering tests of kimberlite from Venetia Diamond Mine. (Data was obtained from ICP analyses of the leachate solutions.)	95
Figure 6.2	XRD analyses of kimberlite from Venetia Mine after being subjected to heterotrophic leaching treatments using <i>Aspergillus niger</i>.	96

	<i>List of Tables</i>	<i>Page</i>
Table 1.1	Diversity of leaching microorganisms known to mediate biohydrometallurgical processes involved in mineral and ore processing or known to be part of the natural microbial leaching consortia found in bioleaching habitats. (Re-drawn and adapted from Brandl, 2001; Rawlings and Johnson, 2007)	13
Table 1.2	Types of silicates present in nature. (Re-drawn and modified from Morkel, 2007)	16
Table 2.1	Initial X-Ray diffraction analyses of the kimberlite samples obtained from Gahcho Kue, Premier, Venetia and Victor diamond mines indicating minerals identified.*	27
Table 2.2	Experimental conditions for ICP-OES.	30
Table 2.3	Preparation and final concentrations of standards used to calibrate the ICP spectrometer.	32
Table 2.4	Experimental conditions for XRD.	33
Table 3.1	Summary of treatments used in the preliminary investigation of the biotransformation of kimberlite. (Mixed chemolithotrophic bioleach cultures (<i>A. caldus</i> , <i>Sulfobacillus spp.</i> and <i>L. ferrooxidans</i>) maintained either on iron sulfate or sulfur were used in the treatments.)	36
Table 3.2	Summary of treatments used in the evaluation of the biotransformation of kimberlite using known and enriched microbial leach cultures maintained either on iron sulfate or sulfur.	38
Table 3.3	ICP analyses of four different microbially leached kimberlite samples (particle size <100µm). (Mixed chemolithotrophic cultures were used in leaching experiments with sulfur or ferrous iron as the energy source. All treatment flasks were incubated at 30°C in a shake incubator set at 120rpm for 6 weeks.)	41
Table 3.4	ICP analyses of different kimberlite samples (particle size < 100µm) treated with enriched microbial cultures from naturally weathered kimberlite. (Sulfur or ferrous iron was used as the energy source for the cultures. Known mesophilic chemolithotrophic cultures were used as controls in leaching experiments. All treatment flasks were incubated at 30°C in a shake incubator set at 120rpm for 6 weeks.)	50
Table 4.1	ICP analyses of treated kimberlite samples of different particle size (<100µm and >2mm<5mm) to determine the effect of microbial leaching treatments on larger kimberlite particles. (Mixed chemolithotrophic cultures were used in leaching experiments with sulfur or ferrous iron as the energy source. All treatment flasks were incubated at 30°C in a shake incubator (120rpm) for 6 weeks.)	63

Table 4.2	ICP analyses of two different kimberlite samples (<100mm) used to determine the influence of energy source concentrations on the biotransformation of kimberlite ores. (Mixed chemolithotrophic cultures were used in leaching experiments with varying concentrations of sulfur or ferrous iron as the energy source. All treatment flasks were incubated at 30°C in a shake incubator (120rpm) for 6 weeks.)	69
Table 4.3	ICP analyses of two different treated kimberlite samples (<100mm) to determine the effect of increasing treatment time during microbial leaching of kimberlite. (Mixed chemolithotrophic cultures were used in leaching experiments with sulfur or ferrous iron as the energy source. All treatment flasks were incubated at 30°C in a shake incubator (120rpm) for 8 weeks.)	75
Table 5.1	ICP analyses of kimberlite (>5.0mm<6.7mm) from Venetia Diamond Mine after treated in a continuous flow bioleach column system.	84
Table 6.1	ICP Analyses of heterotrophically leached kimberlite ores (<100mm) using <i>Aspergillus niger</i>. (All treatment flasks were incubated at 30°C in a shake incubator set at 120rpm for 6 weeks.)	94

CHAPTER 1

Microbial biotransformation of kimberlite ores

1.1 Introduction

It is now well known that microorganisms and related microbial leaching processes play a significant role in the natural weathering of rocks and minerals. Microorganisms facilitate and accelerate this breakdown process, which ultimately leads to the transformation of these rocks and minerals to products that have little resemblance to their original structure, by promoting diagenesis and dissolution (Yatsu, 1988; Ehrlich, 1998). It is not surprising, therefore, that these microbial leaching processes have been commercially exploited and harnessed in the mining industry to aid in the extraction of metals and/or other elements from minerals and ores (Rawlings, 2004).

The term biohydrometallurgy is used to describe the use of microbial processes involved in mineral and elemental biotransformations and incorporates biomining that encompasses bioleaching and biooxidation processes (Rawlings, 2004). Current research on the biomineralization of mineral ores include two main focus areas; one aimed at harnessing heterotrophic microorganisms to produce organic acids for mineralization purposes and the second, aimed at harnessing chemolithotrophic leaching processes. However, much of the biohydrometallurgical processes in mineral processing have focused on large scale bioleaching and biooxidation of sulfide-bearing ores and minerals using acidophilic chemolithotrophic bacteria. The biological treatment of silicate-bearing ores and minerals is still a challenge and it is an important facet of biohydrometallurgy that needs to develop to meet future industry needs (Ehrlich, 2001; Ivanov and Karavaiko, 2004).

Of importance to this study is kimberlite, a silicate-bearing ore that is diamond bearing. Kimberlite is known to weather naturally and extensive weathering of old kimberlite-containing mine dumps has been observed, suggesting possible microbial action (Boshoff *et al.*, 2005; Gericke *et al.*, 2007). Further evidence in the literature documents the ability of certain microorganisms to partially mineralize silicate-

containing rock-material, thereby enhancing the release of metal cations from the mineral structures (Ehrlich, 1996; Gericke *et al.*, 2007).

Therefore, it is hypothesized that microorganisms can accelerate the weathering of kimberlite through the production of metabolites that can enhance mineral dissolution. In this study the microbial biotransformation of kimberlite via microbial leaching processes was investigated. Harnessing these microbial leaching processes to pre-treat mined kimberlite ores has been proposed as a means of improving diamond recovery efficiencies.

This chapter serves to describe the natural weathering of rocks and minerals including silicates and kimberlite. Also, the importance and role of microorganisms in mineral and rock weathering is highlighted whilst a brief description of their biohydrometallurgical application in the mining industry is given.

1.2 Microbial role in the natural weathering of rocks and minerals

Weathering is a natural phenomenon that was previously thought to be confined to physical and chemical processes that brought about mineral diagenesis and dissolution (Yatsu, 1988). More recently it has been shown that microorganisms also play a significant role in the natural weathering of rocks and minerals (Yatsu, 1988; Ehrlich, 1998). Hence, the term biological weathering was coined and is defined as the disintegration process of rocks and minerals brought about or facilitated by microorganisms and their decomposition products (Yatsu, 1988).

Microbes promote mineral dissolution by influencing the kinetics and course of reactions that are involved in the weathering process. Microbes, especially bacteria, are in turn able to gain energy from the process. They are also able to meet their trace element requirements through the dissolution process and in some cases, depending on the mineral dissolution process and the effect it has on the microbial environment, the dissolution process allows the microbes to enhance their competitiveness in their community (Ehrlich, 1996).

Microorganisms promote rock weathering by producing corrosive chemical agents that chemically interact with minerals either through simple acid attack (acidolysis),

mineral complexation or oxidation or reduction reactions (Ehrlich, 1998; Brandl and Faramarzi, 2006). These weathering agents include inorganic acids (e.g. nitric and sulfuric acids), organic acids (e.g. citric, oxalic, lobaric and physolic acids), ferric iron-complexing siderophores as well as oxidizing and reducing agents (e.g. ferric iron and sulfide). These are metabolic end-products formed by bacteria, fungi, or lichens from naturally occurring organic and inorganic substances deposited on or absorbed by the rock (Ehrlich, 1996; Ehrlich, 1998). Therefore, the mineral dissolution process is due to a combination of chemistry and microbiology (Rawlings, 2004).

The microbial processes involved in the natural weathering of rocks and minerals have been harnessed commercially and include processes such as bioleaching and biooxidation (Rawlings, 2004). Although in nature, a wide range of microbes may be involved simultaneously in the mineral dissolution process, much of the industrial application and hence, research has focused on chemolithotrophic and heterotrophic bacteria and fungi and their involvement in the leaching process (Ehrlich, 1996; Gadd, 1999; Rawlings *et al.*, 2003).

1.2.1 Microorganisms involved in the weathering of rocks and minerals

1.2.1.1 Chemolithotrophic microorganisms

It is well documented in literature that the most important microbes in mineral dissolution and degradation are the chemolithotrophic bacteria (Brierley, 1982; Rawlings *et al.*, 2003). Some chemolithotrophic bacteria can grow autotrophically by fixing carbon dioxide (CO₂) from the atmosphere and obtain their energy from inorganic ferrous iron (Fe²⁺) and/or reduced sulfur compounds which act as electron donors (Rawlings *et al.*, 2003).

Leaching chemolithotrophs are found throughout the world and representatives are found in both prokaryote domains, namely, the *Archaea* and *Bacteria*. Biological weathering processes involving chemolithotrophs can occur over a range of temperatures and a variety of microorganisms have been characterized and identified. Amongst these, members of the genus *Acidithiobacillus* (previously known as *Thiobacillus*) were given significant importance (Bosecker, 1989; Krebs *et al.*, 1997). *Acidithiobacillus* are Gram-negative bacteria that exist primarily at mesophilic

temperatures (25-40°C). These include *Acidithiobacillus ferrooxidans* (sulfur- and iron- oxidizing), *Acidithiobacillus thiooxidans* (sulfur oxidizing) and *Acidithiobacillus caldus* (sulfur oxidizing, moderately thermophilic) (Rawlings *et al.*, 2003). Table 1.1 gives an overview of other chemolithotrophic and heterotrophic bioleaching microorganisms and their leaching capacity and potential.

Previously, *Acidithiobacillus spp.* were thought to be the only important leaching microorganisms and therefore much of the literature focused on this group (Brierley, 1982). Subsequently, it has been revealed that other important groups of chemolithotrophs play a significant role in leaching processes. These include the iron-oxidizing *Leptospirillum ferrooxidans* and *Leptospirillum ferriphilum* (Rawlings, 2004). Typically, the microorganisms involved in bioleaching processes exist in consortia. One species may dominate over another depending on the prevailing physiochemical conditions that affect the leaching process (Brandl, 2001; Rawlings, 2005).

Relatively few studies have been done on leaching chemolithotrophs found at temperatures of 50°C and above. At 50°C the microorganisms that have been reported include *A. caldus*, some *Leptospirillum spp.*, bacteria that belong to the Gram-positive genera *Sulfobacillus* (iron-oxidizing) and *Acidimicrobium* and archaeal associates from the genus, *Ferroplasma*. At temperatures greater than 65°C, archaeal species are more dominant than bacteria. These include archaea belonging to the genus, *Sulfolobus* and *Metallosphaera* and *Acidianus* (Brierley, 1982; Rawlings, 2004).

1.2.1.2 Chemolithotrophic mechanisms of bioleaching

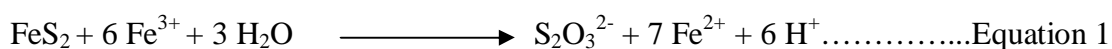
Until recently, it was hypothesized that chemolithotrophic bacteria brought about leaching of minerals and ores via direct and/or indirect mechanisms. Briefly, in the indirect mechanism ferric sulfate [$\text{Fe}_2(\text{SO}_4)_3$] (source of ferric iron, Fe^{3+}) and sulfuric acid is generated through the metabolism of leaching microbes. These metabolites react with other metals and transform them into a soluble oxidized form in a sulfuric acid solution. In direct leaching, it was believed that chemolithotrophic bacteria come into direct contact with a mineral and then brings about dissolution by an enzymatic oxidative attack (Brierley, 1982). However, there is no strong evidence that ‘direct’ leaching does indeed occur and many investigations have further tried to unravel this

phenomenon (Watling, 2006). The role of microorganisms in the ‘indirect’ bioleaching mechanism is also unclear. If their role in leaching is just to generate leaching agents, then the efficiency of the leaching process should be independent of whether the microbes are in contact with the mineral or not. Due to the lack of clarity of what is meant by ‘direct’ and ‘indirect’ and the general debate as to whether bioleaching occurs via the ‘direct’ or ‘indirect’ mechanism, recent studies have proposed that the terms ‘non-contact’ leaching, ‘contact’ leaching and ‘co-operative’ leaching be used (Rawlings, 2002).

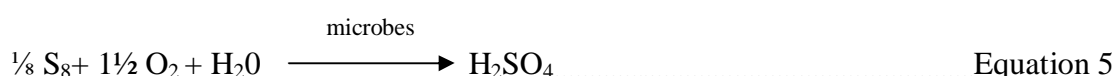
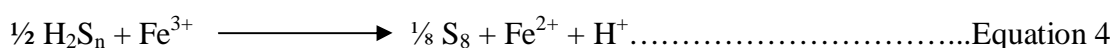
Non-contact chemolithotrophic leaching

Bioleaching is now recognized as a chemical process in which ferric iron and protons play a key role in the leaching reactions. The role of the microorganisms in this process is to generate leaching chemicals and to create a reaction space in which the reactions take place (as in the case of ‘contact’ leaching). The chemolithotrophs generate these leaching chemicals when they bring about the oxidation of ferrous iron and sulfur during their metabolic activities. Depending on the chemical properties and composition of the minerals, microbial leaching of minerals can proceed via different intermediates. For example, it has been recently reviewed that the microbially assisted biooxidation of different metal sulfides proceeds via different intermediates and consequently, the dissolution process for all metal sulfides are not identical. It has been proposed that depending on the acid-solubility properties of the metal sulfides the leaching process may proceed via a thiosulfate mechanism or a polysulfide mechanism (Rawlings, 2002).

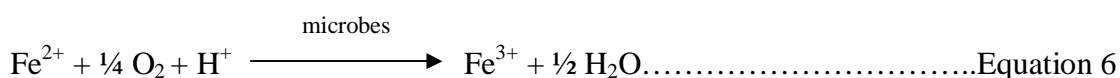
Bioleaching of acid-insoluble metal sulfides such as pyrite (FeS_2), molybdenite (MoS_2) and tungstenite (WS_2) proceed via the thiosulfate mechanism. In this mechanism, solubilization of the acid-insoluble metal sulfide is through a ferric attack on the sulfide minerals. Thiosulfate (S_2O_3) is the main intermediate that is formed during the process reactions whilst sulfate is the main end-product. With reference to the sulfide mineral, pyrite, the reactions may be represented as (Rawlings, 2005):



In the polysulfide mechanism, solubilization of acid-soluble metal sulfides, such as sphalerite (ZnS), chalcopyrite (CuFeS₂) and galena (PbS), is through a combined attack of ferric iron and protons. Elemental sulfur is the main intermediate in this mechanism, which is relatively stable, but may be oxidized to sulfate by sulfur-oxidizing microbial species such as *A. thiooxidans* and *A. caldus*. The reactions in this bioleaching mechanism may be represented as (Rawlings, 2002):



The ferrous iron (Fe²⁺) that is generated in the above reactions (Equations 1-4) may be re-oxidized to ferric iron (Fe³⁺) by iron-oxidizing microbial species such as *A. ferrooxidans* or by species of the genera *Leptospirillum* or *Sulfobacillus*, as represented in Equation 6 (Rawlings, 2005).



Therefore, the role of the microorganisms in the ‘thiosulfate’ and ‘polysulfide’ bioleaching mechanisms is to generate sulfuric acid for proton attack and to keep the iron species present in an oxidized ferric state. Maintenance of acidic conditions will also favour the growth of acidophilic chemolithotrophs (Rawlings, 2005).

Contact chemolithotrophic leaching

In contact bioleaching, the role of chemolithotrophic microorganisms is to provide a reaction space for the bioleaching reactions to occur. Bioleaching microorganisms, in some cases, have a strong affinity for mineral surfaces to which they rapidly adhere to. They form an exopolysaccharide (EPS) layer (but not when growing as planktonic cells), which attaches the microbes to a mineral surface and forms a matrix in which the microbes divide and form a biofilm. It is within this EPS layer that the bioleaching reactions take place more rapidly and efficiently than in comparison to the bulk solution, allowing an accumulation of leaching agents that causes a chemical attack on the valence bonds of the mineral (Rawlings, 2002 and 2005). Because the above

bioleaching mechanism describes the association of the microbes with a surface rather than a means of attack, it has been proposed that 'contact' leaching be used instead of 'direct' leaching (Watling, 2006).

Co-operative leaching

It has been shown that, during the bioleaching of sulfide minerals, sulfur colloids accumulate in the EPS layer. Much of this sulfur is released into the environment, where it is subsequently used by planktonic iron- and sulfur-oxidizing organisms in a co-operative leaching interaction. These organisms produce ferric iron and protons for non-contact leaching (Rawlings, 2002).

1.2.1.3 Chemolithotrophic attachment on mineral/ore surfaces

Bacteria attach themselves to substrates and subsequently develop well structured communities and associations to form biofilms. These biofilms are well adapted in their environment and have well suited mechanisms in place for the delivery of nutrients and removal of waste and toxic by-products. Similarly, chemolithotrophic bacteria attach themselves on mineral/ore surfaces and form biofilms (Watling, 2006). In bioleaching, it is believed that attachment is important because of the '*inferred necessity of close contact by organisms that obtain metabolic energy from constituents released during the dissolution of a solid mineral substrate*' (Edwards *et al.*, 2000).

Biofilm research that has been done has shown that attachment occurs via diffusion, convection and chemotaxis. The former two processes are mostly random, whereas chemotaxis involves bacteria responding to a chemical gradient. These bacteria are able to detect the active dissolution of minerals by sensing changes in dissolved iron or sulfate concentration and are then able to move in the direction of increased concentrations of these ions (Rohwerder *et al.*, 2003). The bacteria then attach themselves to the mineral surfaces. Edwards *et al.* (2000), who also investigated the characteristics of attachment and growth of *A. caldus* on sulfide minerals, reported that attachment of the bioleaching bacteria occurred in an oriented manner relative to the crystal structure of the sulfide mineral. They suggested that oriented attachment may occur, firstly, because of high energy step edges (such as those that bind dissolution pits) or sites (such as scratches and grooves) that control the orientation of

and localize cell attachment and secondly, cell attachment may be controlled by zones enriched in sulfur accumulations. They concluded that cell attachment of *A. caldus* occurred due to their ability to sense and respond to sulfur gradients, which enabled them to be localized on mineral surfaces. Also, although the process is not well understood, it is widely accepted that the EPS layer also plays a key role in the attachment of the bacteria to mineral surfaces (Rohwerder *et al.*, 2003; Watling, 2006). Under acidic conditions, the EPS layer has a net positive charge. This may account for the attachment of bacterial cells to minerals such as pyrite, which has a net negative charge (Rohwerder *et al.*, 2003).

There is also evidence that bacterial attachment maybe mineral and site specific (Watling, 2006). It appears that bacteria will adhere to surfaces to which they are most attracted to and not necessarily to the outer most mineral surface. For example, the hydrophobicity of chemolithotrophic bacteria increases as pH decreases, bacterial cells preferentially adhere to more hydrophobic surfaces such as sulfides than to hydrophilic surfaces such as quartz (Watling, 2006). Additionally, if a bacterial cell has more affinity for a specific mineral in ores, it will preferentially adhere to that mineral if detected in inclusions or cracks, etc. Over time as depletion of energy sources occurs, the bacteria will attach to mineral surfaces that can act as or provide an alternate source of energy (Watling, 2006).

Chemical parameters such as the presence of certain ions may increase or decrease the affinity of bacterial cells to adhere to certain minerals. For example, ferrous iron inhibited the attachment of *A. ferrooxidans* to pyrite and chalcopyrite whilst ferric iron was less inhibiting (Watling, 2006).

1.2.1.4 Advantages and disadvantages of using chemolithotrophic leaching processes

The major advantages of using chemolithotrophic bacteria in leaching processes include the following:

1. In sulfide mineral bioleaching, chemolithotrophic bacteria derive their energy from the oxidation of ferrous iron or reduced inorganic sulfur compounds, or some cases both (Rawlings, 2005). However, this is not necessary the case in silicate bioleaching.

2. Their metabolic activities result in the production of ferric iron and sulfuric acid which promote metal leaching and enhance the dissolution of cations such as K, Mg and Ca from interlayer regions of minerals, thereby promoting weathering and weakening of many minerals and ores (Rawlings, 2005; Gericke *et al.*, 2007).
3. They are mostly acidophiles and therefore can grow in environments of low pH (Rawlings, 2005). With the production of sulfuric acid in some cases, the pH of the leaching environment drops and therefore it is important that the bacteria continue to function normally and efficiently under these conditions.
4. They are also tolerant to a wide range of metallic and other ions and therefore their growth is not inhibited by the release of metals from minerals and ores into solution (Rawlings, 2005).
5. Furthermore, chemolithotrophic microorganisms are not usually subject to contamination by unwanted microbes (Gericke *et al.*, 2007) .
6. In continuous flow systems, the microbes are continuously being washed out but there is a strong selection of microbes that grow most efficiently on the minerals present. The microorganisms once attached to the substrate will not be washed out. This allows for selection of improved and best adapted microorganisms to their environment in the bioleaching process. This is an added advantage as there are very few biological processes where selection of microorganisms that grow most effectively can be selected for (Rawlings, 2005).

The major disadvantages reported include the following:

1. Uncontrolled bioleaching processes leads to acid mine drainage (AMD) or acid rock drainage (ARD). The degradation products of bioleaching, dissolved metals and acids generated if not neutralized will enter soil and water paths and cause environmental pollution (Rohwerder *et al.*, 2003). However, industrial applications of this technology can have measures implemented to ensure that the environment is protected. Furthermore, mine tailings or residues from biomining processes are less chemically active and because they have been subjected to bioleaching, the microbiological activity that they can support is drastically reduced by the extent to which they have already been bioleached (Rawlings *et al.*, 2003).

2. Chemolithotrophic bacteria have slow growing rates and therefore longer growth and reaction times are required in comparison to other leaching microorganisms (Krebs *et al.*, 1997).

1.2.2.1 Heterotrophic microorganisms

Although applications of microbial leaching technologies mostly make use of chemolithotrophic microorganisms, many species of heterotrophic fungi and bacteria are able to leach minerals and ores. Heterotrophic microorganisms require organic carbon substrates for growth and energy generation (Gericke *et al.*, 2007). Although many heterotrophic species capable of causing mineral dissolution have been described (Table 1.1), a great deal of importance is given to fungal species of the genera *Aspergillus* and *Penicillium* because of their ability to produce high concentrations of organic acids that promote mineral and ore leaching (Krebs *et al.*, 1997; Rezza *et al.*, 2001).

1.2.2.2 Heterotrophic mechanisms of bioleaching

Heterotrophic leaching of minerals may occur by several indirect processes. These include:

1. The production of organic acids such as citric and oxalic acid. In most cases of heterotrophic leaching, attack and dissolution of minerals is a result of organic acid production by bacteria and fungi. The organic acids act as a source of protons for solubilization and complexing of organic acid anions with cations that solubilize in solution. Therefore attack on the mineral occurs via acidolysis and complexation (Gadd, 1999; Jain and Sharma 2004).
2. Heterotrophic microorganisms may also produce chelating agents such as siderophores, oxalates, citrates, amino acids and phenolic compounds that complex with the metallic ions and remove them from their sphere of action. Oxalic and citric acids also have strong chelating properties and can also aggressively attack minerals via ligand-promoted dissolution. Oxalic acid can also leach those metals that form soluble oxalate complexes. In some cases, if there is a higher concentration of chelating agents, dissolution of minerals occurs via ligand-promoted dissolution while acidolysis becomes the secondary leaching process (Gadd, 2007).

3. Metal accumulation in the fungal mycelium, which functions as the sink for mobilized metals, also promotes mineral dissolution by ‘pulling’ the equilibrium towards the fungal mycelium (Gadd, 2007).
4. Literature has also shown that fungi may also cause mineral dissolution through redoxlysis, where they are able to precipitate reduced forms of metals and metalloids in and around their fungal hyphae (Gadd, 2007).
5. Heterotrophic organisms may also produce metabolic products that increase the alkalinity of the medium. The alkalization of the media may aid in the dissolution of silicate ores by breaking the silicon-oxygen bond (Jain and Sharma, 2004).

1.2.2.3 Advantages and disadvantages of using heterotrophic leaching processes

Advantages of heterotrophic microorganisms include:

1. Heterotrophic microorganisms, namely fungi, are able to function over a wide pH range and therefore could have potential use in leaching environments where leaching with acidophilic chemolithotrophs is not possible. They also have a high a tolerance to metals (Gadd, 1999).
2. Growth conditions of heterotrophic microorganism are also more easily manipulated in bioreactors than *Acidithiobacillus* spp. and these growth conditions can be altered to increase production of leaching agents (Burgstaller and Schinner, 1993).

Disadvantages of heterotrophic microorganisms include:

1. Heterotrophic microorganisms utilize organic carbon substrates for their growth requirements and energy generation. The cost of the organic carbon substrates is high thus, making heterotrophic leaching on a large commercial scale expensive and less attractive (Jain and Sharma, 2004; Gericke *et al.*, 2007).
2. Since it is not feasible to sterilize ores on a large scale, prevention of contamination is virtually impossible. Current thinking suggests that heterotrophic leaching systems are not suited for *in situ* use and that their application in controlled bioreactors is generally envisaged (Gadd, 1999; Ehrlich, 2001; Gericke *et al.*, 2007).

3. Finally, for leaching of minerals and ores to be effective, high levels of leaching organic metabolites have to be maintained (Gadd, 1999).

Table 1.1 Diversity of leaching microorganisms known to mediate biohydrometallurgical processes involved in mineral and ore processing or known to be part of the natural microbial leaching consortia found in bioleaching habitats. (Re-drawn and adapted from Brandl, 2001; Rawlings and Johnson, 2007)

Domain	Organism	Nutrition Type	Main Leaching Agent	pH Range	Optimum Growth pH	Temperature (°C)
Archaea	<i>Acidianus ambivalens</i>	facultative heterotrophic	sulfuric acid			
	<i>Acidianus brierleyi</i>	facultative heterotrophic	sulfuric acid	acidophilic	1.5-3.0	45-75
	<i>Acidianus infernus</i>	facultative heterotrophic	sulfuric acid			
	<i>Ferroplasma acidiphilum</i>	chemolithoautotrophic	ferric iron	1.3-2.2	1.7	15-45
	<i>Metallosphaera prunae</i>	chemolithoautotrophic	ferric iron, sulfuric acid			
	<i>Metallosphaera sedula</i>	chemolithoautotrophic	ferric iron, sulfuric acid	acidophilic		
	<i>Picrophilus oshimae</i>	chemolithoautotrophic	ferric iron, sulfuric acid	0.9-4.0		
	<i>Picrophilus torridus</i>	chemolithoautotrophic	ferric iron, sulfuric acid	0.9-4.0	2.0-3.0	55-85
	<i>Sulfolobus acidocaldarius</i>	chemolithoautotrophic	ferric iron, sulfuric acid			
	<i>Sulfolobus ambivalens</i>	chemolithoautotrophic	ferric iron, sulfuric acid			
	<i>Sulfolobus brierleyi</i>	chemolithoautotrophic				
	<i>Sulfolobus hakonensis</i>	chemolithoautotrophic				
	<i>Sulfolobus metallicus</i>	chemolithoautotrophic	ferric acid, sulfuric acid			
	<i>Sulfolobus themosulfidooxidans</i>	chemolithoautotrophic	ferric acid, sulfuric acid			
	<i>Sulfolobus yellowstonii</i>	mixotrophic	ferric acid, sulfuric acid	acidophilic		
	<i>Sulfurococcus mirabilis</i>	mixotrophic	ferric acid, sulfuric acid			
	<i>Thermoplasma acidophilum</i>	heterotrophic		acidophilic	1.8	56
	<i>Thermoplasma volcanicum</i>				1.8-2.0	56-60
Bacteria	<i>Acidiphilium cryptum</i>	heterotrophic	organic acid	2.0-6.0		25-30
	<i>Acidiphilium symbioticum</i>	heterotrophic	organic acid		3.0	25-30
	<i>Acidiphilium acidophilum</i>	mixotrophic	sulfuric acid	1.5-6.0	3.0	25-30
	<i>Acidimicrobium ferrooxidans</i>	mixotrophic		3.0-6.0		25-30
	<i>Bacillus coagulans</i>	heterotrophic		5.4-6.0		22
	<i>Bacillus licheniformis</i>	heterotrophic				37

Table 1.1 Continued

Domain	Organism	Nutrition Type	Main Leaching Agent	pH Range	Optimum Growth pH	Temperature (°C)
	<i>Leptospirillum ferrooxidans</i>	chemolithoautotrophic	ferric iron		2.5-3.0	30
	<i>Leptospirillum thermoferrooxidans</i>	chemolithoautotrophic	ferric iron		1.7-1.9	45-50
	<i>Pseudomonas cepacia</i>	heterotrophic		5.4-6.0		22
	<i>Pseudomonas putida</i>	heterotrophic	citrate, gluconate			
	<i>Sulfobacillus thermosulfidooxidans</i>	mixotrophic	ferric acid, sulfuric acid	acidophilic		50
	<i>Sulfobacillus acidophilus</i>	mixotrophic				
	<i>Acidithiobacillus caldus</i>	chemolithoautotrophic	sulfuric acid			45
	<i>Acidithiobacillus ferrooxidans</i>	chemolithoautotrophic	ferric iron, sulfuric acid	1.4-6.0	2.4	28-35
	<i>Acidithiobacillus thiooxidans</i>	chemolithoautotrophic	sulfuric acid	0.5-6.0	2.0-3.5	10-37
	<i>Ferroplasma acidiphilum</i>	heterotrophic			1.7	35-36
Fungi	<i>Alternaria sp.</i>	heterotrophic	citrate, oxalate			32
	<i>Aspergillus awamori</i>	heterotrophic				
	<i>Aspergillus fumigatus</i>	heterotrophic				
	<i>Aspergillus niger</i>	heterotrophic	oxalate, citrate, organic acids			30
	<i>Aspergillus ochraceus</i>	heterotrophic	citrate			28
	<i>Penicillium sp.</i>	heterotrophic	organic acids			25-30
	<i>Cladosporium resinae</i>	heterotrophic				
	<i>Cladosporium sp.</i>	heterotrophic				
	<i>Coriolus versicolor</i>	heterotrophic	oxalate			
	<i>Fusarium sp.</i>	heterotrophic	oxalate, malate, pyruvate			27

1.3 Weathering of minerals

In geochemical terms, minerals are usually defined as inorganic compounds that are of specified chemical composition and structure. They are usually crystalline but sometimes may appear as amorphous material and may be simple or very complex in chemical composition. This definition also includes organic compounds in nature such as coal. Rocks, which may either be igneous, sedimentary or metamorphic are solid, inorganic matter consisting of two or more inter-grown minerals (Ehrlich, 1981).

All types of minerals may be susceptible to natural weathering, which includes chemical, mechanical and biological weathering. Weathering of minerals depends on their chemical structure, composition and stability in the environment. Weathering occurs as a result of weakening of their structural bonds due to physical and chemical stress factors induced by the environment. Some minerals are more stable than others and therefore are more resistant to weathering. Rock weathering occurs according to the type of minerals present, the way the minerals are arranged and the overall stability of the mineralogical structure of the rock. All types of igneous and sedimentary rocks (including sulfides, carbonates and silicates) are susceptible to weathering (Ehrlich, 1998).

1.3.1 Weathering of silicate minerals and rocks

Geologists estimate that silicates make up over 90% of the earth's crust and are therefore the largest group of minerals (Ehrlich, 1981). They also make up about 75% of the exposed surface rocks and are regarded as the most important group of minerals in rock formation. A wide variety of silicate minerals exist naturally, which are largely made up of silicon and oxygen. Due to their ability to occur in numerous structural orientations, they are categorized according to their structural group. Table 1.2 describes the major groups of silicate minerals with examples of each sub-group (Morkel, 2007).

Table 1.2 Types of silicates present in nature. (Re-drawn and modified from Morkel, 2007)

Name of Silicate	Structural Group	General Formula	Example
Neosilicates (Orthosilicates)	Tetrahedra	SiO_4^{4-}	Olivine, zircon, garnet, forsterite
Sorosilicates	Double tetrahedra	$\text{Si}_2\text{O}_7^{2-}$	hemimorphite
Cyclosilicates	Closed rings of tetrahedra	$(\text{SiO}_3^{2-})_n$ $n = 3, 4, 6$	benitoite
Inosilicates	1. Chains of tetrahedral 2. Double chains of tetrahedra	$(\text{SiO}_3^{2-})_n$ $(\text{Si}_4\text{O}_{11}^{2-})_n$	Pyroxenes (diopside), amphibole
Phyllosilicates	Sheets of tetrahedra	$(\text{Si}_2\text{O}_5^{2-})_n$	Clay minerals, mica, serpentine
Tectosilicates	3D framework of tetrahedra	SiO_2	Feldspars

Weathering of silicates also occurs naturally via chemical, physical and biological processes and the degree of weathering depends on the structure of the silicate mineral and the lattice energy of the structure. For example, olivine is easily weathered due to the fact it has a simple structure with low lattice energy. Silicate rocks consist mainly of silicate minerals and their susceptibility to weathering will therefore depend on the silicate minerals present (Morkel, 2007).

With respect to the microbiology of silicate weathering, the literature documents the ability of some bacteria and fungi to accelerate the dissolution process. Leaching results when the microbes produce metabolic by-products such as organic and inorganic acids that promote dissolution of these minerals (Ehrlich, 1996; Benett *et al.*, 2001). However, unlike like sulfide ores, silicate ores contain no energy source for the microbes to utilize. This mineralogical group is of particular significance to this present study as kimberlite (Figure 1.1) is an igneous silicate rock that consists predominantly of silicate minerals that are susceptible to weathering (Morkel, 2007).



Figure 1.1 Image of a typical kimberlite ore found at Kimberley diamond mines in South Africa. (Re-printed from www.guilford.edu/geology/imagelibrary/MVC-061F.JPG)

1.3.1.1 Weathering of kimberlite

Kimberlite ores are a rare type of volcanic rock which are volatile rich (CO_2 predominantly), potassic, ultrabasic/ultramafic igneous rocks that are the main source of diamonds. They consist of many silicate minerals such as olivine, serpentine, phlogopite (mica minerals) and smectite (swelling clay minerals) that are known to weather naturally in the environment (Morkel, 2007). However, the vulnerability of weathering of kimberlite ores and the rate at which the weathering process occurs depends on controlling variables such as ion and acid concentration, temperature and other physiochemical parameters that may affect the mechanisms involved (Morkel, 2007).

Mechanical or physical weathering includes mechanisms such as low temperature-water based weathering, hydration shattering, salt weathering, wetting and drying, insolation weathering and pressure release weathering (Morkel, 2007). Chemical weathering mechanisms include hydration, solution, oxidation (redox reactions), hydrolysis, acidolysis and complex formation (chelation). Living organisms such as bacteria, fungi, lichens, algae, plant roots involved in biological weathering are not usually part of the immediate causes of breakdown but are agents that contribute to the physical and chemical weathering mechanisms by exerting a physical stress or by

emitting substances that enhance mineral dissolution as part of their life processes (Morkel, 2007). Chemolithotrophic and heterotrophic microorganisms may play a similar role as discussed in section 1.2.1 and 1.2.2 by producing metabolites that promote oxidation, acidolysis and chelation.

Kimberlite is primarily made up of silicates, therefore weathering of kimberlite is dependent on the type of silicate minerals present and their susceptibility to weathering (Bennett *et al.*, 2001). Most kimberlite ores contain swelling clays and it has been suggested that kimberlite weathering is associated with the swelling mechanism of these swelling clays (Boshoff *et al.*, 2005). This swelling mechanism is due to the hydration of exchangeable cations which results in a widening of the spacing between the layers. This causes a volume change that produces relatively high pressures that can result in the disintegration of kimberlite. This swelling phenomenon is therefore dependent on the interlayer properties of the clay and the type of spacing cations present and their interlayer spacing exchange properties as well as their ability to absorb water and hydrate (Boshoff *et al.*, 2005; Morkel, 2007). Weathering of kimberlite is also brought about by the dissolution of other silicate minerals such as serpentine and phlogopite (Ivanov and Karavaiko, 2004). The solubilization of phlogopite may occur via two mechanisms. Firstly, solubilization may be mediated by a proton attack or through complexation or secondly, through the removal of the interlayer K and its replacement with Mg and other solvated ions, which may lead to an interstratified phase between vermiculite and phlogopite. In some cases, the complete removal of the interlayer K can lead to the formation of vermiculite or smectites (Štyriaková *et al.*, 2004).

Weathering of kimberlite affects several aspects of diamond processing (Morkel, 2007). Figure 1.2 gives an overview of diamond processing. Weathered kimberlite becomes weaker or 'softer' and therefore is prone to over-crushing which may result in diamond damage (Boshoff *et al.*, 2005; Morkel, 2007).

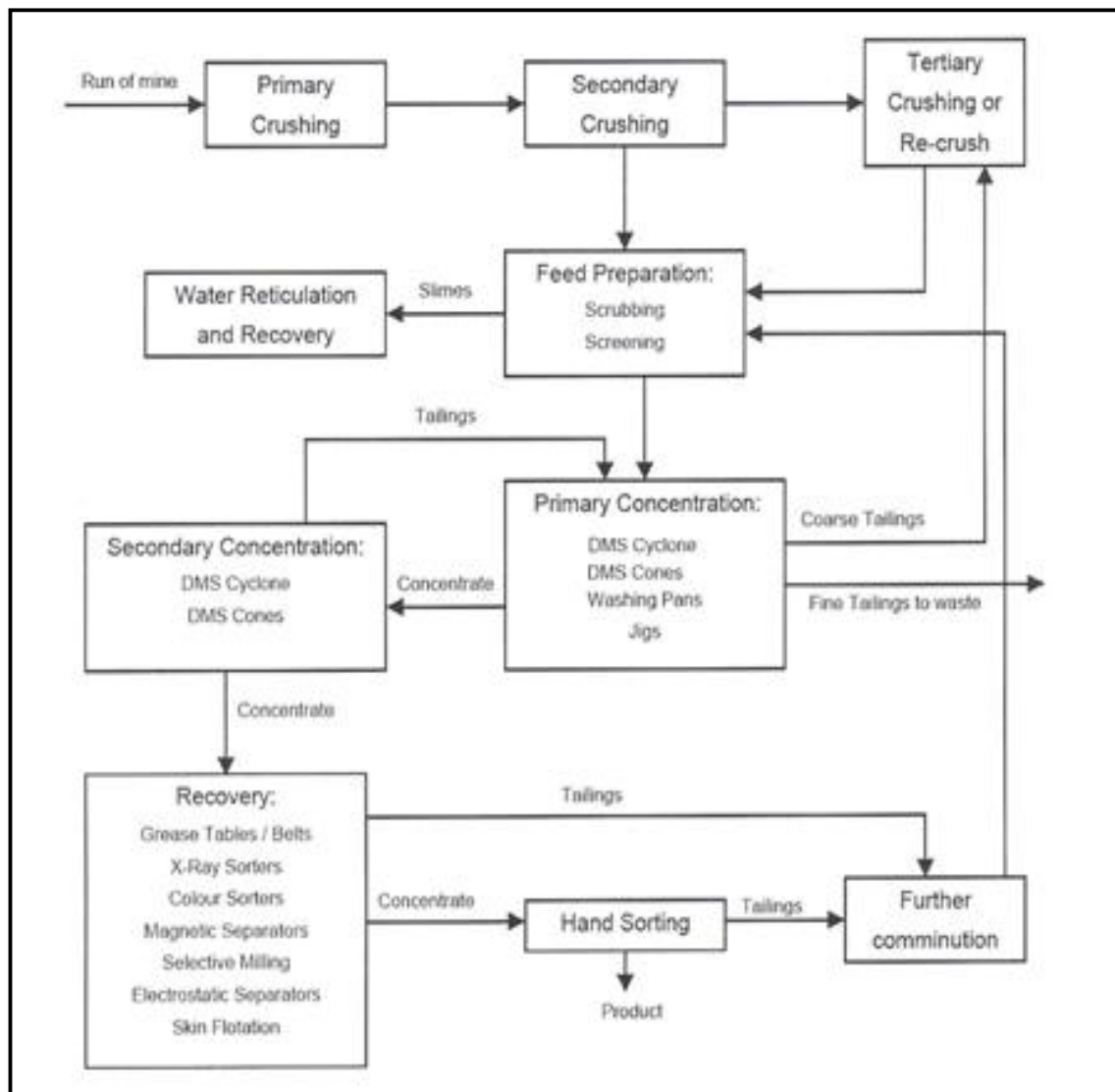


Figure 1.2 Flow diagram of kimberlite processing and diamond liberation. (Re-drawn from Morkel, 2007)

1.4 Biohydrometallurgical applications

Bioleaching processes are currently used successfully for the commercial-scale recovery of metals such as copper, cobalt, gold and uranium from ores and concentrates (Brierley and Brierley, 2001; Rawlings, 2004; Rawlings, 2005). However, much of these biohydrometallurgical applications have been restricted to sulfide-bearing ores and concentrates and to a lesser extent iron-bearing ores with extensive use of chemolithotrophic bacteria (Torma and Bosecker, 1982; Rawlings, 2004). To date, biohydrometallurgical research on silicate ores appear to be limited to laboratory scale investigation (Ehrlich, 2001).

Commercial microbial leaching and oxidation of minerals and ores are carried out on several different scales with various degrees of control (Torma and Bosecker, 1982; Waites *et al.*, 2001). Four distinct industrial microbial leaching approaches have been applied. These include dump, heap, *in situ* and stirred-tank reactor leaching (Bosecker, 1989; Ehrlich, 2001; Rawlings *et al.*, 2003). Before microbial leaching processes are applied on a large scale, the leaching characteristics of the ore and the capabilities of the microbes to be used are investigated. Subsequently, if preliminary findings are positive, further investigations need to be conducted to optimize and scale-up the leaching conditions. Various experimental procedures can be implemented within the laboratory for this purpose. These include percolator leaching, stationary leaching, shake flask suspension leaching as well as column and stirred-tank leaching (Bosecker, 1989).

Currently, industry makes use of microbial leaching processes (MLP) for one of two purposes:

1. MLP are used to convert insoluble metal sulfides or oxides to water soluble metal sulfates. Sulfides of metals such as zinc, copper, etc. are almost insoluble in water. However, when oxidized to its sulfate form, it is soluble in water. Bacteria act as mediators in the chemical attack of the insoluble sulfides by producing ferric iron and acid which enhance mineral solubilization. The metal sulfate is leached into solution where the metal can be extracted using chemical separation and extraction procedures. This microbial leaching process is referred to as bioleaching and an example of this is the conversion of insoluble copper present in sulfide minerals such as covellite (CuS) or chalcocite (Cu_2S) to soluble copper sulfate. Copper is currently the largest metal recovered using bioleaching processes that are mostly applied in dump and heap leaching technologies (Rawlings *et al.*, 2003; Rawlings, 2004; Rawlings, 2005).
2. MLP are used as part of a pre-treatment process to weaken and open up the mineral structure so that other chemicals can better penetrate through the mineral and solubilize the desired metal. Because the metal is not solubilized and remains in the mineral, the microbial leaching process is referred to as biooxidation. An example of this is the removal of gold from arsenopyrite ores and concentrates. Gold is obtained by chemical solubilization using cyanide.

Gold is inert to attack by ferric and sulfuric acid but using biooxidation as a pre-treatment allows the minerals of the ores to become weakened and allows cyanide to better penetrate the minerals and get better access to the gold during the subsequent extraction procedure thereby allowing > 95% of the gold to be recovered. Biooxidation of gold largely makes use of stirred-tank reactor leaching technology. There are about 10 commercial stirred-tank biooxidation plants that operate in 6 countries including South Africa (Rawlings *et al.*, 2003; Rawlings, 2004; Rawlings, 2005).

1.4.1 Industrial biohydrometallurgical processes

1.4.1.1 Dump leaching

Dump leaching is the oldest commercial microbial leaching method used to extract metals from ores and concentrates (Bosecker, 1989). In practice, low-grade ores are deposited in natural valleys or basins with impermeable floors to ensure that leachate does not contaminate the surrounding environment. Acidic leaching liquid is irrigated onto the dump and allowed to percolate through the mineral ores carrying dissolved oxygen and carbon dioxide. The resulting leachate contains microbial metabolites and solubilized metals flowing out of the dump can be collected at the base of the pile in catch streams. After removal of relevant metals, the leachate is then recycled and pumped back to the dump (Bosecker, 1989; Waites *et al.*, 2001). The limitations of large-scale dump leaching include (Waites *et al.*, 2001; Rawlings, 2004):

1. Provision of adequate growth limiting factors of which oxygen being the most important;
2. Ensuring even percolation of leaching liquid through the dump and prevention of channeling;
3. Ensuring the prevention of overheating in the dump as temperatures can exceed 80°C, which is detrimental to the leaching bacteria; and
4. Although the natural movement of microbes will eventually inoculate the heap, initial mineral dissolution rates can be improved by effective heap inoculation. However, this is difficult to achieve in dump leaching.

1.4.1.2 Heap leaching

Heap leaching is similar to dump leaching except that it is carried out on higher quality ores on a smaller scale (Waites *et al.*, 2001). It usually involves ores being crushed to a particular size (Bosecker, 1989). Added advantages are that the process is generally much shorter (months rather than years) and is more easily controlled than dump systems (Waites *et al.*, 2001). Figure 1.3 illustrates a microbial heap-leach processing plant.



Figure 1.3 Heap-leaching processing plant of copper operational at Cerro Colorado, Chile. (Re-drawn from Rawlings, 2004)

1.4.1.3 *In situ* leaching

In situ leaching is typically carried out in disused mines where some of the metals such as uranium and copper may still be present but are not economically feasible to mine. The mines are flooded with leaching liquid containing microorganisms and the outflowing leachate is collected after about 3-4 months and the metals in solution are recovered (Bosecker, 1989; Waites *et al.*, 2001). The advantage of this approach is that ores do not need to be removed making it an energy efficient and cost effective option (Rawlings, 2004). However, the major disadvantages of *in situ* leaching are that control of the leaching process is difficult to achieve and that the process is dependent on geological factors. Porous rock or adequate permeability of the ores is needed to allow for efficient percolation of the leach solution whilst a high

impermeability of the surrounding rocks is required so that seepage of the leaching liquid into the environment is prevented (Bosecker, 1989; Waites *et al.*, 2001).

1.4.1.4 Stirred-tank reactor leaching

Stirred-tank leaching processes make use of highly aerated continuous flow reactors that offer the possibility of increased leaching efficiency under controlled leaching conditions (Waites *et al.*, 2001; Rawlings, 2004). The ores and mineral concentrates are finely ground and then added together with inorganic nutrients to a slurry which is stirred and mixed. Subsequently, the stirred suspension flows through a series of pH and temperature controlled tanks in which mineral dissolution and ore decomposition takes place. Mineral leaching in stirred-tank leaching reactors can take days rather than weeks and/or months. Another advantage of stirred-tank leaching is that little adaptation of the set-up is required for different mineral types in stirred tanks operating at 40-50°C. However, the major constraint of stirred-tank leaching is that leaching efficiency is dependent on pulp density. The maximum pulp density that can be maintained in suspension in the reactors is limited to about 20% (w/v). Physical and microbiological problems occur at higher pulp densities due to lowered gas transfer efficiency and shear forces that cause physical damage to the microbial cells. Pulp density constraints together with higher capital and running costs when compared to the other leaching technologies has led to the application of this technology to only high-value minerals (Rawlings, 2004). Figure 1.4 shows an example of the stirred-tanks reactors used in the biooxidation of gold-bearing ores.

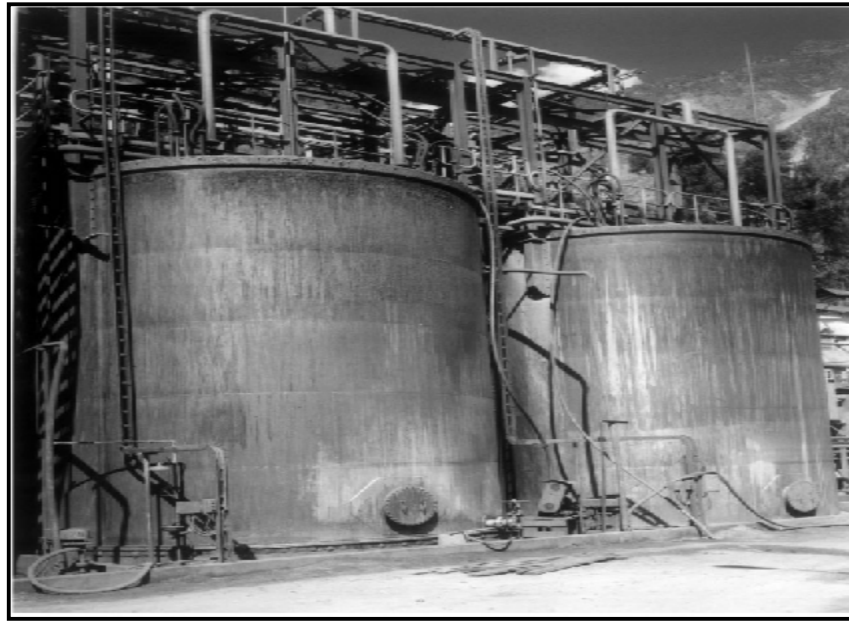


Figure 1.4 Photograph of stirred-tank reactors used in the biooxidation of gold found at Tamboraque gold mine, 90 km east of Lima, Peru. (Re-drawn from Rawlings, 2004)

1.4.2 Advantages of biohydrometallurgical processes

There are several advantages of using biohydrometallurgical processes in mineral and metal extraction. These include:

1. As sources of higher-grade ores become depleted, there is an increasing need to recover metals from lower-grade ores. Bioleaching can also be applied to low grade ores to economically extract minerals and metals (Waites *et al.*, 2001; Rawlings, 2004).
2. Microbial leaching processes have shown increased and improved mineral dissolution and recovery rates, economically, in comparison to other leaching processes (Waites *et al.*, 2001).
3. They have reduced operating costs with less energy requirements and are generally more environmentally friendly when compared to many other physicochemical metal extraction methods (Waites *et al.*, 2001; Rawlings, 2004).
4. Because microbial leaching processes are more economical, they are now also being applied to higher grade ores to recover metals (Rawlings, 2004).

1.4.3 Possible application of biohydrometallurgical processes to kimberlite

The ability of kimberlite to weather naturally was previously exploited in the 19th century where this phenomenon was used as a pre-treatment step for kimberlite diamond processing. However, the weathering process of kimberlite took about two years before the rock was sufficiently weakened to extract the diamonds. Hence, this pre-treatment was replaced with mechanical crushing. Crushing devices are expensive and also have high operational costs with respect to maintenance and energy consumption. Furthermore, harsh crushing reduces the quality of diamonds because it sometimes leads to diamond breakage and damage (Boshoff *et al.*, 2005).

The concept of using accelerated weathering processes to pre-treat kimberlite has recently been revisited (Gericke *et al.*, 2007). With the successful development of biomining technology over the years coupled with a greater understanding of the role of microbes in the weathering of silicate-containing ores, accelerated weathering of kimberlite may become an attractive pre-treatment option once again.

It has been proposed that microbial leaching processes in the form of dump/heap technology be exploited to accelerate the weathering of kimberlite. Kimberlite, which does not have readily available energy sources for the microorganisms, will be mixed with supplemented energy sources whilst the dump/heap will be irrigated with leaching liquid. This pre-treatment would be beneficial, as weathering is significantly promoted using microbial leaching processes. This would lead to a weakening of the ores at a faster rate when compared to weathering with water, which leads to less harsh crushing procedures and consequently a reduction in power costs and diamond damage during the liberation process. Furthermore, with strict regulations about conserving energy and practicing more eco-friendly processes, this microbial pre-treatment offers a promising alternative to conventional processing of kimberlite during diamond liberation.

1.5 Dissertation overview

Kimberlite is known to be prone to natural weathering processes which results in a weakening of its mineralogical structure. Evidence from the literature documents the ability of microorganisms to partially mineralize silicate-containing rock-material, thereby enhancing and accelerating the weathering process. Further studies have shown that the weathering of silicate minerals such as serpentine, smectite, phlogopite, etc., which kimberlite largely consists of, is significantly promoted in the presence of sulfuric acid and organic acids such as oxalic and citric acid which are examples of naturally produced microbial metabolites (Bhigam *et al.*, 2001; Ivanov and Karavaiko, 2004; Gericke *et al.*, 2007). Hence, it has been proposed that these microbial leaching processes be harnessed for the pre-treatment of kimberlite ores during kimberlite processing for diamond liberation. Therefore, this study investigated the feasibility of harnessing microbial leaching processes to accelerate the weathering of kimberlite ores. Research on the biomineralization of kimberlite ores is sparse and therefore this investigation focused on harnessing both chemolithotrophic and heterotrophic leaching processes.

1.5.1 Aims and objectives:

1. Evaluation of the biotransformation of kimberlite ores using known heterotrophic and autotrophic microorganisms and assessing their feasibility and efficiency in accelerating the weathering of kimberlite ores.
2. Enriching and selecting for autotrophic communities from naturally weathered kimberlite ores and investigating their role and efficiency in mineralization.
3. Optimization and scale-up studies to determine how energy source availability, kimberlite particle size and the use of a mixed chemolithotrophic culture in a continuous system affects the microbial weathering of kimberlite.

CHAPTER 2

Material and Methods

2.1 Kimberlite

The four kimberlite samples used in this study were sourced from different diamond mines, namely Gahcho Kue (Northwest Territories, Canada), Premier (Cullinan, East of Pretoria, RSA), Venetia (near Alladays, Limpopo, RSA) and Victor (Northeastern Ontario, Canada) diamond mines. These samples were crushed (*Mintek*, Randburg, RSA) to approximately 6.7mm. An initial X-Ray Diffraction (XRD) analysis performed on the kimberlite samples was also provided by *Mintek* and represented in Table 2.1.

Table 2.1 Initial X-Ray diffraction analyses of the kimberlite samples obtained from Gahcho Kue, Premier, Venetia and Victor diamond mines indicating minerals identified.*

Mineral Group	Mineral	Chemical Composition	Gahcho Kue	Premier	Venetia	Victor
Clay	Smectite	Mg-Na-Ca- $\text{Al}_2\text{Si}_4\text{O}_{10}(\text{OH})_2 \cdot x\text{H}_2\text{O}$	Trace			Major
Serpentine	Lizardite Antigorite	$\text{Mg}_3\text{Si}_2\text{O}_5(\text{OH})_4$	Major	Major	Major	Minor
Olivine	Forsterite	Mg_2SiO_4	Minor	Trace		Minor
Mica	Phlogopite	$\text{KMg}_3(\text{Si}_3\text{Al})\text{O}_{10}(\text{OH})_2$	Major	Trace	Trace	Trace
Pyroxene	Diopside Augite	$\text{Ca}(\text{Mg},\text{Al})(\text{Si},\text{Al})_2\text{O}_6$ $\text{Ca}(\text{Mg},\text{Al})(\text{Si},\text{Al})_2\text{O}_6$	Trace	Minor		
Fe-oxides	Magnetite Hematite	Fe_3O_4 Fe_2O_3	Minor	Minor Minor	Minor	Trace
Calcite	Calcite Dolomite	CaCO_3 $\text{CaMg}(\text{CO}_3)_2$		Minor	Minor Minor	Trace Major
Corundum	Ilmentite	FeTiO_3				
Perovskite	Perovskite	CaTiO_3		Minor	Minor	

* (Estimates based on relative peak intensities as determined by XRD: Levels of occurrence — Major: >20 mass % of sample, minor: 5 - 20 mass %, and trace <5 mass %) (Initial XRD supplied by Mintek, Randburg, RSA)

2.2 Microorganisms

2.2.1 Chemolithotrophic microorganisms

The mixed mesophilic bacterial bioleach cultures used in this study were sourced from Ms M. Gericke, *Mintek*, Randburg, RSA. The mixed cultures contained bacterial species such as *Acidithiobacillus caldus*, *Leptospirillum ferrooxidans* and *Sulfobacillus spp.* (Gericke, pers comm, Biotechnology Division).

2.2.2 Heterotrophic microorganisms

The oxalic and citric acid producing test fungus used in the heterotrophic leaching experiments was *Aspergillus niger*, which was sourced from a culture collection housed within the Discipline of Microbiology, School of Biochemistry, Genetics, Microbiology and Plant Pathology, University of KwaZulu-Natal, RSA.

2.3 Maintenance and storage of microorganisms

2.3.1 Maintenance and storage of chemolithotrophic microorganisms

The chemolithotrophic consortia were maintained as fed-batch cultures. These were prepared by taking 10ml of inoculum of the given *Mintek* cultures that were maintained either on ferrous sulfate (FeSO_4) or elemental sulfur (S^0) concentrate and inoculating it into Erlenmeyer flasks (250ml) containing prepared basal inorganic maintenance media (50ml) (described in 2.4.1). These inoculated flasks were either amended with 15g/l of FeSO_4 or 10g/l of elemental sulfur as energy sources. The pH of the media were adjusted to 1.4 -1.5 using concentrated sulfuric acid (H_2SO_4). Flasks containing basal media and sulfur as the energy source were autoclaved at 105°C for 15 minutes prior to inoculation. The pH of the media containing sulfur was adjusted after autoclaving. The flasks containing basal media and ferrous iron as the energy source were filtered through a sterile membrane filter (0.45µm). The inoculated flasks were incubated at 30°C and shaken at 120rpm. Subcultures were prepared every 2 months. This ensured that an active culture was always available for experimental purposes.

2.3.2 Maintenance and storage of heterotrophic microorganisms

Aspergillus niger was also maintained as a fed-batch culture. Mycelial plugs (1.5mm x 1.5mm) taken from *A. niger* grown on Potato Dextrose Agar (PDA) plates were transferred using a sterile scalpel to Erlenmeyer flasks (250ml) containing a standard growth medium (50ml) (described in 2.4.2). The pH of the medium was adjusted to 7.5 using sodium hydroxide (NaOH). Flasks containing growth media were autoclaved at 120°C for 15 minutes prior to inoculation. The inoculated flasks were incubated on a shaker at 120rpm at 30°C. Subcultures were prepared every 2 weeks during the investigation period. Spores (10^8 spores/ml) which were harvested from a 7-day-old *A. niger* culture that had been incubated at 30°C were used for the preparation of inocula. Initial cell counts were performed using a Petroff-Hausser counting chamber (Neubauer). Stock cultures of *A. niger* were grown on PDA media and incubated at 25°C for 7 days and then stored at 4°C.

2.4 Media

2.4.1 Inorganic basal medium

The basal inorganic maintenance medium contained 1g of $(\text{NH}_4)_2\text{SO}_4$, 0.1g of KCl, 0.22g of MgSO_4 and 0.5g of K_2HPO_4 in 1000ml distilled water (Silverman and Lundgren, 1959).

2.4.2 Heterotrophic medium

The standard growth medium for *A. niger* contained 150g of sucrose, 0.25g of $\text{MgSO}_4 \cdot 7\text{H}_2\text{O}$, 2.5g of $(\text{NH}_4)_2\text{CO}_3$, 2.5g of KH_2PO_4 , 0.06mg ZnCl_2 and 1.3mg $\text{Fe}_2(\text{SO}_4)_3$ in 1000ml distilled water (Castro *et al.*, 2000). The PDA medium (Merck) that was used for sub-culturing of stock cultures of *A. niger* was made up according to the manufacturer's instructions.

2.5 Analyses

2.5.1 Inductive coupled plasma-optical emission spectroscopy (ICP-OES)

Leach solutions from leaching experiments were sampled for chemical analysis by ICP at periodic intervals over the course of each study. The samples were prepared as described in 2.5.1.1.

2.5.1.1 Sample preparation

Five milliliter aliquots of the leachate solution were aseptically removed from treatment flasks in all leaching experiments and placed into McCartney bottles. The pH of the contents of the bottles were recorded and adjusted to their initial pH if changes were observed. The pH was altered to ensure that the cations were in their 'ionic' state. Two milliliter aliquots of the leachate solution after pH alteration were then transferred into minifuge tubes and centrifuged at 13,000xg (Hermle Z 160M) for 20 minutes. The resultant pellets were discarded and 1ml of the remaining supernatants were added to volumetric flasks (100ml) and made up to the mark with distilled water. These solutions were thereafter filtered through a membrane filter (0.45µm pore size) and then analyzed for dissolution of magnesium (Mg), calcium (Ca), iron (Fe), Silica (Si) and potassium (K) using an ICP spectrometer (conditions described in 2.5.1.2).

2.5.1.2 ICP conditions

All elemental analyses of leachate solutions were performed using a Varian 720-ES ICP-OES according to the operating conditions given in Table 2.2.

Table 2.2 Experimental conditions for ICP-OES.

ICP spectrometer	Varian 720-ES ICP-OES
Power (kw)	1.00
Argon Plasma Flow (L/min)	15.0
Auxillary Argon Flow (L/min)	1.50
Photomultiplier (V)	800
Intergration time (s)	1
Nebuliser (kPa)	240

The analytical wavelengths (nm) were set at the following spectral lines for each analyte: Mg (279.553), Ca (396.847), Fe (259.940), Si (251.611) and K (769.896). Distilled water was used as a blank and the standards used to calibrate the instrument were made up from a working solution containing Mg, Ca, Fe, K and Si (described in 2.5.1.3). Results were obtained as ppm (mg/l) and then converted to mg of cation species/g of kimberlite used in the experiments for graphical purposes.

Sample calculation:

Result obtained from ICP: 4500mg/l

Conversion: $4500\text{mg}/1000\text{ml}$ (ICP result) $\times 1/1000\text{ml} = 4.5\text{mg/ml}$

$4.5\text{mg/ml} \times 75\text{ml}$ (amount of basal/growth media used) $\times 1/3.75\text{g}$
(amount of kimberlite used in most experiments unless otherwise stated)
 $= 90\text{mg/g}$.

2.5.1.3 Chemicals and elemental species standard solutions

All chemicals and elemental standard stock solutions used were of analytical reagent grade purchased from Sigma-Aldrich, Riedel de Haën, Fluka or Merck.

The ICP standard stock working solution contained all 5 elemental species analyzed with a final concentration as follows: Mg (200mg/l), Ca (40mg/l), Fe (200mg/l), Si (200mg/l) and K (20mg/l).

To obtain these final concentrations of the elemental species, the working solution was prepared by placing 50ml of Mg (1000mg/l), 5ml of Ca (2000mg/l), 50ml of Fe (1000mg/l), 5ml of Si (1000mg/l) and 5ml of Si (1000mg/l) in a volumetric flask (250ml) and making it up to the mark with distilled water.

From the working solution, standards that were used to calibrate the ICP instrument were prepared by taking the appropriate dilution amount and adding it to volumetric flasks (100ml) to obtain a final concentration of the elements (Table 2.3).

Table 2.3 Preparation and final concentrations of standards used to calibrate the ICP spectrometer.

	Standard 1	Standard 2	Standard 3	Standard 4	Standard 5
Final volume of flask (ml)	100	100	100	100	100
Amount pipetted from working solution (ml)	1.0	2.0	5.0	10	25
Concentration of Mg (mg/l)	2.0	4.0	10	20	50
Concentration of Ca (mg/l)	0.4	0.8	2.0	4.0	10
Concentration of Fe (mg/l)	2.0	4.0	10	20	50
Concentration of Si (mg/l)	0.2	0.4	1.0	2.0	5.0
Concentration of K (mg/l)	0.2	0.4	1.0	2.0	5.0

2.5.2 X-Ray diffraction powder analysis (XRD)

Random treated kimberlite particles were sampled for mineralogical analysis by XRD at the end of an experimental period and the results presented were representative of the entire sample. The XRD results were verified by cross-checking the XRD results of the duplicated treatments.

2.5.2.1 Sample preparation

The contents of the treated flasks were placed in centrifuge bottles at the end of each experiment and centrifuged at 9,000xg for 20 minutes (Beckman J2-HS centrifuge) to precipitate the suspended kimberlite particles. Subsequently, the treated kimberlite samples were rinsed with distilled water, dried and then gently ground to ‘powder-like’ form using a mortar and pestle. These were then mounted on back-filled aluminum (Al) holders and run as randomly oriented powders. XRD analyses were also performed on untreated kimberlite samples. The untreated kimberlite samples were also finely ground and mounted on back-filled Al holders.

2.5.2.2 XRD conditions

All mineralogical analyses of all kimberlite samples were performed using a Philips PW 1050 Diffractometer according to the operating conditions given in Table 2.4.

Table 2.4 Experimental conditions for XRD.

XRD Diffractometer	Philips PW 1050 Diffractometer
Radiation	CoK α
Temperature	25°C
Detector	Sietronics 122D automated micro-processor
Range	3-43° 2 θ
Scanning Step	0.02° at 1° per minute

After the kimberlite samples were run in the XRD instrument, the peaks on the XRD spectra obtained on the XRD diffractogram were analyzed and assigned to a diffraction angle. These diffraction angles of the major peaks were then assigned to minerals according to the XRD reference data (Berry, 1974) for minerals. It must also be noted that the major minerals have repetitive peaks in the XRD diffractogram (i.e. they have a sequence of peaks that allows for their identification) and only their major peaks were labelled in the XRD results.

CHAPTER 3

Susceptibility of kimberlite ores to microbial weathering using known and enriched natural microbial populations from weathered kimberlite

3.1 Introduction

Research on the treatment of silicate containing ores, namely kimberlite, using bioheap leach technology and chemolithotrophic bacteria is novel (Gericke *et al.*, 2007). Although the role of microorganisms in mineral and rock weathering has been the subject of investigation for many years (Liermann *et al.*, 2000), relatively few studies have focused on the mechanisms and mineralogical pathways of microbial weathering of silicate ores (Ivanov and Karavaiko, 2004).

Previous research in this area focused mostly on chemical processes and the use of heterotrophic microorganisms that utilize organic carbon sources for their metabolism and growth. However, a major disadvantage of heterotrophic leaching is the use of organic carbon sources by the heterotrophs which makes their application expensive on a large commercial scale. An alternative to this would be to exploit chemolithotrophic microorganisms. In contrast to heterotrophs, chemolithotrophs utilize inorganic CO₂ as their sole source of carbon and derive energy from the oxidative cycling of elemental sulfur and/or ferrous iron, resulting in the production of sulfuric acid and ferric iron respectively (Rawlings, 2005). Evidence has shown that these microbially produced inorganic compounds have a similar effect on silicate ores as they do on sulfide ores. They promote weathering by enhancing the leaching of cations from interlayer regions resulting in the transformation of mineralogical structure of the ores (Bigham *et al.*, 2001; Boshoff *et al.*, 2005; Gericke *et al.*, 2007). Thus, application of these chemolithotrophic bacteria and their leaching mechanisms for the treatment of silicate-bearing kimberlite appears to have promising potential in improving diamond recovery technologies.

Hence, this chapter details preliminary investigations into the dissolution of kimberlite ores using known chemolithotrophic microorganisms (*Acidithiobacillus caldus*, *Leptospirillum ferrooxidans* and *Sulfobacillus sp.*).

As previously mentioned, kimberlite is known to weather naturally and in some cases extensive weathering of run-off kimberlite has been observed at kimberlite mines, possibly indicating that there are natural microbial populations involved in the dissolution process. Therefore this chapter also focuses on and describes the isolation and enrichment of natural chemolithotrophic populations present on weathered kimberlite samples. Their ability and efficiency in accelerating the weathering of kimberlite ores in comparison to bioleach tests using a known mixed chemolithotrophic culture was also assessed.

3.2 Experimental Procedure

3.2.1 Preliminary evaluation of the biotransformation of kimberlite using known chemolithotrophic bioleach cultures

3.2.1.1 Kimberlite

The four different kimberlite samples described in Section 2.1 were used. These were finely ground, sieved to a particle size of less than a 100µm and subjected to shake flask weathering tests (Section 3.2.1.3).

3.2.1.2 Microorganisms

The microorganisms used in this investigation were a mixed culture consisting of mesophilic chemolithotrophs, namely, *A. caldus*, *L. ferrooxidans* and *Sulfobacillus sp.* (Section 2.2.1). Culturing, maintenance and storage of microorganisms were described in Section 2.3.1 of Chapter 2.

3.2.1.3 Shake flask weathering tests

Preliminary kimberlite leaching experiments for all 4 kimberlite samples were carried out in Erlenmeyer shake flasks (250ml) containing basal inorganic media (Section 2.4.1) (75ml) and kimberlite (3.75g, 5% w/v). Prior to weathering tests, the basal media and ore samples in shake flasks were sterilized depending on the energy source used (Section 2.4.1). The shake flasks were then subjected to 4 different treatments (Table 3.1). The first treatment served as an uninoculated control to ensure that the basal media had no effect on the dissolution process. These consisted of inorganic maintenance media (pH 7.67) and kimberlite only. Treatment 2 served as a chemical

control where the pH of the contents of the flasks (basal media and kimberlite) was kept more or less constant at pH 1.4. The pH was monitored weekly using a pH meter (Crison micro pH 2000) and any increases in the pH were corrected to pH 1.4-1.5 using concentrated sulfuric acid (7.5M). In Treatment 3 ('sulfur treatment'), the flasks containing kimberlite and basal media were inoculated with the mixed mesophilic culture maintained on sulfur as the energy source (Section 2.3.1) (10ml)(10^7 cells/ml). Sulfur (0.75g) was added as the energy source and the pH was subsequently adjusted to 1.4 after sterilization and prior to inoculation. Treatment 4 ('iron treatment') was similar to Treatment 3 except that the inoculum used in Treatment 4 was the culture maintained on iron sulfate (Section 2.3.1) and Fe^{2+} in the form of FeSO_4 (1.1g) was added as the energy source. Initial cell counts were performed and standardized using a Petroff-Hausser counting chamber (Neubauer). All treatment flasks were incubated at 30°C in a shake incubator set at 120rpm for 6 weeks. All treatments were performed in duplicate for each kimberlite sample.

Table 3.1 Summary of treatments used in the preliminary investigation of the biotransformation of kimberlite. (Mixed chemolithotrophic bioleach cultures (*A. caldus*, *Sulfobacillus spp.* and *L. ferrooxidans*) maintained either on iron sulfate or sulfur were used in the treatments.)

Treat- ment	Contents of Erlenmeyer shake flasks (250ml)				
1 Control	3.75g kimberlite sample	+	75ml basal inorganic solution (pH 7.67)		
2 Chemical Control	3.75g kimberlite sample	+	75ml basal inorganic solution	+	H_2SO_4 (pH 1.4)
3 'sulfur treatment'	3.75g kimberlite sample	+	75ml basal inorganic solution (pH 1.4)	+	0.75g Sulfur
4 'iron treatment'	3.75g kimberlite sample	+	75ml basal inorganic solution (pH 1.4)	+	1.1g FeSO_4
				+	Mixed mesophilic culture maintained on S^0
				+	Mixed mesophilic culture maintained on FeSO_4

For each treatment flask, the initial weight of the flask and its contents were recorded. During the course of the experiment, the flasks were periodically (day 7, 14, 28 and 35) monitored for weight loss due to evaporation. Weight losses due to evaporation

were compensated by addition of sterile distilled water (1g \approx 1ml). The pH was also monitored periodically (day 7, 14, 28 and 42).

At days 7, 14, 28 and 42 leachate samples (5ml) were taken for ICP analyses (Section 2.5.1). After 6 weeks, the contents of each flask were centrifuged and XRD analyses (Section 2.5.2) were performed on the final remaining pellets that were air dried.

3.2.2 Selective enrichment of microbial communities from naturally weathered kimberlite and investigating their role and efficiency in the mineralization of kimberlite

3.2.2.1 Kimberlite

The two kimberlite samples used in this investigation were from Premier and Venetia Diamond Mines (Section 2.1.2). The weathered kimberlite sample was provided by Mr B. Benvie, *De Beers Diamond Group*, Randburg, RSA (Benvie, pers comm., Minerals Division). The weathered kimberlite particle sizes varied and were randomly selected for the enrichment procedure.

3.2.2.2 Enrichment of leaching microbial populations from naturally weathered kimberlite

Unknown natural populations were isolated from the weathered kimberlite in basal inorganic maintenance media (Section 2.1) under different conditions and energy sources. The isolation procedure was performed in Erlenmeyer shake flasks (250ml) containing naturally weathered kimberlite (4g) and sterile basal media (75ml). In the first treatment no amendments were made to the flask and the isolation procedure was carried out at an initial pH of 7.67. The second treatment mirrored the first except that the pH of the medium was adjusted pH 1.4. In the third treatment, sulfur (0.75g) was supplemented to the flasks as an energy source and the initial pH of the contents of the flasks was adjusted to 1.4 using concentrated sulfuric acid. Treatment 4 was similar to Treatment 3 except that Fe^{2+} in the form of FeSO_4 (1.1g) was used as the energy source. Treatments were performed in duplicate and treatment flasks were incubated at 30°C in a shake incubator set at 120rpm for 8 weeks. During the treatment time the flasks were periodically observed for turbidity and Gram-stains were performed for each treatment to determine the presence of bacteria. After 8 weeks the final pH was recorded and 10ml of inoculum from each treatment flask was

sub-cultured into new flasks containing their new respective sterile media. These new treatment flasks were incubated at 30°C in a shake incubator set at 120rpm for 4 weeks. Their initial and final pH's were also monitored.

3.2.2.3 Batch culture shake flask weathering tests using enriched microbial cultures from naturally weathered kimberlite

The isolated and enriched cultures (Section 3.2.2.2) were used for the weathering tests. The known chemolithotrophic cultures (Section 3.2.1.2) were also used as controls in the bioleach experiments used to evaluate the weathering capabilities of the chemolithotrophic populations isolated from naturally weathered kimberlite. The two test kimberlite samples (Section 3.2.2.1) were therefore subjected to 5 different treatments that were performed similar to the procedure described above in 3.2.1.3. Table 3.2 describes the treatments used.

Table 3.2 Summary of treatments used in the evaluation of the biotransformation of kimberlite using known and enriched microbial leach cultures maintained either on iron sulfate or sulfur.

Treat- ment		Contents of Erlenmeyer shake flasks (250ml)				
1	3.75g kimberlite sample	+	75ml basal inorganic solution (pH 7.67)			
2	3.75g kimberlite sample	+	75ml basal inorganic solution (pH 1.4)	+	0.75g Sulfur	'Known' culture maintained on S ⁰
3	3.75g kimberlite sample	+	75ml basal inorganic solution (pH 1.4)	+	0.75g Sulfur	Enriched culture maintained on S ⁰
4	3.75g kimberlite sample	+	75ml basal inorganic solution (pH 1.4)	+	1.1g FeSO ₄	'Known' culture maintained on FeSO ₄
5	3.75g kimberlite sample	+	75ml basal inorganic solution (pH 1.4)	+	1.1g FeSO ₄	Enriched culture maintained on FeSO ₄

Similar chemical and mineralogical analyses were performed on the leachate solutions and treated kimberlite particles as described in Section 3.2.1.3.

3.2.3 Statistical analyses

Statistical analysis was carried out using SAS software (Version 6.12) (SAS, 1987). A general linear model (GLM) was used to run an analysis of variance (ANOVA) for ICP results derived from each set of kimberlite ore treatments. Separations of means was based on the principle of least significant difference (LSD) at $P < 0.05$.

3.3 Results

3.3.1 Preliminary evaluation of the biotransformation of kimberlite using known chemolithotrophic bioleach cultures

During the course of the preliminary investigation, it was observed that the turbidity of the content of the flasks inoculated with bioleach cultures increased as incubation time increased, indicating microbial growth and/or an increase in total dissolved solids. It was also observed that a greyish precipitate formed in the treatment flasks containing S^0 as the energy source whereas a yellowish-mustard precipitate formed in the treatment flasks supplemented with Fe^{2+} as the energy source for all kimberlite samples tested.

Initially, the pH readings of the treatment flasks containing S^0 and Fe^{2+} as the energy source increased to a pH range 7.5-8.0 but after week 2 and onwards the final pH readings decreased to a pH range of 1.5-2.0 and 3.2-3.7, respectively. Figure 3.1 illustrates the trend described above for the kimberlite sample from Victor mine. Similar trends were seen for the kimberlite samples from Gahcho Kue, Premier and Venetia mines (data not shown).

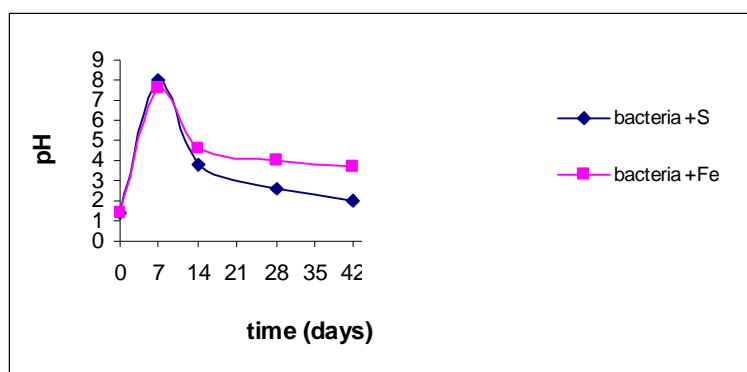


Figure 3.1 Changes in pH over time (days) observed during the chemolithotrophic microbial transformation of kimberlite ores from Victor mine.

3.3.1.1 ICP results

Over the six week period, ICP analyses of the leach solutions showed that varying amounts of Ca, Si, Fe, Mg and K were solubilized (Table 3.3) indicating that mineral dissolution had been initiated. The negative controls in each case, showed virtually no dissolution of cations.

From Table 3.3, it was evident that Mg was the major cation that solubilized in solution followed by Ca, Fe and to a lesser extent, Si. Solubilization of Fe varied according to different kimberlite ore types, whilst no significant changes were seen in the solubilization of K.

For all kimberlite types, it was observed that the treatment in which sulfur was used as the energy source produced superior Mg solubilization when compared to the treatment in which ferric iron was used as the energy source and the chemical control (with the exception of Gahcho Kue diamond mine) (Figure 3.2). Differences in Ca and Fe solubilization for the two treatments were less distinct.

From the ICP data (Table 3.3), it was deduced that the kimberlite samples from Victor, Venetia and Premier diamond mine were most prone to weathering whereas the Gahcho Kue kimberlite sample was most resistant (Figure 3.3).

In general, it was also observed in Table 3.3 and Figures 3.2 and 3.3 that initially there is a distinct increase in cation dissolution, more specifically in the case of Mg, when compared to the negative control and thereafter the amount of cation dissolution increases rather slightly until very little variation is seen. In the case of Ca, the increases in cation dissolution were as not as marked. Iron dissolution varied according to different kimberlite samples and increases in Fe were mainly apparent for the Premier and Venetia kimberlite ores in the ‘sulfur’ and ‘iron’ treatments.

Table 3.3 ICP analyses of four different microbially leached kimberlite samples (particle size <100mm). (Mixed chemolithotrophic cultures were used in leaching experiments with sulfur or ferrous iron as the energy source. All treatment flasks were incubated at 30°C in a shake incubator set at 120rpm for 6 weeks.)*

Sample	[Ca][mg/l]				[Si][mg/l]				[Fe][mg/l]				[Mg][mg/l]				[K][mg/l]			
	Day 7	Day 14	Day 28	Day 42	Day 7	Day 14	Day 28	Day 42	Day 7	Day 14	Day 28	Day 42	Day 7	Day 14	Day 28	Day 42	Day 7	Day 14	Day 28	Day 42
Gahcho Kue Diamond Mine																				
Kimberlite + basal media – control	13d	13d	13d	14d	8a	25ab	25c	25c	4c	4a	4b	4b	5c	5c	14d	14d	9a	9b	9b	9b
Kimberlite + H ₂ SO ₄ – chemical control	107b	161a	215a	227a	8a	26b	26b	27b	4a	4a	5a	5b	55b	137b	333c	414c	10a	10a	11a	11a
Kimberlite + bacteria + S ⁰	119a	147b	174b	176b	8a	26a	28a	41a	4ab	4a	4ab	14a	5c	5c	480a	548a	7b	7c	11a	12a
Kimberlite + bacteria + Fe ²⁺	54c	107c	138c	159c	8a	9c	9d	26d	4b	4a	4ab	14a	253a	240b	453b	481b	6b	6c	6c	6c
F Ratio	1.E+03	1.E+04	4.E+03	4.E+03	8.E-01	2.E+03	5.E+03	4.E+02	4.E+00	3.E+00	4.E+00	2.E+02	3.E+04	5.E+03	6.E+05	3.E+05	2.E+01	3.E+01	5.E+01	5.E+01
LSD	5.93	2.46	5.24	5.64	0.72	0.84	0.50	1.57	0.39	0.50	0.64	1.75	2.92	6.20	1.08	1.68	1.56	1.29	1.19	1.24
Premier Diamond Mine																				
Kimberlite + basal media – control	16d	16d	16d	16d	9c	26d	26c	27c	4c	4c	4d	5d	9d	9d	9d	9d	9c	9a	9a	10a
Kimberlite + H ₂ SO ₄ – chemical control	174a	202a	226a	254a	9c	28c	28c	42b	9b	5c	9c	41c	360a	682a	1028a	1492a	9ab	9a	10a	8a
Kimberlite + bacteria + S ⁰	159b	187b	213b	240b	55a	67a	81a	82a	9b	28b	65b	535b	613b	1560b	2173b	2333b	10a	9a	10a	10a
Kimberlite + bacteria + Fe ²⁺	121c	133c	146c	159c	40b	40b	53b	78a	42a	93a	174a	652a	241c	533c	615c	633c	9bc	9a	10a	10a
F Ratio	1.E+04	8.E+03	5.E+04	8.E+03	7.E+02	8.E+03	2.E+03	6.E+02	6.E+03	1.E+04	7.E+03	1.E+05	3.E+05	1.E+06	7.E+05	7.E+05	1.E+01	5.E-02	1.E+00	1.E+00
LSD	2.35	3.60	1.69	4.90	3.53	0.81	2.56	4.29	0.89	1.35	3.70	3.81	1.68	2.50	4.18	4.71	0.02	1.12	0.96	4.28
Venetia Diamond Mine																				
Kimberlite + basal media – control	16c	16b	16c	17d	11b	11c	11b	11c	5d	5d	5c	5d	17d	17d	17d	17d	9b	10b	10b	10a
Kimberlite + H ₂ SO ₄ – chemical control	162a	188a	214a	241a	42a	42b	54a	55b	29a	68b	69b	135c	306b	668b	1004b	1363b	10a	10a	10a	11a
Kimberlite + bacteria + S ⁰	161a	173a	213a	214b	42a	54a	55a	69a	106b	375a	521a	452a	480a	1347a	2081a	2200a	10a	10a	10a	11a
Kimberlite + bacteria + Fe ²⁺	107b	120a	147b	147c	42a	54a	54a	68a	17c	17c	68b	174b	201c	373c	440c	466c	4c	4c	4c	5b
F Ratio	9.E+03	1.E+04	1.E+05	2.E+03	8.E+03	4.E+04	1.E+04	3.E+03	2.E+00	5.E+00	4.E+02	3.E+02	5.E+05	1.E+04	2.E+06	2.E+06	1.E+01	1.E+01	3.E+00	8.E+00
LSD	3.17	1.99	2.23	2.88	0.81	0.77	0.73	0.61	0.99	2.74	1.40	3.90	1.08	2.91	8.85	5.09	0.58	0.38	0.68	0.94
Victor Diamond Mine																				
Kimberlite + basal media – control	19c	19d	19c	19c	6b	18c	19d	19c	5a	5b	5b	5c	6d	6d	6d	19d	11b	11b	12a	12b
Kimberlite + H ₂ SO ₄ – chemical control	186a	226a	241a	262a	19a	19b	31b	32b	6a	6a	19a	19a	546b	640b	1010b	1876b	12a	12a	12a	12a
Kimberlite + bacteria + S ⁰	187a	215b	243a	252a	19a	93a	121a	123a	6a	6a	6b	19	653a	1987a	2388a	3002a	12a	12a	12a	12a
Kimberlite + bacteria + Fe ²⁺	160b	175c	206b	210b	6b	6d	6d	6d	6a	6ab	6b	14	226c	586c	653c	840c	12b	12b	12a	12b
F Ratio	9.E+03	1.E+04	1.E+05	2.E+03	8.E+03	4.E+04	1.E+04	3.E+03	2.E+00	5.E+00	4.E+02	3.E+02	5.E+05	1.E+04	2.E+06	2.E+06	1.E+01	1.E+01	3.E+00	8.E+00
LSD	3.26	3.68	11.62	11.47	0.34	0.80	1.76	3.92	1.16	0.74	1.24	1.55	1.68	1.00	2.53	3.44	0.54	0.49	1.08	0.46

* ICP values represented rounded off to the nearest whole number * Mean values from duplicate samples represented. Means with the same letter within a column for each kimberlite ore type are not significantly different (P=0.05). P < 0.0001

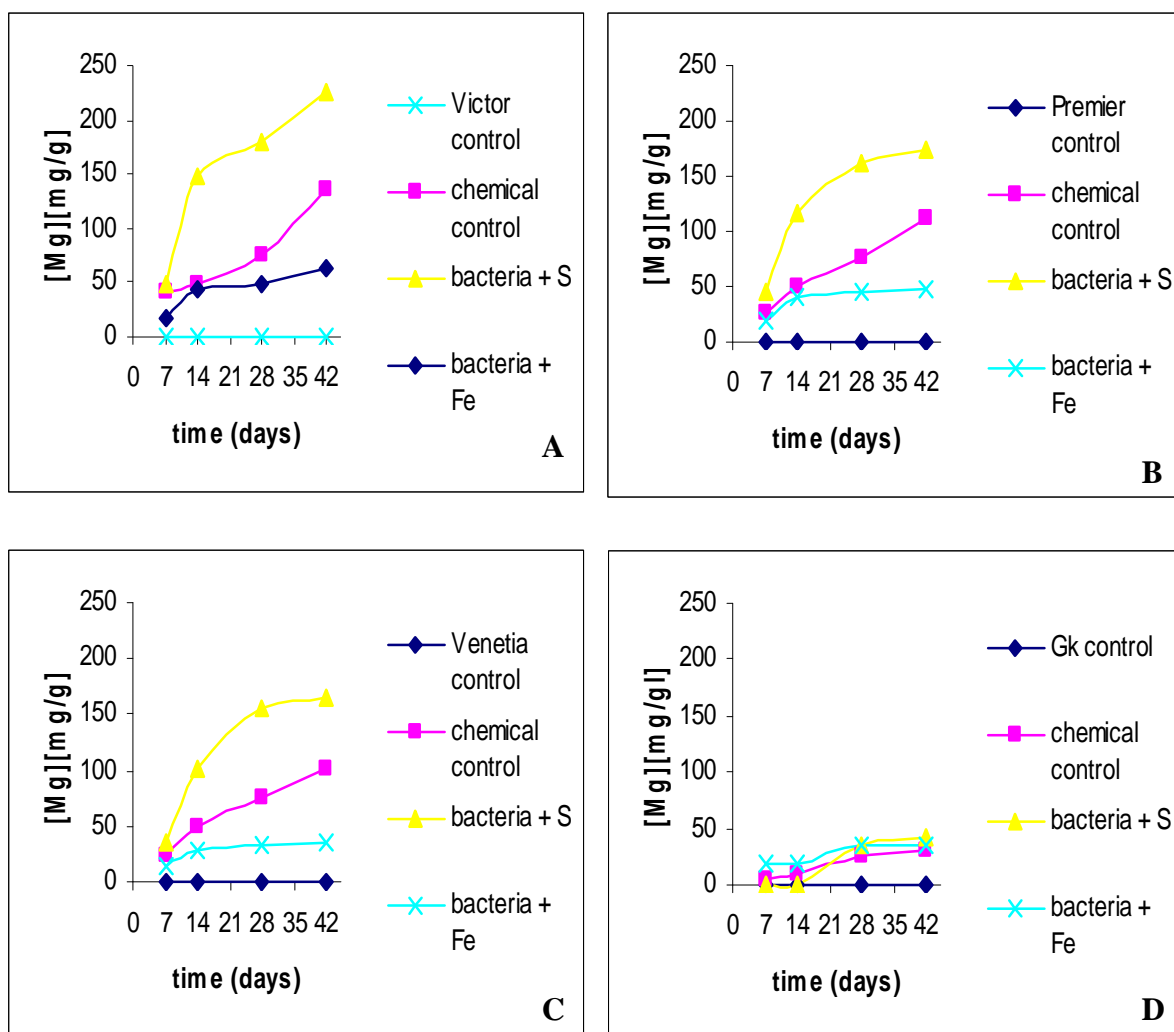


Figure 3.2 Magnesium ion dissolution trends of four kimberlite ores from different diamond mines subjected to various leaching treatments. (A, B, C, D represents the ICP results for the kimberlite sample from Victor, Premier, Venetia and Gahcho Kue diamond mine, respectively.)

Figure 3.2 represents the dissolution of Mg over a six week period. With the exception of the Gahcho Kue kimberlite sample, the ‘sulfur treatment’ achieved the best effect on the dissolution process and produced results that were significantly better than the positive chemical control (Figure 3.2 and Table 3.3). The graphs also illustrate that the chemical controls showed fairly consistent rates of solubilization over time whereas the sulfur and iron amendments showed rapid rate of mineralization early on followed by a ‘tailing off.’

The ‘iron treatment’ also had a positive influence on the dissolution process but to a lesser extent as indicated by the ICP results in Table 3.3 and Figure 3.2. It was further

shown that the kimberlite samples from different mines weathered at different rates (Figure 3.3).

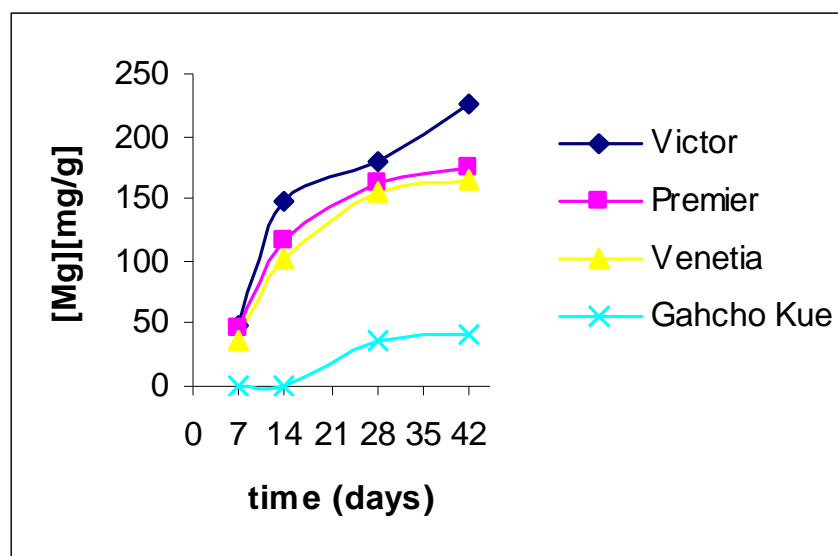


Figure 3.3 Magnesium ion dissolution trends illustrating the weathering susceptibility of the treated kimberlite samples from different diamond mines.
(Data was obtained from ICP analyses of the leachate solutions of the ‘sulfur treatment.’)

Figure 3.3 represents the leaching of Mg from different kimberlite samples subjected to treatment with chemolithotrophic bacteria and sulfur as the energy source (data plotted are represented values of ICP data recorded in Table 3.3). The graph was plotted to show that the dissolution rates and hence the weathering susceptibility of the different kimberlite samples varied. From Table 3.3 and Figure 3.3 the kimberlite sample from Victor mine seems to be the most susceptible to weathering followed by the kimberlite samples from Premier and Venetia mine. The kimberlite sample from Gahcho Kue mine seems to be the most resistant to weathering.

A similar trend was also seen in the solubilization of Ca and Si. Again, it must be noted that iron dissolution varied in treatments and kimberlite sample types, no set trend was observed. Similar susceptibilities of kimberlite weathering were observed in the ‘iron treatment.’

3.3.1.2 XRD results

XRD analyses showed the mineralogical structure and the changes thereof of the treated kimberlite samples (Figures 3.4-3.7). XRD results showing mineral composition for the different kimberlite ores are shown in Table 2.1. After the six week period, no changes were seen in the negative controls of all kimberlite ore types. Overall, differences with respect to changes in the mineralogical structure between all ore types were evident for each of the treatments tested, including the chemical controls. Alteration to major mineral components was evidenced by changes to their assigned peak spectra in the XRD diffractograms. Additional peaks were also evident. These additional peaks represented the formation of gypsum ($\text{CaSO}_4 \cdot 2\text{H}_2\text{O}$), which was evident in all treatments and jarosite, ($\text{KFe}^{3+}_3(\text{OH})_6(\text{SO}_4)_2$), which was mostly observed in all the kimberlite samples treated with Fe^{2+} . Minor jarosite peaks were also evident in some of the other treatments (Figures 3.4 C and 3.7 C).

It must be noted that only peaks where changes were seen were labelled. Repeated peaks for the major minerals were not labelled in the XRD diffractograms, therefore the unlabelled peaks represent mostly the reoccurring peaks of the major minerals. The peaks for the minor minerals were also not labelled.

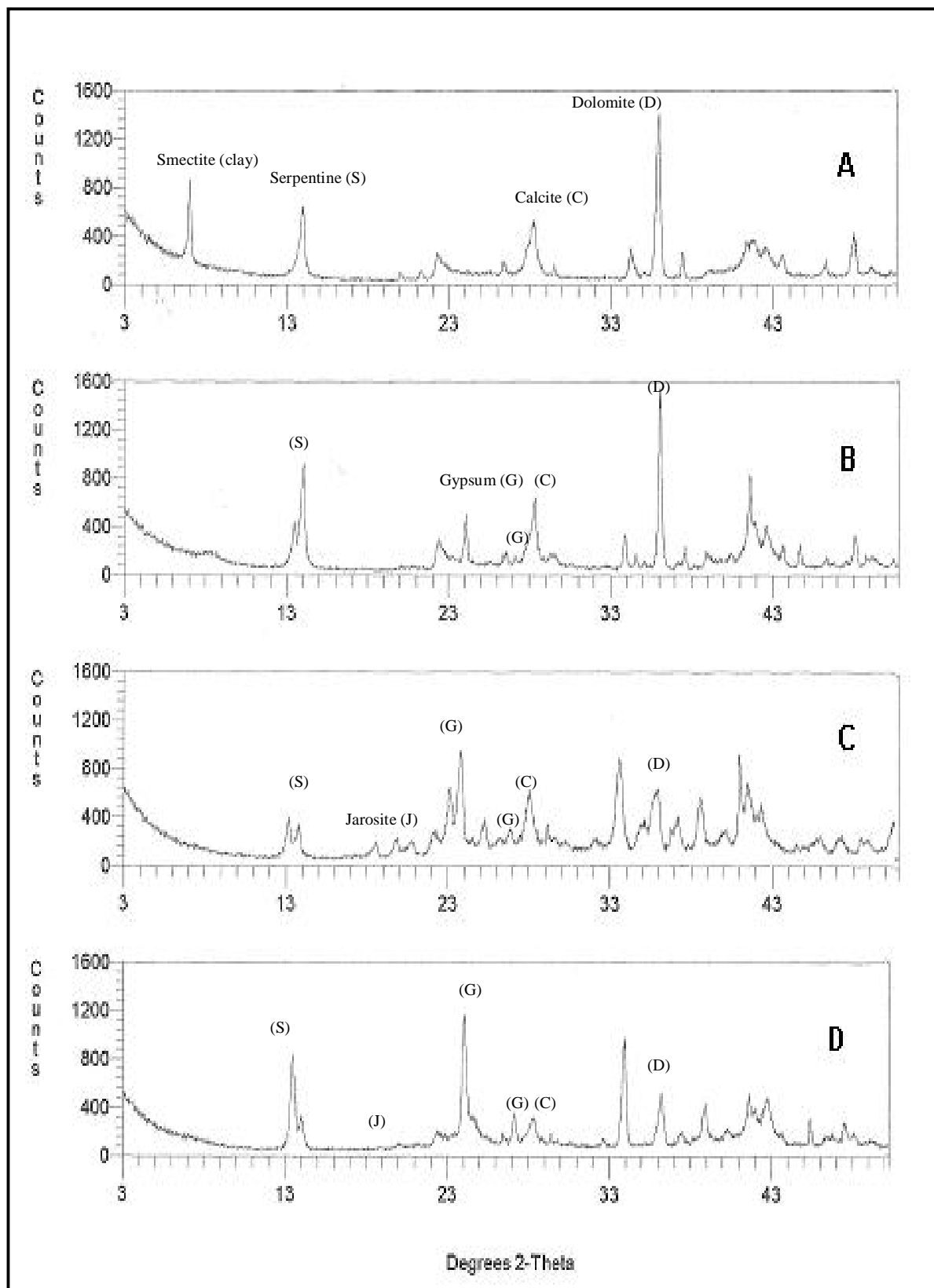


Figure 3.4 XRD analyses of kimberlite from Victor mine that was subjected to various leaching treatments. [A (negative control), B (positive chemical control), C (chemolithotrophic bacteria in the presence of 1% (w/v) S^0), D (chemolithotrophic bacteria in the presence of 10% (w/v) Fe^{2+})].

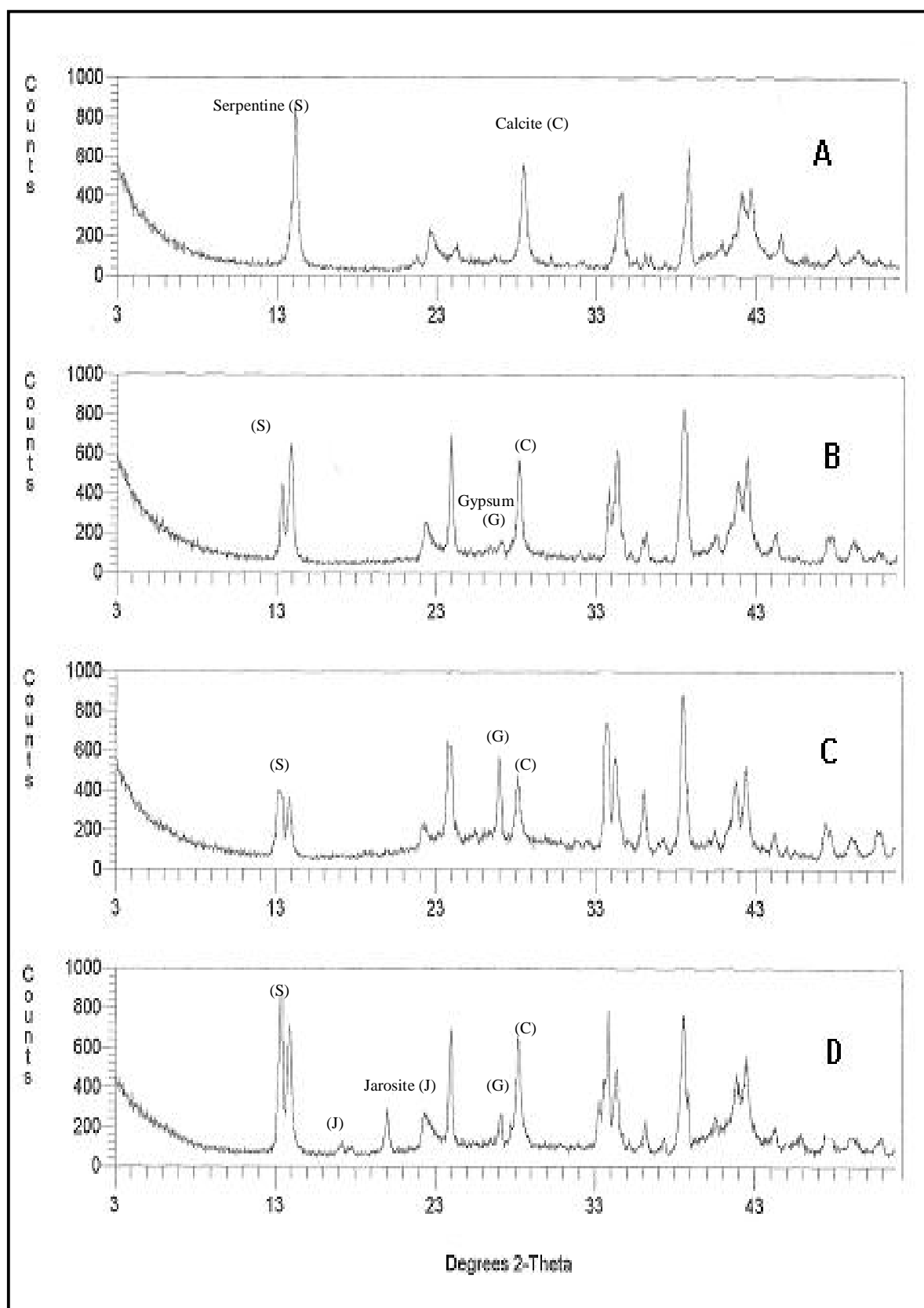


Figure 3.5 XRD analyses of kimberlite from Premier mine that was subjected to various leaching treatments. [A (negative control), B (positive chemical control), C (chemolithotrophic bacteria in the presence of 1% (w/v) S⁰), D (chemolithotrophic bacteria in the presence of 10% (w/v) Fe²⁺)].

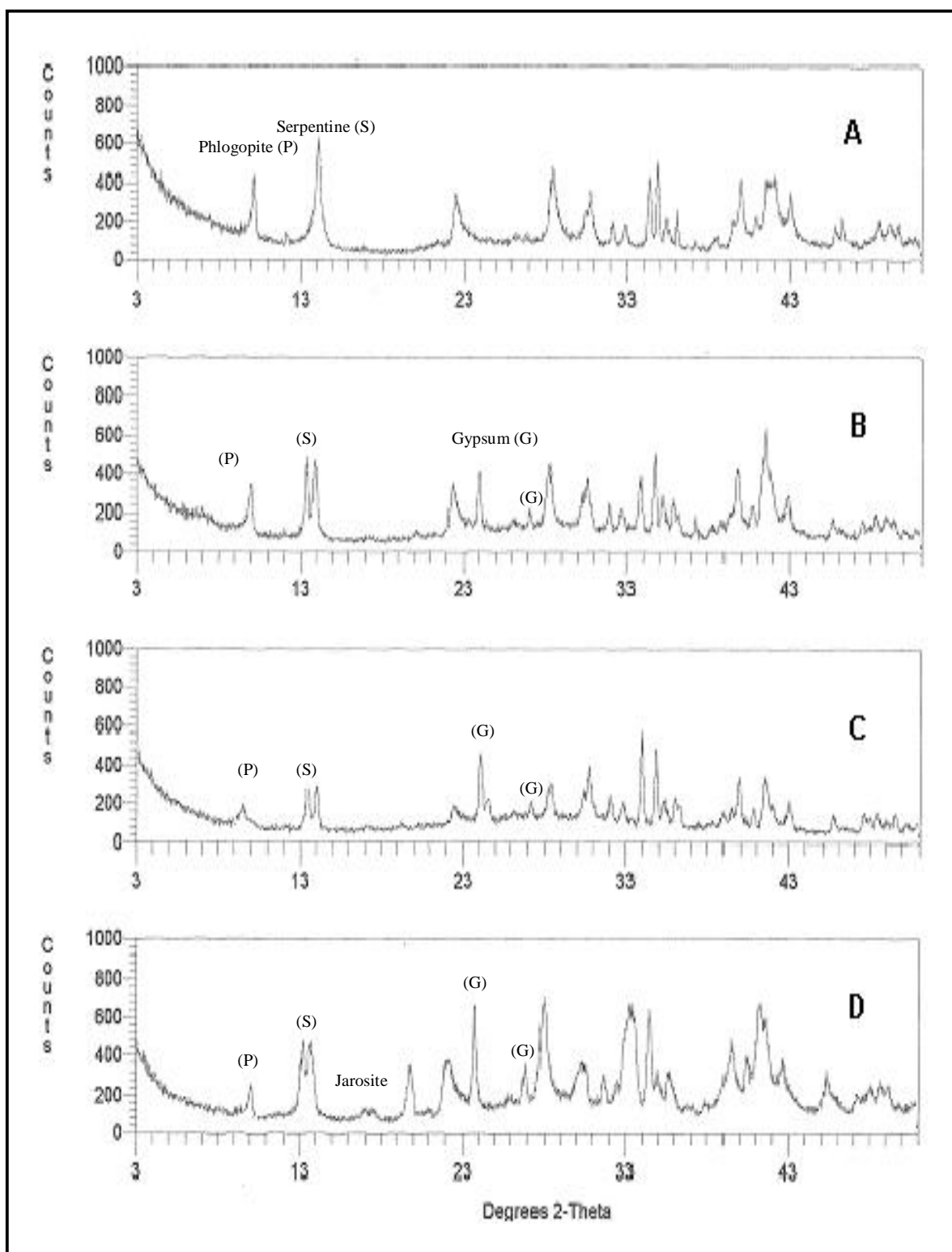


Figure 3.6 XRD analyses of kimberlite from Venetia mine that was subjected to various leaching treatments. [A (negative control), B (positive chemical control), C (chemolithotrophic bacteria in the presence of 1% (w/v) S⁰), D (chemolithotrophic bacteria in the presence of 10% (w/v) Fe²⁺)].

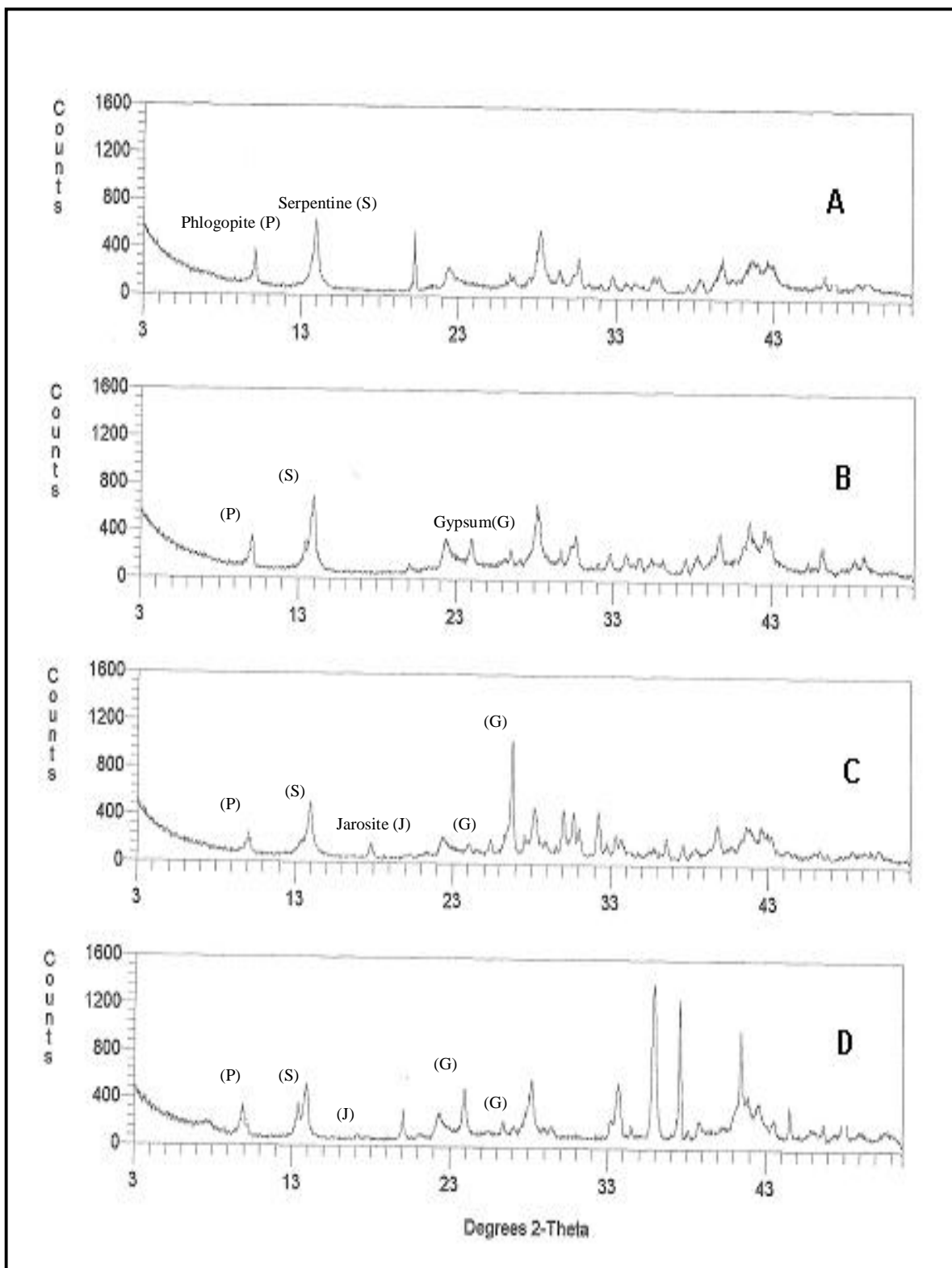


Figure 3.7 XRD analyses of kimberlite from Gahcho Kue mine that was subjected to various leaching treatments. [A (negative control), B (positive chemical control), C (chemolithotrophic bacteria in the presence of 1% (w/v) S^0), D (chemolithotrophic bacteria in the presence of 10% (w/v) Fe^{2+})].

The XRD analyses of kimberlite from Victor mine (Figure 3.4) showed that the peak for smectite completely disappeared after each treatment, indicating its complete dissolution. Changes in mineralogical structure of other mineral components, namely, serpentine, calcite and dolomite were also evident.

Figure 3.5 showed the XRD analyses of kimberlite from Premier, which illustrated alterations to the serpentine and calcite peaks indicating that partial dissolution of these minerals had occurred. The treated kimberlite samples from Venetia and Gahcho Kue mine exhibited mineralogical structural changes in phlogopite and serpentine as displayed in their XRD analyses represented in Figures 3.6 and 3.7 respectively.

It was also noted that although both ‘sulfur’ and ‘iron’ treatments cause changes to the mineralogical structures of the treated kimberlites, the ‘sulfur’ treatment resulted in more pronounced changes. In some cases, the changes observed were more marked in the bacterial treatments than in the chemical treatments.

3.3.2 Selective enrichment of microbial communities from naturally weathered kimberlite and investigating their role and efficiency in the mineralization of kimberlite

Gram stains, pH and redox monitoring all illustrated that microbial populations were successfully enriched from naturally weathered kimberlite in all treatments described in Section 3.2.2.2.

3.3.2.1 ICP results

The ICP analyses of the leach solutions from weathering tests using enriched bacteria illustrated the solubility of Mg, Ca, Si, Fe and K (Table 3.4). The results indicated that the enriched cultures performed very similarly to the ‘control cultures.’ Again it was observed that Mg had the highest solubilized concentration followed by Ca and that the ‘sulfur’ treatment produced more pronounced cation dissolution. It was also seen in Table 3.4 and Figure 3.8 that the dissolution rates of each treatment using the enriched cultures for each kimberlite sample were very similar to their respective positive controls.

Table 3.4 ICP analyses of different kimberlite samples (particle size < 100mm) treated with enriched microbial cultures from naturally weathered kimberlite. (Sulfur or ferrous iron was used as the energy source for the cultures. Known mesophilic chemolithotrophic cultures were used as controls in leaching experiments. All treatment flasks were incubated at 30°C in a shake incubator set at 120rpm for 6 weeks.)*

Sample	[Ca][mg/l]				[Si][mg/l]				[Fe][mg/l]				[Mg][mg/l]				[K][mg/l]			
	Day 7	Day 14	Day 28	Day 42	Day 7	Day 14	Day 28	Day 42	Day 7	Day 14	Day 28	Day 42	Day 7	Day 14	Day 28	Day 42	Day 7	Day 14	Day 28	Day 42
Premier Diamond Mine																				
Kimberlite + basal media - control	14d	15d	15d	15d	8b	8c	8d	8c	4d	4c	4e	4e	4e	4e	4e	5e	4d	8c	8c	8c
Kimberlite + 'Mintek' culture + S ⁰ - control	106a	133a	159a	201a	39a	52a	53a	54a	9c	9d	41c	79c	227a	361a	1508a	2266a	8a	9a	9a	9a
Kimberlite + Enriched culture + S ⁰	106a	125b	136b	159b	8b	26b	40b	40b	4d	4c	8d	40d	173b	257b	1322b	1572b	8b	8b	8b	8b
Kimberlite + 'Mintek' culture + Fe ²⁺ - control	80b	121c	131c	147c	8c	8c	8d	40b	27b	106b	267b	333b	146d	213d	388c	401d	4c	4d	4d	4d
Kimberlite + Enriched culture + Fe ²⁺	67c	122c	133c	147c	5c	25b	25c	53a	161a	241a	333a	466a	167c	240c	333d	466c	4d	8b	8c	8c
F Ratio	1.E+04	6.E+04	3.E+03	2.E+04	9.E+04	1.E+03	2.E+03	4.E+03	6.E+04	2.E+05	1.E+05	2.E+05	4.E+04	5.E+04	5.E+05	5.E+06	1.E+03	1.E+03	3.E+02	2.E+02
P value	<1.E-04	<1.E-04	<1.E-04	<1.E-04	<1.E-04	<1.E-04	<1.E-04	<1.E-04	<1.E-04	<1.E-04	<1.E-04	<1.E-04	<1.E-04	<1.E-04	<1.E-04	<1.E-04	<1.E-04	<1.E-04	<1.E-04	<1.E-04
LSD	1.17	2.25	3.87	1.94	0.56	1.74	1.72	1.09	1.02	0.95	1.50	1.69	1.43	2.13	3.42	1.54	0.23	0.20	0.39	0.43
Venetia Diamond Mine																				
Kimberlite + basal media - control	16d	16d	16c	17d	9a	9b	9b	9d	3c	4d	4e	4e	5d	5d	27e	20e	4c	4c	4d	4d
Kimberlite + 'Mintek' culture + S ⁰ - control	134a	171a	213a	227b	5c	5c	10b	41b	5c	29c	54c	58c	308a	646a	1551a	2388a	9a	9a	9a	9a
Kimberlite + Enriched culture + S ⁰	131b	172a	219a	254a	5b	9a	29a	55a	5c	5d	9d	45d	216b	598b	126b	2043b	9a	9a	9a	9ab
Kimberlite + 'Mintek' culture + Fe ²⁺ - control	121c	133c	147b	174c	5d	9a	9b	26c	56a	94a	123a	337a	206c	251c	489c	656c	4b	4b	4c	5c
Kimberlite + Enriched culture + Fe ²⁺	133ab	146b	160b	173c	4e	9ab	9b	26c	42b	57b	82b	122b	201c	243c	398d	545d	4bc	4b	9b	9b
F Ratio	3.E+03	2.E+03	2.E+04	2.E+04	2.E+03	3.E+02	4.E+02	3.E+02	8.E+02	3.E+03	4.E+03	8.E+03	3.E+03	8.E+03	8.E+04	6.E+04	5.E+02	4.E+02	6.E+02	4.E+02
P value	<1.E-04	<1.E-04	<1.E-04	<1.E-04	<1.E-04	<1.E-04	<1.E-04	<1.E-04	<1.E-04	<1.E-04	<1.E-04	<1.E-04	<1.E-04	<1.E-04	<1.E-04	<1.E-04	<1.E-04	<1.E-04	<1.E-04	<1.E-04
LSD	3.28	4.85	22.45	2.54	0.17	0.40	1.56	3.46	3.28	2.43	2.82	5.28	7.87	11.29	8.38	15.50	0.44	0.48	0.39	0.48

* ICP values represented rounded off to the nearest whole number * Mean values from duplicate samples represented. Means with the same letter within a column for each kimberlite ore type are not significantly different (P=0.05).

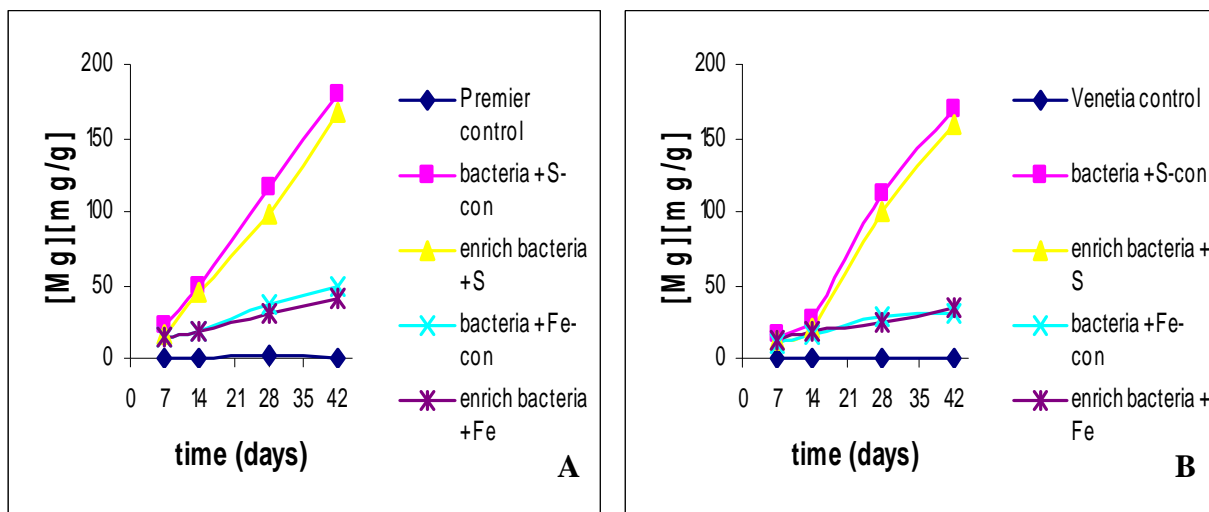


Figure 3.8 Magnesium ion dissolution trends illustrating the efficiency of enriched microbial populations from naturally weathered kimberlite in the weathering of two kimberlite ores. (A, B represents the ICP results for the kimberlite sample from Premier and Venetia diamond mine, respectively.)

Figure 3.8 represents the dissolution of Mg over the six week treatment time (data plotted are represented values of ICP data recorded in Table 3.4) showing that the ‘sulfur treatment’ in which the enriched culture was used produced similar results to the ‘sulfur treatment’ in which the known ‘*Mintek* culture’ was used. Again it was observed that the ‘sulfur treatment’ produced superior results than the ‘iron treatment.’

3.3.2.2 XRD results

XRD analyses showed that the enriched cultures used in the treatments produced similar results to the treatments in which the known mesophilic cultures were used. Typical results as indicated in Figure 3.9 and 3.10 demonstrated the breakdown of most of the major mineral peaks such as phlogopite and serpentine as described in Section 3.3.1.2. The formation of gypsum and jarosite was also evident in the XRD spectra of the treated kimberlite samples.

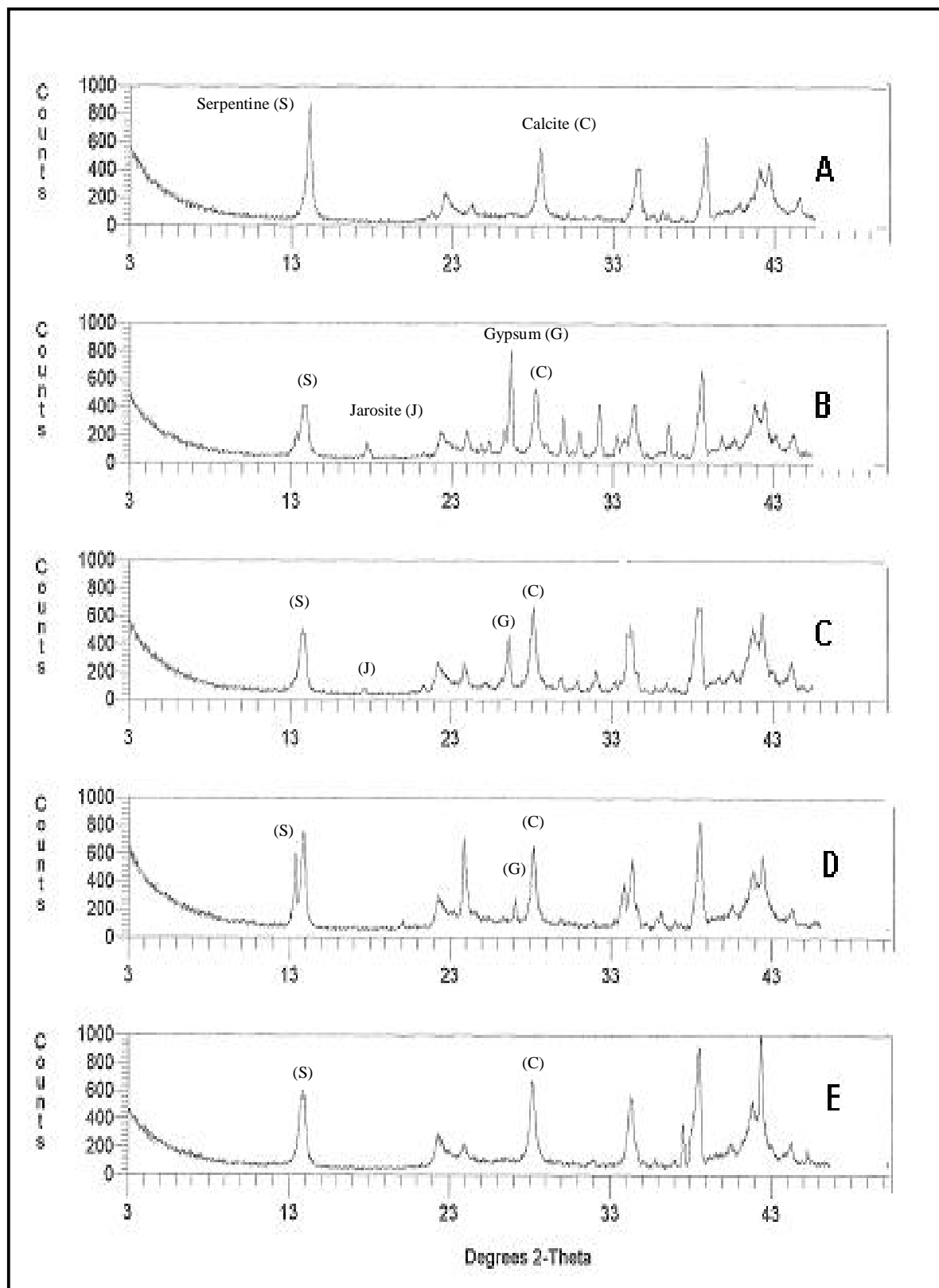


Figure 3.9 XRD analyses of kimberlite from Premier mine that was subjected to leaching treatments with enriched microbial cultures from naturally weathered kimberlite. [A (negative control), B (positive control-known mesophilic chemolithotrophic culture + S^0), C (enriched chemolithotrophic culture + 1% (w/v) S^0), D (positive control-known mesophilic chemolithotrophic culture + Fe^{2+}), E (enriched chemolithotrophic culture + 10% (w/v) Fe^{2+})].

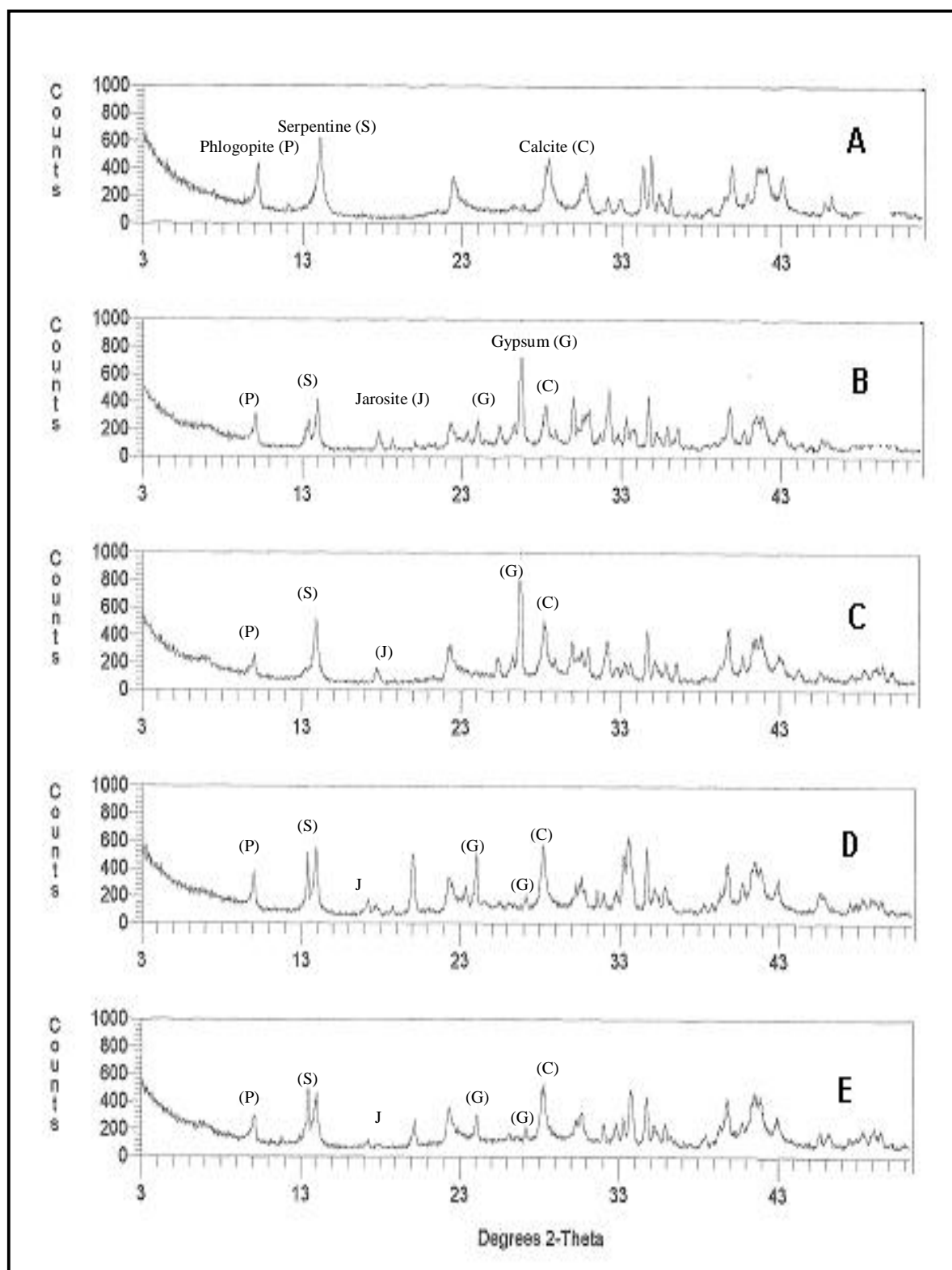


Figure 3.10 XRD analyses of kimberlite from Venetia mine that was subjected to leaching treatments with enriched microbial cultures from naturally weathered kimberlite. [A (negative control), B (positive control-known mesophilic chemolithotrophic culture + S^0), C (enriched chemolithotrophic culture + 1% (w/v) S^0), D (positive control-known mesophilic chemolithotrophic culture + Fe^{2+}), E (enriched chemolithotrophic culture + 10% (w/v) Fe^{2+})].

3.4 Discussion

A combination of pH, ICP and XRD data yielded promising results in the preliminary investigation of kimberlite weathering indicating that kimberlite is susceptible to accelerated mineralization and weathering processes in the presence of acidophilic chemolithotrophic microorganisms. The mineralization process is believed to be a result of an oxidative/proton attack brought about by the microbial production of sulfuric acid and ferric iron.

ICP data in Tables 3.3 and 3.4 showed that cations Mg, Fe and Ca and to a lesser extent, K and Si were solubilized over time indicating that mineral dissolution had occurred. This was further emphasized by the XRD data (Figures 3.4 -3.7 and Figures 3.9-3.10) in which the disappearance and alteration of some of the kimberlite minerals were observed. A similar investigation undertaken by Gericke *et al.* (2007) yielded results consistent with the findings in this investigation.

Tables 3.3 and 3.4 also showed that Mg was the predominant cation that leached into solution followed by Ca over the course of the experiment. Similar observations were made by Platonova *et al.* (1989) who performed experiments on kimberlite using the chemolithotrophic bacterium *Acidithiobacillus thiooxidans*. They reported that Mg leached most intensely into solution followed by Ca and then Si. They deduced that the active removal of Mg from kimberlite was an indication of the mineralization of serpentine. Further experiments performed by Platonova *et al.* (1994) on kimberlite ores consisting primarily of the minerals saponite and serpentine indicated that Mg and Ca passed into solution at different rates and amounts depending on the mineralogical structure of kimberlite. Thus, the leaching of Mg and Ca in comparatively higher amounts was therefore attributed to the breakdown of minerals such as smectite, serpentine, phlogophite, dolomite and calcite which are rich in Mg and Ca. The XRD results also supported this deduction.

From the ICP data, it was observed that as time passed, solubilization of the cations in the ‘sulfur’ and ‘iron’ treatment reached more or less constant levels. This phenomena could be due to the solubilization of the more easily silicate minerals (causing the increase in dissolution rates) leaving only the more resistant silicate minerals that leach more slowly and causing the curve in the graph to ‘flatten’ because of the

significantly reduced mineral dissolution. Another possible reason for the weathering rates decreasing could be because of the release of ions and cations or the formation of secondary minerals that inhibit mineral dissolution (Welch and Banfield, 2002). Alternatively, it could be attributed to a pH effect where a slight increase in pH inhibits the dissolution of certain minerals. The increase in pH is usually brought about by the release of elemental species into solution and their precipitation in solution, which sometimes may act as buffering agents. An example of this is the precipitation of Ca into gypsum, which has strong pH buffering abilities. Also, in the case of Fe dissolution, the lack of Fe during the initial stages of the leaching treatments was probably due to iron precipitation at high pHs. As the pH drops, iron precipitation decreases but because the pH did not decrease as far as 1.6, some Fe would have still precipitated.

The XRD results for the Victor kimberlite showed that smectite (clay) disappeared from each of the chemical and biological treatments after 6 weeks indicating that this mineral had the highest susceptibility to the mineralization processes. Dissolution of clay minerals alters their interlayer spacing cations. The interlayer spaces of clay minerals such as smectite are occupied by exchangeable cations such as Ca, K, Na, etc., which usually replace Mg ions that are removed during the dissolution process (the high concentration of Mg in solution could also be indicative of this) (Platonova *et al.*, 1989). The changing of the interlayer cation spacing and properties in clays play a significant role in the swelling mechanism of the clays present in kimberlite. This swelling mechanism of clays increases the rate of kimberlite weathering. A complete dissolution of the clay minerals in kimberlite is not required but rather an adequate change in the interlayer and interlayer spacing cation exchange properties is needed to weaken the kimberlite structure sufficiently to accelerate the weathering process (Boshoff *et al.*, 2005; Gericke *et al.*, 2007).

The presence of Mg, Ca, Si, K and Fe in solution could also be an indication that interlayer cation exchange is occurring in other minerals and these cations are possibly being replaced by H⁺ ions (Jonckbloedt, 1998). This would denote that the dissolution process is also occurring via proton attack of the mineral structure with the chemolithotrophic organisms acting as mediators and catalysts.

Dissolution of the cations and minerals permitted for the formation of secondary minerals jarosite ($\text{KFe}^{3+}_3(\text{OH})_6(\text{SO}_4)_2$) and gypsum (CaSO_4). The presence of gypsum as a new mineral in the treated kimberlite samples and in some cases the presence of jarosite, which arises from the precipitation of ferric iron during the oxidation of ferrous to ferric iron, indicates that weathering of kimberlite is occurring as these are common by-products of kimberlite and mineral weathering (Gericke *et al.*, 2007; Hakkou *et al.*, 2008). However, in the case of the ‘iron treatments’, ferrous iron was added to the leaching treatments, which was oxidised by the microorganisms to ferric iron, thus providing another source for jarosite production.

The ICP and XRD analyses showed that the weakening and the degree of transformation of the different kimberlite samples varied. Certain silicate minerals weather at different rates depending on the mineral internal bonding structure. For example, olivine is the fastest weathering silicate mineral because the SiO_4 tetrahedra structure is interconnected by weak Si-O-Si bonds (Jonckbloedt, 1998). Also according to the ‘Goldich Weathering Sequence,’ the most unstable silicate mineral will weather first, with more resistant silicates taking longer to dissolve (Bennett *et al.*, 2001). Therefore, the rate of weathering and the degree of weakening and transformation of the kimberlite structure depends on the mineralogy of the different kimberlite samples. From the results represented overall, the kimberlite sample from Victor mine was the most susceptible to weathering. The kimberlite sample from Victor mine had a high proportion of smectite (swelling clays). According to Boshoff *et al.* (2005), the weathering of kimberlite containing high levels of swelling clays can be greatly accelerated in the presence of cations. The rate of cation exchange also affects weathering (Boshoff *et al.*, 2005). Mica and serpentine minerals are much more resistant to weathering and therefore this would explain why the Venetia and Gahcho Kue kimberlite samples were more resistant to weathering since they had a combination of mica (phlogophite) and serpentine minerals as a major component of their mineralogical structure (Table 2.1).

Both the XRD and ICP results illustrated that although both energy sources used in the biological treatments positively influenced the dissolution process, sulfur produced superior results. During the dissolution process, the chemolithotrophs continually oxidized S^0 to sulfuric acid thus lowering the pH of the basal medium

(Equation 5). Dissolution increases with decreasing pH (Wilson, 2004), therefore because acid is continually being produced in the ‘sulfur treatment’ the dissolution rates are relatively higher than the ‘iron treatment.’ In Figure 3.1, it was seen that initially that the pH increased significantly, indicating silicate leaching, and then decreased for both energy sources used in the leaching treatments. This was possibly due to the cation dissolution of silicate minerals and their buffering effect, which caused the pH to increase initially, however, the oxidation of sulfur to sulfuric acid (mediated by the microorganisms) and/or the formation of jarosite, thereafter, decreased the pH (Dopson *et al.*, 2009). In the ‘iron’ treatment, the chemolithotrophs oxidized Fe^{2+} (ferrous sulphate) to Fe^{3+} (ferric sulfate) (Equation 6), which is a strong oxidizing agent. Although the ferric iron produced by the microorganisms produces an oxidative attack of the silicate minerals, it does however, increase the pH. The subsequent jarosite precipitation from ferric iron lowers the pH. In comparison to the ‘sulfur treatment’ the pH drop is not that much to make conditions more favourable for the growth of the bacteria or to cause the silicate minerals to become more unstable. It has been observed that over the 6 week period the pH drop is comparatively slower than the ‘sulfur’ treatment and lies in the pH range of 3.2 -5.7. Ivanov and Karavaiko (2004) stated that sulfuric acid does not cause significant changes in kimberlite silicate minerals in the pH range of 3.0-6.0 due to most silicate minerals being relatively stable at this pH range. In the ‘sulfur treatment’ the pH varied in the range of 1.5-2.0, which resulted in the silicate minerals being more unstable and susceptible to weathering. Even more encouraging was that the results from the ‘sulfur’ treatment were even superior to the chemical control, as the bacteria counteracted the buffering effect of the solubilized cations by continually producing sulfuric acid whereas the pH of the chemical control was altered and reduced during monitoring periods.

Microbial populations were successfully enriched from naturally weathered kimberlite and used for the treatment of kimberlite ores under parallel conditions as in the preliminary investigation. Similar results were observed as described in the preliminary investigation suggesting that the microbes involved are possibly analogous to the known mesophilic cultures (Section 3.2.1.2). However, this needs to be confirmed by further identification tests using molecular techniques such as

denaturing gradient gel electrophoresis (DGGE), analyses of the 16S rRNA genes and DNA sequencing and investigation of physiological traits (Okibe *et al.*, 2003).

Overall, the results presented here have shown that the sulfuric acid and ferric iron generated by the chemolithotrophic microorganisms were successful in transforming and weakening of the kimberlite ores under study. Whilst, the extent of transformation and weakening depends on the internal mineralogical structure of the kimberlite ores, it can be positively concluded that there is potential use of chemolithotrophic bacteria in accelerating the weathering and weakening of kimberlite ores. These results are consistent with prior studies of kimberlite weathering that suggested '*bacterial leaching of kimberlites may find practical use in the enrichment of diamond-bearing concentrates (<1mm) through dissolution of the main minerals of the rock*' (Platonova *et al.*, 1994). However, further test work and optimization studies will be required before this technology can be successfully implemented and applied on a larger technological scale.

CHAPTER 4

Optimization studies to determine the influence of particle size and energy source concentration on the biotransformation of kimberlite ores

4.1 Introduction

Microbial leaching processes have been successfully applied industrially to aid in recovering metals and minerals from ores and residues of conventional mining. However, the profitability and effectiveness of these processes depends essentially on the chemical and mineralogical characteristics of the ore to be leached and the activity of the microorganisms involved (Bosecker, 1989). Optimum bioleaching and accelerated bioweathering can only be achieved when optimum growth conditions of the microorganisms are met (Bosecker, 1989). Therefore, before applying microbial leaching processes on a large technical scale, it is important to assess if the material is suitable for microbial leaching. This is usually followed by laboratory based investigations to optimize leaching conditions (Bosecker, 1989). It has already been established in the preliminary investigations (Chapter 3) that kimberlite ores of fine particle size ($<100\mu\text{m}$) are prone to weathering to an extent where the mineralogy of the ores is altered and weakened in the presence of chemolithotrophic microorganisms. Thereby, giving rise to the possibility of applying heap/dump-leaching technology for the microbial treatment of kimberlite ores. Consequently, this chapter further investigated the effects of chemolithotrophic leaching on larger particle sizes of kimberlite to determine if a similar weathering effect could be achieved. Other parameters such as energy source concentration and time were varied and also investigated to optimize microbial growth and, hence microbial leaching and weathering.

4.2 Experimental Procedure

4.2.1 Evaluation of the effect of kimberlite particle size on biotransformation by a known chemolithotrophic bioleach consortia

4.2.1.1 Kimberlite

Two kimberlite samples from Victor and Gahcho Kue diamond mines were used (2.1). Two particle sizes of each kimberlite sample were used. These samples were crushed and sieved to a particle size of less than 5mm and greater than 2mm ($>2\text{mm}<5\text{mm}$) and less than a $100\mu\text{m}$ ($<100\mu\text{m}$) for a series of shake flasks weathering tests.

4.2.1.2 Microorganisms

The microorganisms used were a mixed mesophilic culture consisting of *A. caldus*, *L. ferrooxidans* and *Sulfobacillus sp.* (Section 2.2.1). Culturing, maintenance and storage of microorganisms were described in Section 2.3.1.

4.2.1.3 Shake flask weathering tests

Each set of the different particle size of the two kimberlite samples were subjected to same leaching experimental treatments and chemical and mineralogical analyses as described in Section 3.2.1.3 of Chapter 3.

4.2.2 Influence of energy source concentration on the biotransformation of kimberlite ores by chemolithotrophic bioleach cultures

4.2.2.1 Kimberlite

Two kimberlite samples, namely from Premier and Venetia diamond mines, were used (Section 2.1). These samples were crushed to a particle size of less than a $100\mu\text{m}$ and then subjected to shake flasks weathering tests.

4.2.2.2 Microorganisms

The microorganisms used were a mixed mesophilic culture consisting of *A. caldus*, *L. ferrooxidans* and *Sulfobacillus sp.* (Section 2.2.1). Culturing, maintenance and storage of microorganisms were described in Section 2.3.1.

4.2.2.3 Energy Sources

The two energy sources used were elemental sulfur (S^0) and ferrous iron (Fe^{2+}) (obtained from $FeSO_4$). A set of different concentrations of each energy source was used and evaluated to determine its affect on kimberlite mineralization. The amounts used for each energy source is as follows:

1. S^0 : 0.75g (20% w/w); 0.38g (10% w/w); 0.19g (5% w/w); 0.1g (2.5% w/w)
2. Fe^{2+} : 1.30g (35% w/w); 0.65g (18% w/w); 0.33g (9% w/w); 0.17g (4.5% w/w)

The percentages recorded were calculated as energy source concentration with respect to the mass of kimberlite (w/w) used during the shake flask weathering tests.

4.2.2.4 Shake Flask weathering tests

Weathering tests and analyses for each kimberlite sample was carried out as described in Treatments 3 and 4 in 3.2.1.3 of Chapter 3 for each of the different concentrations of S^0 and Fe^{2+} (4.2.2.3) respectively.

4.2.3 Effect of longer treatment time on the biotransformation of kimberlite ores using chemolithotrophic bioleach cultures

4.2.3.1 Kimberlite

Two kimberlite samples, namely from Premier and Venetia Diamond Mines (Section 2.1), of particle size of less than a $100\mu m$ were used. These were subsequently subjected to shake flasks weathering tests.

4.2.3.2 Microorganisms

The microorganisms used were a mixed mesophilic culture consisting of *A. caldus*, *L. ferrooxidans* and *Sulfobacillus sp.* (Section 2.2.1). Culturing, maintenance and storage of microorganisms were described in Section 2.3.1.

4.2.3.4 Shake Flask weathering tests

The kimberlite samples were subjected to the same treatments and conditions as described in Section 3.2.1.3 except the incubation time was increased from 6 weeks to 8 weeks. Sample monitoring on leachate solutions were carried out on days 14, 28, 42 and 64. Similar chemical and mineralogical analyses were also made on the treated kimberlite samples.

4.2.3 Statistical analyses

Statistical analysis was carried out using SAS software (Version 6.12) (SAS, 1987). A general linear model (GLM) was used to run an analysis of variance (ANOVA) for ICP results derived from each set of kimberlite ore treatments. Separations of means was based on the principle of least significant difference (LSD) at $P < 0.05$.

4.3 Results

4.3.1 Evaluation of the effect of kimberlite particle size on biotransformation by a known chemolithotrophic bioleach consortia

Visually, the changes observed in the flasks were similar for both particle sizes of the kimberlite particles. Microbial growth and precipitate formation occurred as described in Section 3.3.1 of Chapter 3.

4.3.1.1 ICP results

ICP analyses over the six week treatment time illustrated that all cations investigated were solubilized and weathering via mineral dissolution of both kimberlite samples of both particle sizes had occurred (Table 4.1). Again it was shown in Table 4.1 that Mg was the major cation to solubilize followed by Ca and to a much lesser extent, Si. Negligible dissolution of Fe was only seen in the 'sulfur treatment' of both kimberlite types.

The ICP data in Table 4.1 also illustrated that the kimberlite sample from Victor mine was more prone to dissolution. The influence of particle size was also more apparent for the kimberlite sample from Victor mine. This was also seen in Figure 4.1 where the weathering rates of both particle sizes of kimberlite from Victor mine was higher than the kimberlite sample from Gahcho Kue mine.

It was also observed that the concentration of cations released during the shake flasks experiment were lower for the larger particle size when compared to the finely ground ore samples. Differences between the two particle sizes of the kimberlite sample from Gahcho Kue mine were less marked as seen in Figure 4.1.

Table 4.1 ICP analyses of treated kimberlite samples of different particle size (<100mm and >2mm<5mm) to determine the effect of microbial leaching treatments on larger kimberlite particles. (Mixed chemolithotrophic cultures were used in leaching experiments with sulfur or ferrous iron as the energy source. All treatment flasks were incubated at 30°C in a shake incubator (120rpm) for 6 weeks.)*

Sample	[Ca][mg/l]				[Si][mg/l]				[Fe][mg/l]				[Mg][mg/l]				[K][mg/l]			
	Day 7	Day 14	Day 28	Day 42	Day 7	Day 14	Day 28	Day 42	Day 7	Day 14	Day 28	Day 42	Day 7	Day 14	Day 28	Day 42	Day 7	Day 14	Day 28	Day 42
Gahcho Kue Diamond Mine (<100mm)																				
Kimberlite + basal media - control	11g	11e	12f	12f	6d	21c	22c	22c	3c	3d	3e	3e	5d	5f	11e	11g	6c	7d	7d	7e
Kimberlite + H ₂ SO ₄ – chemical control	67e	147b	174c	216a	8bc	24b	25b	27c	4b	4c	4dc	4de	50c	133d	333d	509a	8b	9b	9b	9b
Kimberlite + bacteria + S ⁰	133a	161a	202b	209c	8b	26b	26b	41b	13a	14b	14b	35a	6d	6f	483a	548a	6c	7d	9b	9cb
Kimberlite + bacteria + Fe ²⁺	92d	132c	147d	174d	7cd	8e	8e	23c	4bc	4dc	4de	12c	4d	240b	453b	484c	6c	7d	7d	8ed
Gahcho Kue Diamond Mine (>2mm<5mm)																				
Kimberlite + basal media - control	13g	13e	13f	13f	7cd	8e	8e	9d	3bc	4d	4de	4e	5d	5f	6f	7g	7c	7d	7cd	8cd
Kimberlite + H ₂ SO ₄ – chemical control	107c	162a	213a	223a	8b	14d	14d	28c	4bc	5c	5c	12c	6d	95e	388c	441d	13a	13a	14a	15a
Kimberlite + bacteria + S ⁰	121b	147b	176c	177d	28a	41a	57a	95a	13a	16a	16a	25b	227a	269a	389c	428e	14a	14a	15a	15a
Kimberlite + bacteria + Fe ²⁺	51f	109d	127e	161e	8b	8e	8e	13d	4bc	4cd	4d	12dc	217a	219c	335d	381f	7bc	8b	8bc	8cb
F Ratio	3.E+03	6.E+03	5.E+03	3.E+03	8.E+02	3.E+02	6.E+01	2.E+02	6.E+04	2.E+02	8.E+03	2.E+01	5.E+03	2.E+04	3.E+04	1.E+04	5.E+01	1.E+02	2.E+02	3.E+02
P value	<1.E-04	<1.E-04	<1.E-04	<1.E-04	<1.E-04	<1.E-04	<1.E-04	<1.E-04	<1.E-04	<1.E-04	<1.E-04	<1.E-04	<1.E-04	<1.E-04	<1.E-04	<1.E-04	<1.E-04	<1.E-04	<1.E-04	<1.E-04
LSD	1.71	2.25	3.80	5.04	0.86	2.11	1.36	6.38	1.02	1.09	0.77	7.51	4.74	4.56	3.76	6.07	0.23	0.93	0.85	0.61
Victor Diamond Mine (<100mm)																				
Kimberlite + basal media - control	18f	18g	19f	19f	7d	13d	13d	13e	5d	5b	5c	5a	10e	10f	10f	16g	10	10cd	10de	10c
Kimberlite + H ₂ SO ₄ – chemical control	188a	228a	243a	268a	13	13d	27c	28d	6bc	6b	12b	13b	548b	643b	1000c	1825c	10ab	11b	11dbc	11c
Kimberlite + bacteria + S ⁰	184a	216b	241a	254b	15b	93a	123a	124a	6d	6b	13b	13b	654a	1988a	2388a	3001a	11a	11b	11b	12b
Kimberlite + bacteria + Fe ²⁺	160b	173c	203b	214c	8dc	8e	9e	9f	5d	5b	6c	11b	227c	588c	652d	844d	10ab	10d	10de	11c
Victor Diamond Mine (>2mm<5mm)																				
Kimberlite + basal media - control	18f	18g	18f	19f	10c	10ed	10e	10f	6b	6b	6c	6c	9e	9f	9f	9f	9	9d	9e	11c
Kimberlite + H ₂ SO ₄ – chemical control	53d	81e	93d	160d	10c	27c	28c	40c	6b	7b	13b	14b	9e	10f	14f	14f	9b	13a	13a	14a
Kimberlite + bacteria + S ⁰	79c	136d	148c	161d	41a	52b	66b	107a	13a	27a	43a	202a	230c	268d	2265b	2335b	7c	10d	12b	13ab
Kimberlite + bacteria + Fe ²⁺	41e	56f	80e	107e	10c	10de	27c	27d	6b	6b	7c	7c	212d	216e	335e	377e	5	6e	6f	6d
F Ratio	2.E+03	4.E+03	6.E+03	1.E+04	3.E+02	6.E+02	1.E+03	3.E+03	9.E+01	1.E+02	9.E+02	7.E+03	7.E+04	2.E+05	1.E+05	5.E+06	2.E+01	3.E+01	4.E+01	5.E+01
P value	<1.E-04	<1.E-04	<1.E-04	<1.E-04	<1.E-04	<1.E-04	<1.E-04	<1.E-04	<1.E-04	<1.E-04	<1.E-04	<1.E-04	<1.E-04	<1.E-04	<1.E-04	<1.E-04	<1.E-04	<1.E-04	<1.E-04	<1.E-04
LSD	5.43	4.60	4.01	2.75	2.30	4.12	3.30	2.54	0.87	2.23	1.38	2.60	3.05	5.41	9.76	3.81	1.41	1.20	1.08	1.09

* ICP values represented rounded off to the nearest whole number * Mean values from duplicate samples represented. Means with the same letter within a column for each kimberlite ore type are not significantly different (P=0.05).

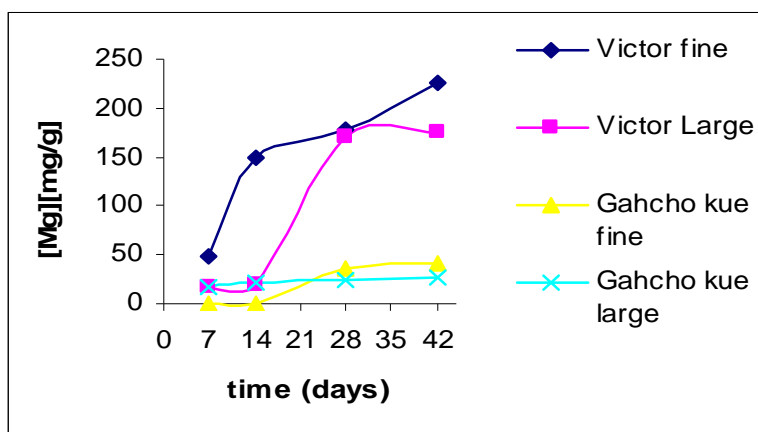


Figure 4.1 Influence of kimberlite ore particle size on magnesium ion dissolution trends. (The larger particles were in size range of >2mm<5mm whilst the finer particles were < 100mm. Data was obtained from ICP analyses of the leachate solutions of the ‘sulfur treatment’ (Table 4.1)).

Figure 4.1 represents the dissolution of Mg from the two kimberlite samples, each of different particle sizes were subjected to treatment with chemolithotrophic bacteria and sulfur as the energy source. The graph showed that the dissolution rates differed between the two particle sizes for each kimberlite sample. Initially, there was a delay in the onset of dissolution of the larger kimberlite particles from Victor mine when compared to its finer particles but thereafter dissolution occurs with the dissolution rates being slightly less than that of the finer particles. In the case of the kimberlite samples from Gahcho Kue mine, there seems to be very little variation in the amount of Mg released in solution. Again, it can be seen that the kimberlite sample from Victor mine is more susceptible to weathering than the kimberlite sample from Gahcho Kue mine. Similar trends were also observed for Ca and Si. Similar observations were made for the kimberlite samples subjected to the ‘iron treatment’ (Table 4.1).

4.3.1.2 XRD results

After the six week treatment period, the XRD analyses of both the treated kimberlite samples showed changes in their mineralogical structure when compared to their controls in Figures 4.2 and 4.3 A. The larger treated kimberlite sample from Victor mine showed the complete disappearance of clay mineral with minor breakdown of serpentine, calcite and dolomite (Figure 4.2). The larger particle kimberlite sample from Gahcho Kue mine only showed significant changes in the phlogopite and serpentine peaks (Figures 4.3 C and D). Additional XRD peaks were also seen on

both the treated kimberlite XRD spectra indicating the presence of jarosite and gypsum (Figure 4.2). XRD results for the fine particles of the kimberlite samples from Victor and Gahcho Kue mine were identical to Figures 3.3 and 3.6 of Chapter 3, respectively, therefore they are not represented here.

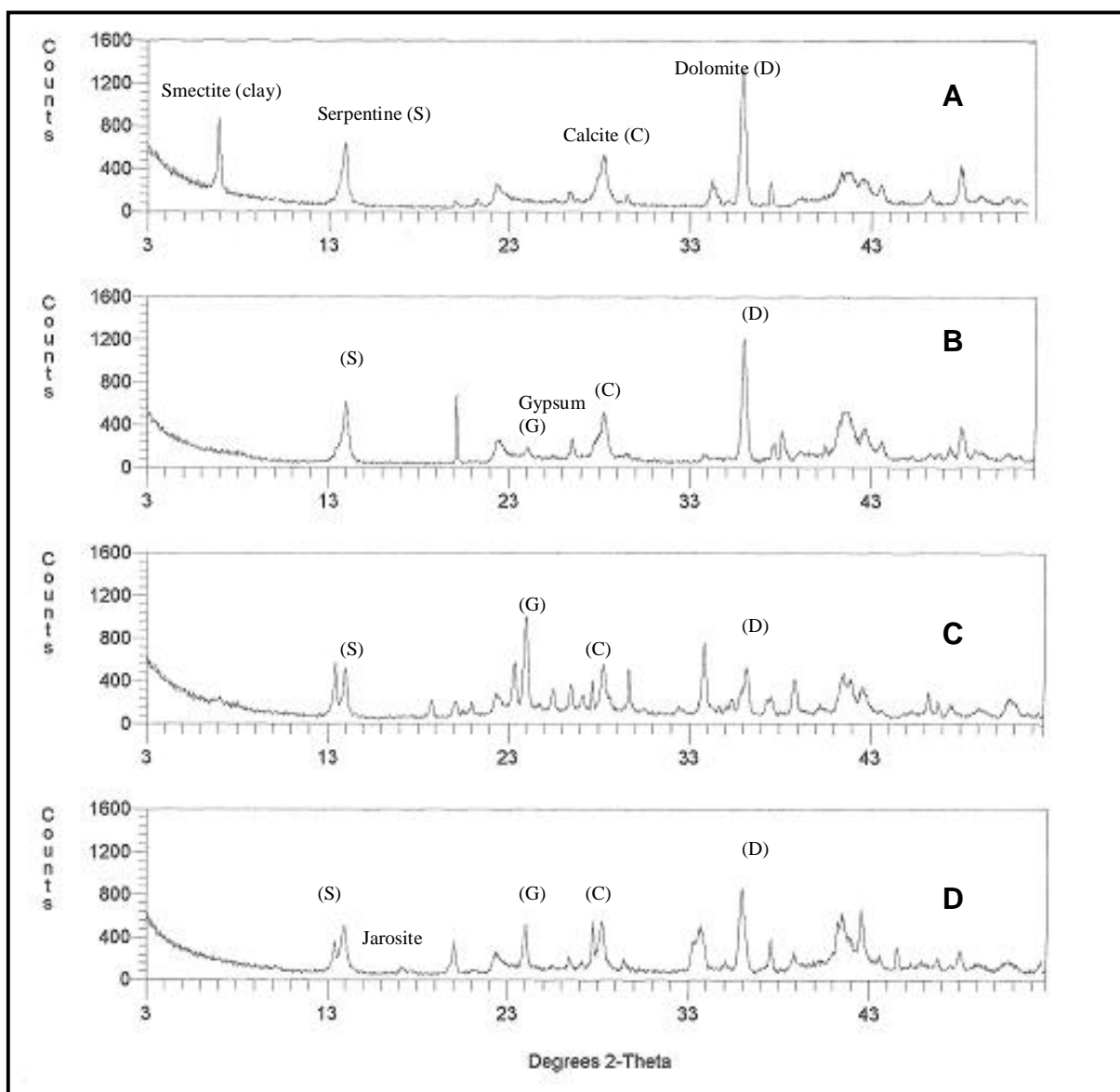


Figure 4.2 XRD analyses of kimberlite of particle size >2mm<5mm from Victor mine that was subjected to various leaching treatments. [A (negative control), B (positive chemical control), C (chemolithotrophic bacteria in the presence of 1% (w/v) S⁰), D (chemolithotrophic bacteria in the presence of 10% (w/v) Fe²⁺)].

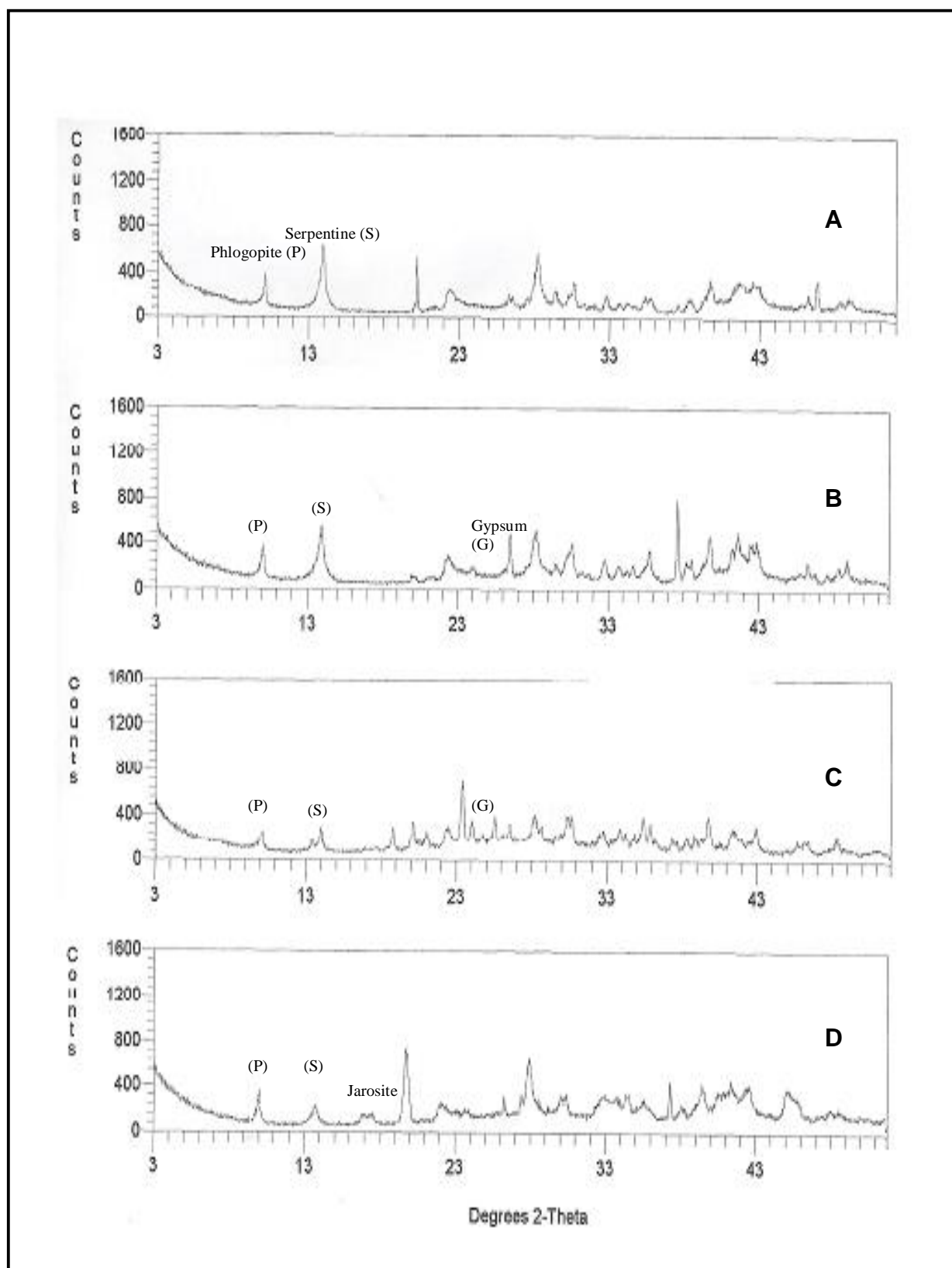


Figure 4.3 XRD analyses of kimberlite of particle size >2mm<5mm from Gahcho Kue mine that was subjected to various leaching treatments. [A (negative control), B (positive chemical control), C (chemolithotrophic bacteria in the presence of 1% (w/v) S⁰), D (chemolithotrophic bacteria in the presence of 10% (w/v) Fe²⁺)].

4.3.2 Influence of energy source concentration on the biotransformation of kimberlite ores by chemolithotrophic bioleach cultures

Over the course of the experiment, it was observed that the flasks amended with the highest concentration of energy sources were the most turbid. This turbidity decreased with lower concentrations of energy sources.

Figure 4.4 represents changes in pH over time for the kimberlite sample from Venetia mine during the course of the experiment where energy source concentrations were varied. The graphs illustrate that initially the pH increased and from day 7 onwards the pH decreased for all of the energy source concentration evaluated. However, this decrease in pH is greater as energy source concentration increases. This trend was seen for both energy sources with sulfur producing lower pH values. This trend in pH change was also seen for the kimberlite sample from Premier mine (data not shown).

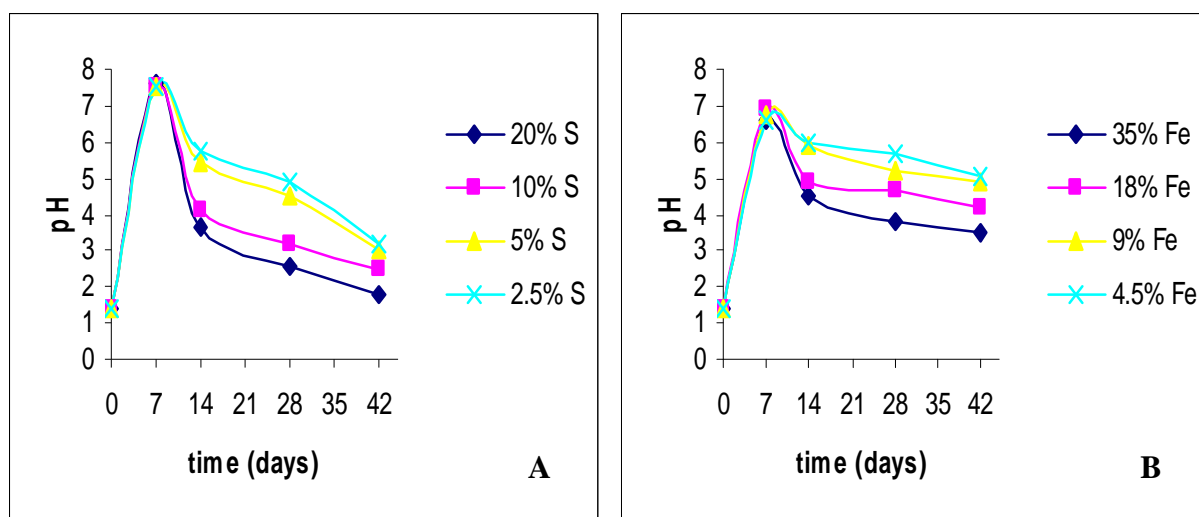


Figure 4.4 Changes in pH over time (days) observed during the biotransformation of kimberlite ores from Venetia Mine. Energy source concentrations were varied to determine its influence on kimberlite mineralization. [A (sulfur was used as the energy source), B (ferrous iron was used as the energy source)].

It was also observed that the final pH readings for the flasks supplemented with 5 and 2.5% S^0 (w/w) were slightly higher than the flasks that contained 20 and 10% S^0 (w/w). Their final pH reading was in the range of 3.0-3.3 as compared with the pH range of 1.8-2.5 of the flasks that contained 20 and 10% S^0 (w/w).

The pH range of the flasks containing Fe^{2+} in higher concentrations fluctuated between the pH range of 3.5-4.2 whereas the pH range of the flasks containing 4.5 and 9% (w/w) of Fe^{2+} was in the range of 4.8-5.0.

4.3.2.1 ICP results

The results obtained were very similar to those obtained for the preliminary study (Section 3.3.1.1 of Chapter 3). The ICP analyses illustrated that the cations investigated solubilized in solution for all concentrations of energy sources used. In Table 4.2, it was seen that the highest solubilized cation was Mg followed by Fe and Ca and then Si. It was also observed that the rate of solubilization increased as the concentration of energy source increased. In the case of sulfur as the energy source, the highest rate of cations leached into solution was observed for the 20% (w/w) concentration of sulfur (Figure 4.5), although the leaching efficiency of the cations does not increase that much with an increase in energy source concentrations. For the Premier and Venetia mine sample an 800% increase in the sulfur concentration (20% w/w) resulted only in a 48.3% and 114% increase in Mg solubilization respectively. This was calculated by taking the concentration of dissolved Mg at the 20% w/w sulfur treatment and dividing it by the concentration of Mg at the lowest concentration sulfur (2.5% w/w) used $((172/116)*100\%)$ (Table 4.2).

This leaching trend was also seen in the treatments where Fe^{2+} was used as the energy source (Table 4.2 and Figure 4.5). The leaching efficiency only increased by 123% and 105% when the concentration of Fe^{2+} was increased by 800% for the kimberlite samples from Venetia and Premier mine respectively. This percentage was calculated as described above except the dissolved Mg values were taken for the highest and lowest concentration of Fe^{2+} used during the experiment.

Table 4.2 ICP analyses of two different kimberlite samples (<100mm) used to determine the influence of energy source concentrations on the biotransformation of kimberlite ores. (Mixed chemolithotrophic cultures were used in leaching experiments with varying concentrations of sulfur or ferrous iron as the energy source. All treatment flasks were incubated at 30°C in a shake incubator (120rpm) for 6 weeks.)*

Sample	[Ca][mg/l]				[Si][mg/l]				[Fe][mg/l]				[Mg][mg/l]				[K][mg/l]			
	Day 7	Day 14	Day 28	Day 42	Day 7	Day 14	Day 28	Day 42	Day 7	Day 14	Day 28	Day 42	Day 7	Day 14	Day 28	Day 42	Day 7	Day 14	Day 28	Day 42
Premier Diamond Mine																				
Kimberlite + 0.75g S ⁰ (20% w/w)	201a	243a	264a	305a	39a	54a	55b	55b	43c	162b	202c	480b	748a	1269a	2247a	2295a	9a	9a	10a	10a
Kimberlite + 0.38g S ⁰ (10% w/w)	148b	199b	222b	268b	27b	41b	43c	43c	14e	122b	162d	334d	604b	962b	1668b	2109b	7bc	8c	8b	9b
Kimberlite + 0.19g S ⁰ (5.0% w/w)	121d	160d	201c	242c	25b	25c	26d	39c	5f	83e	122f	231g	429c	842c	1508c	1664c	6d	7d	7c	7c
Kimberlite + 0.10g S ⁰ (2.5% w/w)	107f	132f	174d	206e	24b	25c	25d	26d	4f	79e	95g	147h	372d	788d	1348d	1548d	5e	5e	5d	5d
Premier Diamond Mine																				
Kimberlite + 1.30g Fe ²⁺ (35% w/w)	132c	174c	205c	217d	37a	42b	68a	94a	107a	205a	417a	563a	485e	588e	615e	568e	8b	8b	9b	9b
Kimberlite + 0.65g Fe ²⁺ (18% w/w)	122e	145e	162e	198e	25b	26c	26d	27d	80b	163b	322b	405c	388f	456f	456f	469f	7dc	7d	7c	7c
Kimberlite + 0.33g Fe ²⁺ (9.0% w/w)	95g	124g	148f	163f	14c	14d	17e	19de	44c	133c	203c	267e	269g	364g	390g	406g	5ef	5e	5d	5d
Kimberlite + 0.17g Fe ²⁺ (4.5% w/w)	82h	96h	138g	140g	13c	13d	13e	14e	27d	64f	149e	242f	188h	295h	283h	296h	4f	4f	4d	4d
F Ratio	7.E+02	4.E+03	5.E+02	4.E+02	1.E+02	4.E+02	2.E+02	1.E+02	3.E+02	6.E+02	4.E+03	3.E+03	7.E+03	2.E+05	1.E+05	3.E+05	6.E+01	1.E+02	3.E+01	4.E+01
P value	<1.E-04	<1.E-04	<1.E-04	<1.E-04	<1.E-04	<1.E-04	<1.E-04	<1.E-04	<1.E-04	<1.E-04	<1.E-04	<1.E-04	<1.E-04	<1.E-04	<1.E-04	<1.E-04	<1.E-04	<1.E-04	<1.E-04	<1.E-04
LSD	4.44	4.42	6.41	8.92	2.88	2.32	4.79	5.44	1.02	1.48	5.61	8.69	5.99	5.99	6.10	5.13	0.74	0.53	1.06	1.02
Venetia Diamond Mine																				
Kimberlite + 0.75g S ⁰ (20% w/w)	198a	213a	240a	253a	39a	54a	56b	68a	92a	212a	478a	651a	344	1623a	2076a	2129a	6b	7b	8a	9a
Kimberlite + 0.38g S ⁰ (10% w/w)	185b	209a	226b	227b	35a	40b	52b	53b	63b	184b	281b	331b	263	1185b	1608b	1664b	6b	6b	6b	7b
Kimberlite + 0.19g S ⁰ (5.0% w/w)	173c	187b	225b	226b	24b	36b	37c	43c	39c	135c	203c	264c	207	1000c	1163c	1062c	5c	5c	6bc	6c
Kimberlite + 0.10g S ⁰ (2.5% w/w)	132d	159c	161c	174c	21b	23b	29d	34de	23d	66d	144d	240d	172	876d	931d	972d	4d	5d	5c	5de
Venetia Diamond Mine																				
Kimberlite + 1.30g Fe ²⁺ (35% w/w)	104e	136d	159c	161d	38a	39c	63a	68a	64b	96e	136d	210e	279	453e	481e	522e	6a	6a	7a	7a
Kimberlite + 0.65g Fe ²⁺ (18% w/w)	93f	120e	123d	147e	24b	28c	51b	54b	43c	67e	106e	187f	223	332f	358f	431f	4b	4b	5b	5b
Kimberlite + 0.33g Fe ²⁺ (9.0% w/w)	81g	104f	117d	126f	24b	25d	30dc	41dc	37c	49f	78f	130g	158	261g	272g	315g	2d	2d	2c	2dc
Kimberlite + 0.17g Fe ²⁺ (4.5% w/w)	63h	65g	79e	92g	21b	22d	26d	26e	23d	26g	60g	102h	122	206h	217h	249h	2e	2e	2d	2e
F Ratio	5.E+02	3.E+02	9.E+02	6.E+03	2.E+01	5.E+01	4.E+01	4.E+01	1.E+02	2.E+02	2.E+03	4.E+03	3.E+02	2.E+04	9.E+05	4.E+05	6.E+01	7.E+02	4.E+01	2.E+04
P value	<1.E-04	<1.E-04	<1.E-04	<1.E-04	<1.E-04	<1.E-04	<1.E-04	<1.E-04	<1.E-04	<1.E-04	<1.E-04	<1.E-04	<1.E-04	<1.E-04	<1.E-04	<1.E-04	<1.E-04	<1.E-04	<1.E-04	<1.E-04
LSD	7.79	9.48	6.56	4.78	2.19	2.11	2.21	7.92	1.02	15.99	9.47	9.21	4.74	12.52	12.12	5.21	0.72	0.63	0.85	1.02

* ICP values represented rounded off to the nearest whole number * Mean values from duplicate samples represented. Means with the same letter within a column for each kimberlite ore type are not significantly different (P=0.05).

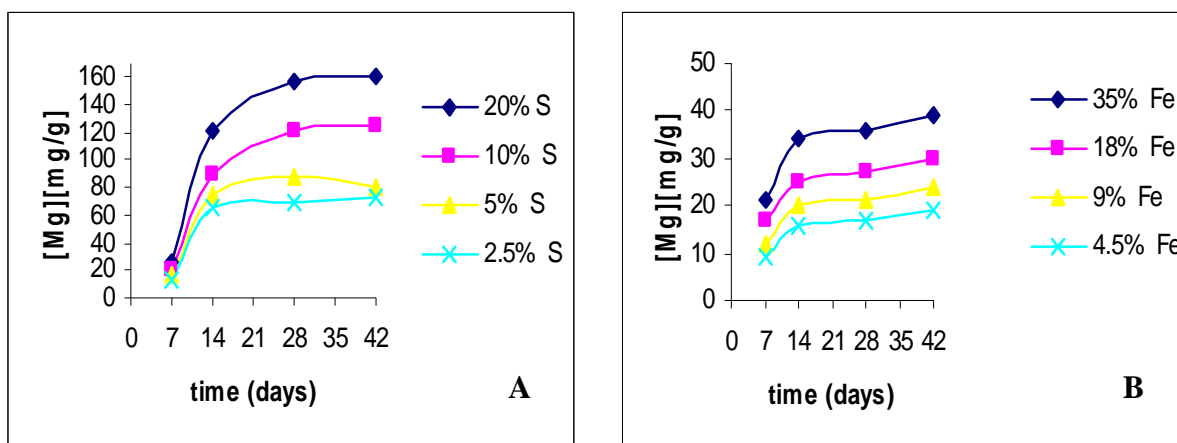


Figure 4.5 Magnesium ion dissolution trends illustrating the effect of the different concentrations of energy sources used in the microbial leaching treatments of kimberlite ores from Venetia Mine. [A (sulfur was used as the energy source), B (ferrous iron was used as the energy source). Data was obtained from ICP analyses (Table 4.2)].

Figure 4.5 represents the dissolution of Mg from the kimberlite sample from Venetia mine during the optimization tests. Similar trends were also observed for other major cations solubilized in solution. Therefore using Mg as the major leached cation, the graph was plotted to illustrate the trend that as the concentration of energy source increased, dissolution of the cations present in kimberlite increased (data plotted are represented values of ICP data recorded in Table 4.2). Similar results were also seen for the kimberlite sample from Premier mine (data not shown).

Based on the ICP data and Figure 4.5, it was observed that levels and rates of Mg solubilization significantly increased with increasing concentration of energy source. The concentration of Mg in solution stabilized over time for all energy source concentrations suggesting possible saturation and precipitation of Mg. It was also observed that the sulfur energy source was more effective at solubilizing Mg even at the lowest concentration viz., 2.5% versus 35% Fe^{2+} .

4.3.2.2 XRD results

The XRD analyses of both the treated kimberlite samples showed that the degree of change in their mineralogical structures was seen in the treatments where higher concentrations of energy sources were used. In the optimization studies of sulfur as the energy source, typical XRD results, as represented in the XRD analyses of the treated kimberlite from Venetia mine in Figure 4.6, showed alterations in the

phlogopite and serpentine peaks when compared to its control. Although this occurred in all the concentration of S^0 investigated, it was evident that the 20% (w/w) concentration of S^0 brought about the most change. The formation of gypsum was seen in the XRD spectra of all treated kimberlite ores whereas the formation of jarosite was only seen in Figure 4.6 B, C, D and Figure 4.7 B, C.

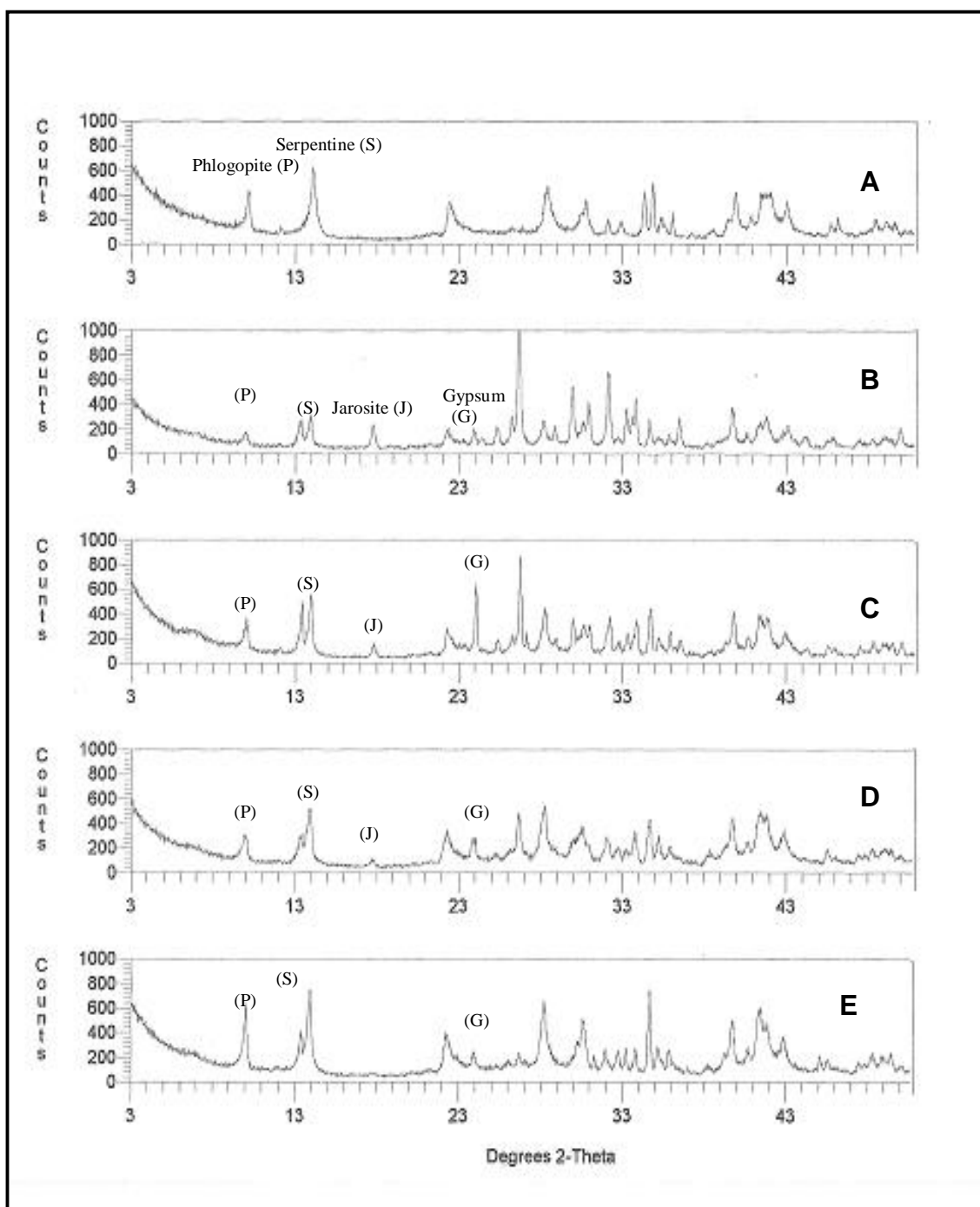


Figure 4.6 XRD analyses of kimberlite from Venetia mine after treatment with a mixed chemolithotrophic culture in the presence of different concentrations of elemental sulfur. [A (negative control), B (20% (w/w) S^0), C (10% (w/w) S^0), D (5% (w/w) S^0), E (2.5% (w/w) S^0)].

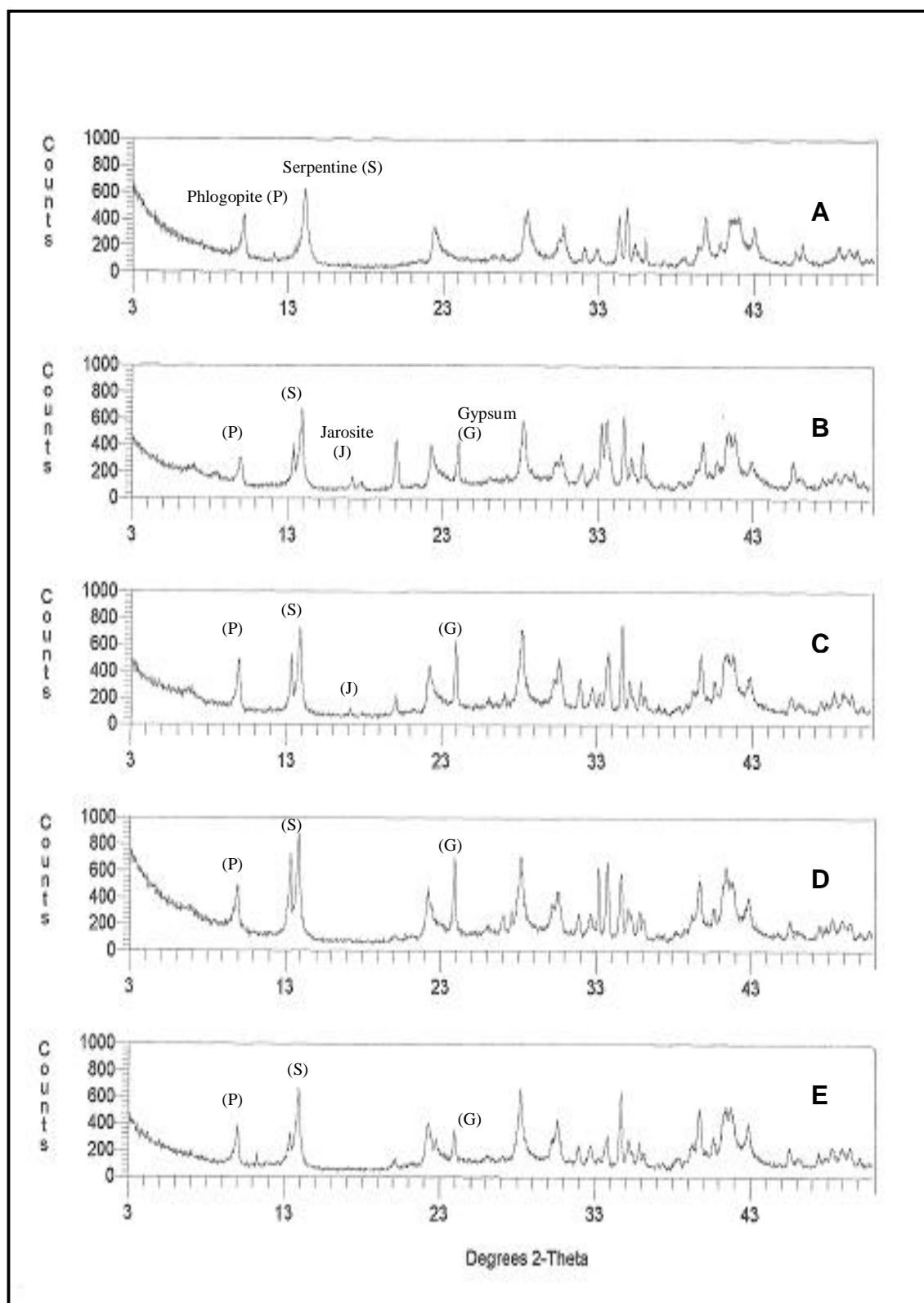


Figure 4.7 XRD analyses of kimberlite from Venetia mine after treatment with a mixed chemolithotrophic culture in the presence of different concentrations of ferrous iron. [A (negative control), B (35% (w/w) Fe^{2+}), C (18% (w/w) Fe^{2+}), D (9% (w/w) Fe^{2+}), E (4.5% (w/w) Fe^{2+})].

Based on Figures 4.6 and 4.7, the concentration of sulfur and ferrous iron that caused major breakdown of the kimberlite minerals is 20% (w/w) S^0 and 35% (w/w) Fe^{2+} . The XRD analyses of kimberlite from Premier mine (data not shown) also exhibited alterations to its major mineral serpentine and similar trends as the kimberlite sample from Venetia mine were also seen.

4.3.2 Effect of increasing treatment time of kimberlite ores during microbial leaching processes

The general observations made were similar to that described in Section 3.3.1 of Chapter 3. The pH results of the treated kimberlite sample from Venetia mine are represented in Figure 4.8 to illustrate the pH trends for the ‘sulfur treatment’ observed for both kimberlite samples. The pH readings decreased as time increased. The final pH readings of the ‘sulfur treatments’ were between 1.4 and 1.5 and between 3.0 and 3.3 for the ‘iron treatments.’

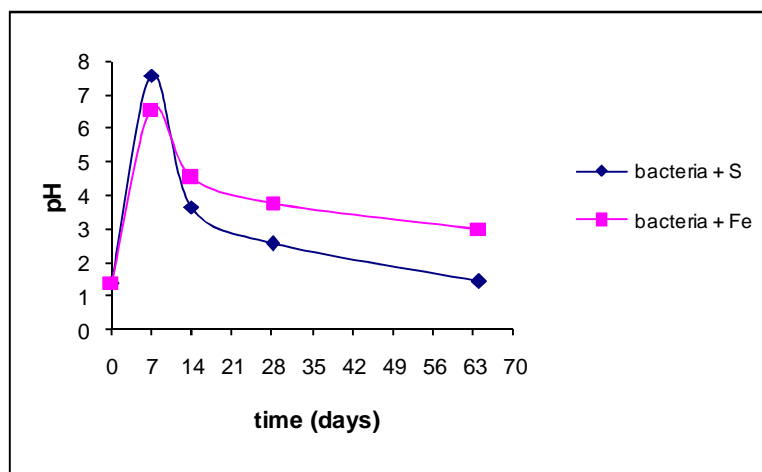


Figure 4.8 Changes in pH over time (days) observed during the biotransformation of kimberlite ores from Venetia Mine.

Figure 4.8 represents changes in pH over time for the kimberlite sample from Venetia mine during the course of the 8 week experimental investigation. The graph shows an initial increase in pH and thereafter, from day 7 onwards, the pH continually decreases. This trend is seen for both energy sources with sulfur producing lower pH values. This trend in pH change was also seen for the kimberlite sample from Premier mine (data not shown).

4.3.3.1 ICP results

Over the 8 week period, the ICP results obtained showed that as time increased beyond the 6 week normal treatment time, the dissolution of the cations occurred slowly with slight variation in the amount of cations that solubilized into solution (Figure 4.9). In comparison to the ICP data in Table 3.3 (Chapter 3), the ICP data obtained for this investigation (Table 4.3) showed that similar ICP values were obtained for all the cations present in the leachate solution with only slight increases observed on day 64. All other trends described in Section 3.3.1.1 (Chapter 3) were also observed here.

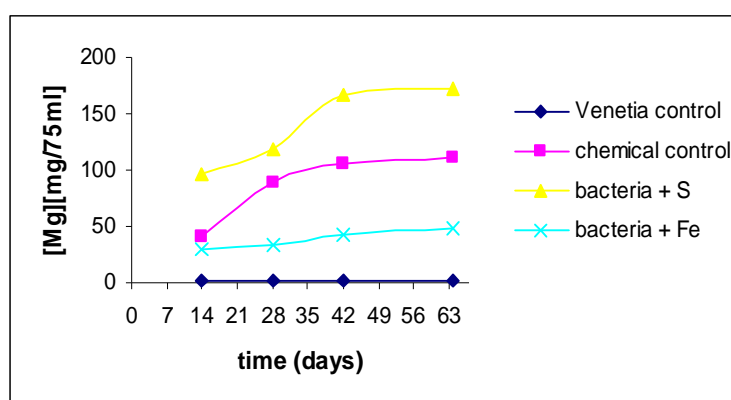


Figure 4.9 Magnesium ion dissolution trends illustrating the effect of increasing the microbial leaching time of kimberlite ores from Venetia Mine. [Data was obtained from ICP analyses (Table 4.3)].

Figure 4.9 represents the dissolution of Mg from the kimberlite sample from Venetia mine and illustrates the effect of increasing treatment time during the microbial leaching of kimberlite. An increase in the amount of Mg solubilized into solution as time increased was noticed in the graph, except, from day 42 onwards where negligible amounts of Mg was released into solution causing the graphical curve to flatten and almost becoming constant at the end. These results are representative of all other major cations leached into solution for both kimberlite types.

Table 4.3 ICP analyses of two different treated kimberlite samples (<100mm) to determine the effect of increasing treatment time during microbial leaching of kimberlite. (Mixed chemolithotrophic cultures were used in leaching experiments with sulfur or ferrous iron as the energy source. All treatment flasks were incubated at 30°C in a shake incubator (120rpm) for 8 weeks.)*

Sample	[Ca][mg/l]					[Si][mg/l]				[Fe][mg/l]				[Mg][mg/l]				[K][mg/l]			
	Day 14	Day 28	Day 42	Day 64	Day 14	Day 28	Day 42	Day 64	Day 14	Day 28	Day 42	Day 64	Day 14	Day 28	Day 42	Day 64	Day 14	Day 28	Day 42	Day 64	
Premier Diamond Mine																					
Kimberlite + basal media - control	15d	15d	16c	17c	13c	14c	15c	15d	4d	4d	5d	5d	13d	13d	14d	14	7c	7b	7c	8c	
Kimberlite + H ₂ SO ₄ – chemical control	205a	241a	263a	282a	30a	37a	41a	43a	70c	119c	203c	216c	572b	1311b	1627b	1750	8a	9b	9b	9b	
Kimberlite + bacteria + S ⁰	174b	207b	252a	284a	27b	29b	31b	37b	104b	152b	224b	298b	1365a	2288a	2380a	1336	9a	12a	22a	27a	
Kimberlite + bacteria + Fe ²⁺	150c	162c	184b	202b	25b	26b	27b	31c	133a	173a	583a	618a	466c	525c	608c	697	8b	8b	8b	9b	
F Ratio	5.E+02	6.E+02	1.E+03	9.E+03	1.E+02	9.E+02	2.E+03	3.E+03	8.E+02	9.E+01	5.E+01	4.E+03	5.E+043	3.E+04	4.E+04	4.E+04	5.E+01	1.E+01	7.E+02	2.E+03	
P value	<1.E-04	<1.E-04	<1.E-04	<1.E-04	<1.E-04	<1.E-04	<1.E-04	<1.E-04	<1.E-04	<1.E-04	<1.E-04	<1.E-04	<1.E-04	<1.E-04	<1.E-04	<1.E-04	<1.E-04	<1.E-04	<1.E-04	<1.E-04	
LSD	12.71	16.91	4.58	5.04	2.86	2.15	3.48	2.50	1.02	10.09	10.77	5.63	18.05	24.53	13.48	6.07	0.53	0.93	0.85	0.81	
Venetia Diamond Mine																					
Kimberlite + basal media - control	12c	13c	14c	14c	3d	4d	4d	5	2d	3d	4d	4d	12d	13d	14d	14d	4d	4d	4b	4c	
Kimberlite + H ₂ SO ₄ – chemical control	159a	215a	227a	254a	17c	18c	19c	20	42c	79c	118c	144c	527b	1181b	1407b	1487b	7b	8b	8b	8b	
Kimberlite + bacteria + S ⁰	147a	203a	223a	239a	27a	39a	40a	53	144a	383a	488a	537a	1286a	1563a	2219a	2301a	9a	10a	21a	27a	
Kimberlite + bacteria + Fe ²⁺	121b	136b	163b	203b	22b	25b	26b	26	64b	164b	215b	319b	405c	452c	555c	640c	6c	6c	6b	8b	
F Ratio	3.E+02	6.E+02	8.E+03	7.E+02	8.E+02	1.E+04	2.E+03	1.E+02	6.E+04	2.E+03	2.E+03	1.E+03	1.E+04	1.E+04	3.E+04	4.E+04	4.E+02	1.E+02	2.E+02	5.E+02	
P value	<1.E-04	<1.E-04	<1.E-04	<1.E-04	<1.E-04	<1.E-04	<1.E-04	<1.E-04	<1.E-04	<1.E-04	<1.E-04	<1.E-04	<1.E-04	<1.E-04	<1.E-04	<1.E-04	<1.E-04	<1.E-04	<1.E-04	<1.E-04	
LSD	5.62	12.05	4.09	6.01	2.45	5.92	7.26	6.38	1.42	6.09	3.22	7.51	9.74	6.82	3.76	10.45	1.23	0.86	1.31	0.52	

* ICP values represented rounded off to the nearest whole number * Mean values from duplicate samples represented. Means with the same letter within a column for each kimberlite ore type are not significantly different (P=0.05).

4.3.2.2 XRD results

Typical XRD results, as represented by the XRD analyses of the treated kimberlite sample from Venetia mine in Figure 4.10 showed the complete dissolution of phlogopite in B and C and major breakdown of serpentine coupled with the formation of gypsum in all treated kimberlite ore. Jarosite formation was only seen in Figure 4.10 D.

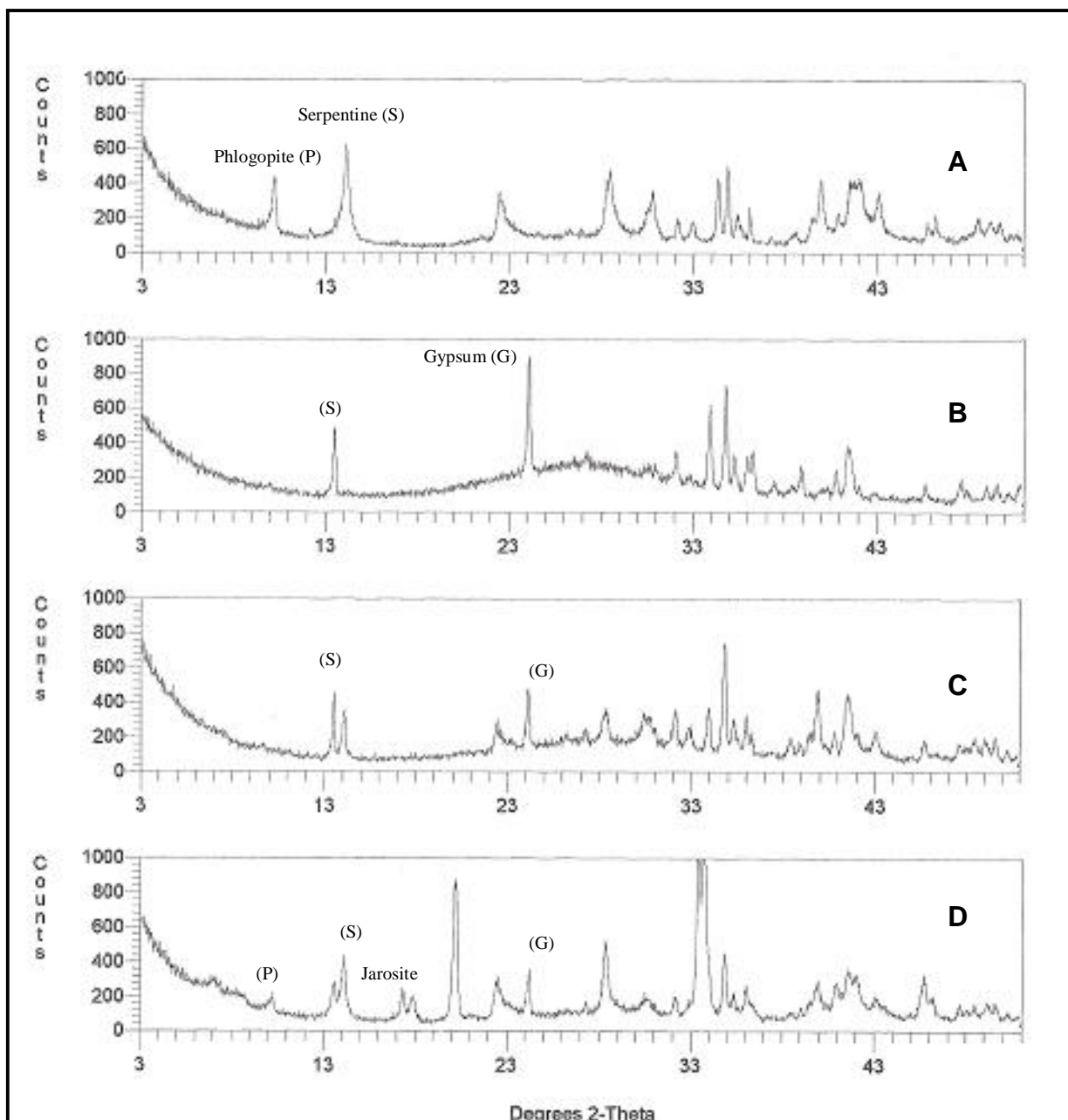


Figure 4.10 XRD analyses of kimberlite from Venetia mine after extending microbial leaching treatment time of the kimberlite ores from 6 to 8 weeks. [A (negative control), B (positive chemical control), C (chemolithotrophic bacteria in the presence of 1% (w/v) S^0), D (chemolithotrophic bacteria in the presence of 10% (w/v) Fe^{2+})].

4.4 Discussion

Given that dump/heap-leach technology could be applied to the microbial leaching of kimberlite, the effects of microbial leaching activities on larger kimberlite particles was evaluated. From Figure 4.1 and the ICP results in Table 4.1, it was observed that the larger particles weathered at slightly lower rates than the finer particles. This was however expected as weathering rates are inversely proportional to surface area (White and Brantley, 2003). Larger particles have a decreased surface area on which microbial leaching reactions and mechanisms can occur, therefore slowing down dissolution and weathering rates (Bosecker, 1989; White and Brantley, 2003; Hossain *et al.*, 2004). This was also confirmed by the XRD results (Figure 4.2 and 4.3) where the degree of transformation of the mineralogical structure was slightly less than the finer particles (Figures 3.3 and 3.6, Chapter 3).

However, although the biotransformation of kimberlite of particle size $>2\text{mm}<5\text{mm}$ was slightly less than the fine particles ($<100\mu\text{m}$), the microbial weathering tests still exhibited an alteration in the kimberlite mineralogical structure. It is known that changing the interlayer cation exchange properties of the swelling clays (Figure 4.2 showed the complete dissolution of smectite) coupled with the alteration of major minerals (serpentine) and formation of new minerals (gypsum and jarosite) would adequately weaken the kimberlite structure to promote accelerated weathering (Gericke *et al.*, 2007).

Optimization studies of energy sources were performed to determine the effect of energy source concentration on subsequent leaching of minerals. The ICP (Figure 4.5) results indicated that rates of Mg dissolution increased with increasing concentrations of S^0 and Fe^{2+} . Lower pH ranges were also achieved at the higher concentrations (Figure 4.4) suggesting that at higher concentrations the bacteria were able to produce more sulfuric acid in the ‘sulfur treatment’ (Equation 5) as well as the jarosite formation with the higher concentrations of ferric iron that caused the pH to drop significantly (more than the rest of the lower concentrations). The increased dissolution rates associated with increasing concentrations of S^0 and Fe^{2+} were therefore attributed to more acid and ferric iron being generated. It is evident that the pH needs to remain low to overcome the neutralization effect of the subsequent silicate dissolution and to ensure that an acidic environment for the bacteria to

function optimally must be maintained. This would thus ensure a continual proton and ferric iron attack on the kimberlite ores.

Comparing both energy sources, it was again observed that the sulfur produced superior results in all the individual parameters investigated suggests that sulfur would be preferable for use as the energy source for the chemolithotrophic bacteria in larger microbial leaching processes that would be used for the treatment of kimberlite.

The effect of time on the microbial leaching process was investigated by increasing treatment time. The ICP results illustrated that as time increases, weathering increases until a 'plateau' or area of little variation is reached (Figure 4.9). However, the XRD results (Figure 4.10) demonstrated that although weathering rates decreased after day 42, more changes were observed in the mineralogical structure as compared to the XRD analyses of the kimberlite samples when the treatment time was 6 weeks (Figure 3.5, Chapter 3). A complete dissolution of phlogopite was observed in the 8 week treatment whereas in the 6 week treatment a slight breakdown of phlogopite was observed in the treated kimberlite sample from Venetia mine. The serpentine peak was altered more in the 8 week treatment than in the 6 week treatment, thus indicating that the longer treatment time had a more drastic weakening effect on the mineralogical structure of kimberlite. Therefore, it was deduced that an increase in treatment time causes kimberlite to weather and weaken more extensively. Apart from a longer chemical reaction time, this phenomenon was also attributed to a longer microbial growth time, which is advantageous to the chemolithotrophs, considering they are 'slow growing.' This suggests that the bacteria were able to produce more acid or ferric iron that enhances leaching. The pH was also continually decreased (Figure 4.8) thereby promoting dissolution. Therefore, it was deduced that although weathering rates decrease with time, the leachate solution still has a positive effect on the dissolution of kimberlite minerals.

Apart from the reasons discussed in Chapter 3, possible further reasons why weathering rates slow down as time increases include (White and Brantley, 2003):

1. As dissolution increases, pitting and etching occur on the surface of the particles causing a decrease in surface area which leads to a decrease in weathering rates. As time increases, surfaced leached layers and precipitation

of new minerals may also decrease particle surface area and decrease weathering rates.

2. As time increases, weathering of the most susceptible and reactive minerals occur the fastest resulting in the removal of these minerals and leading to a decrease in weathering rates.

In general, the results presented in this investigation also serve to validate the results obtained in the preliminary investigation of the biotransformation of kimberlite. Most of the descriptions and deductions of the results discussed in Chapter 3 were also observed in these sets of experiments.

The results obtained in this investigation have shown that there is potential for the microbial treatment of kimberlite on a larger technical scale with respect to particle size and if such technology is applied, longer treatment times and elemental sulfur as the energy source should be used.

CHAPTER 5

Evaluation of a continuous flow bioleach column system to determine the influence of chemolithotrophic cultures on the biotransformation of kimberlite ores

5.1 Introduction

Laboratory scale bioleach columns have been used to simulate and model conditions present in dump- and heap-leaching systems (Bosecker, 1989; Lizama, 2004). Column leaching experiments have been used to assess leaching conditions and changes that hypothetically could be expected to occur during a dump- or heap-leaching process. In this way, important information on the variables that play significant roles in dump- and heap-leaching and factors that affect these variables and the leaching efficiency may be investigated so as to improve and optimize the bioleaching process (Torma and Bosecker, 1982; Bosecker, 1989). In order to optimize leaching conditions, each variable is investigated individually while all other parameters remain constant. Whilst batch cultures can be used for preliminary biotransformation studies, they are closed systems which do not necessarily reflect changes that occur in an open system as found in a dump- or heap-leaching system (Middelbeek and Jenkins, 1992). In a continuous plug-flow system, steady state conditions can be achieved that reflect more accurately the behaviour of microbial communities/consortia in dump- and heap-leaching systems. In this chapter, the biotransformation of kimberlite ores in a continuous plug-flow bioleach column system was investigated.

5.2 Experimental Procedure

5.2.1 Kimberlite

Kimberlite samples from Venetia diamond mine were used (Section 2.1). Crushed kimberlite sieved to a particle size of greater than 5.0mm and less than 6.7mm ($>5.0\text{mm}<6.7\text{mm}$) was used for the column weathering test (Section 5.2.3).

5.2.2 Microorganisms

The microorganisms used were a mixed mesophilic culture consisting of *A. caldus*, *L. ferrooxidans* and *Sulfobacillus sp.* (Section 2.2.1). Culturing, maintenance and storage of these microorganisms were described in Section 2.3.1.

5.2.3 Column weathering test

Column leaching of the kimberlite sample was carried out in two glass columns (3cm wide, 12cm high). To both columns autoclaved kimberlite (40g) was added gently to obtain an even distribution of packed ore. Prior to filling of kimberlite, a thin layer of glass wool was packed at the bottom of both the columns. To the first column, kimberlite was mixed with elemental sulfur (8g, 20% w/w) and inoculated with 100ml of mixed mesophilic culture (10^7 cells/ml) maintained on sulfur as the energy source (2.3.1). The leachate was allowed to percolate through the first column into the second column which was situated directly below it. The second column contained no sulfur. Using a peristaltic pump (Watson-Marlow 503M), basal inorganic growth medium (Section 2.4.1) (pH 1.4, autoclaved at 120°C for 15 minutes) was pumped from a reservoir bottle (10L) into the first column at a flow rate at 1ml/min. Subsequently, the leachate solution from the first column drained into the second column. A perforated glass diffuser was used in both columns to allow for even distribution of the growth medium and leachate solution during leaching. Parafilm was used to cover the surfaces of the columns and the bottle containing the growth medium to prevent evaporation. Figure 5.1 illustrates the setup of the two columns.

The displacement volume of each column was estimated by pouring basal media into each packed column to a known volume (which covered the kimberlite ore). This was followed by draining and collecting the liquid into a volumetric glass cylinder. The displacement volume for each column was approximately 240ml. Using the

displacement volume, the dilution rate (D) and hydraulic retention time (HRT) was calculated to be 0.25h^{-1} and 4 hours, respectively.

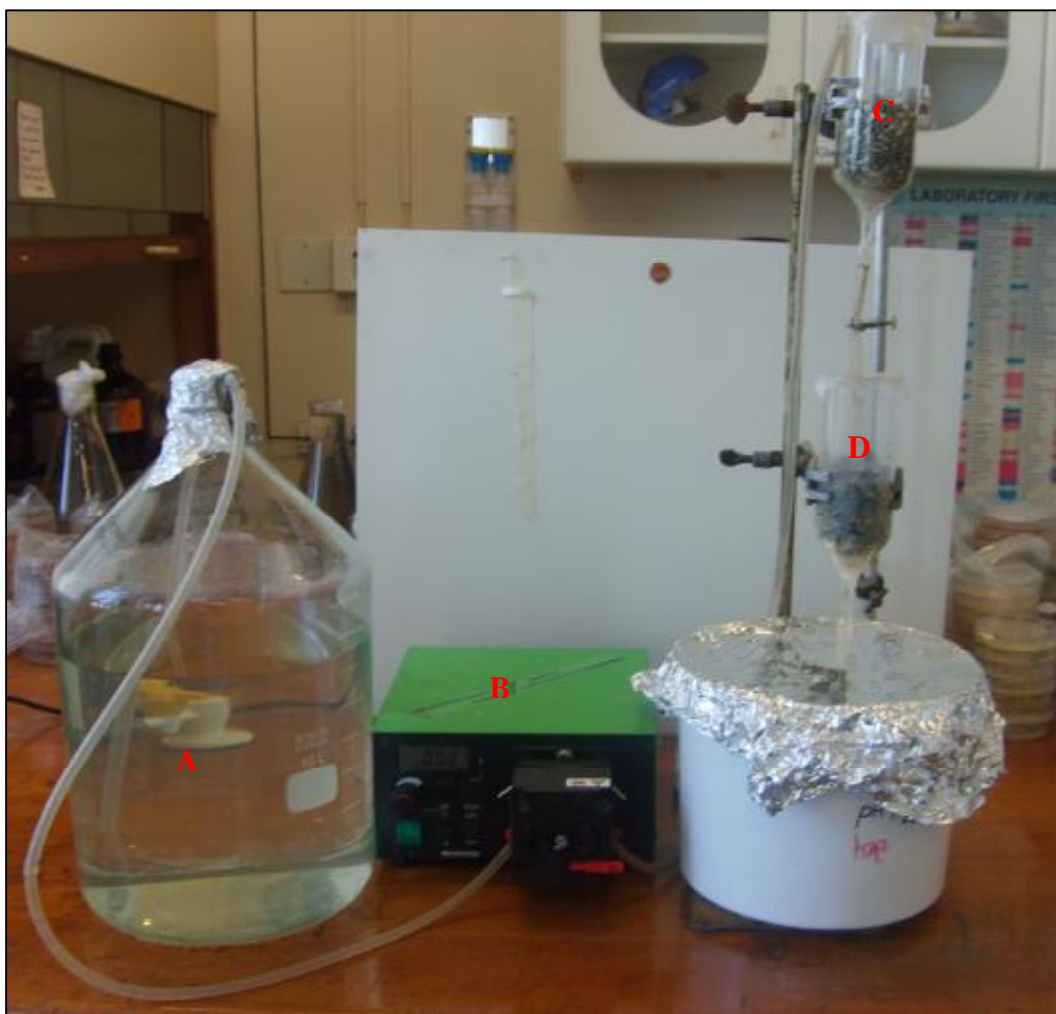


Figure 5.1 Experimental continuous flow bioleach column setup using a chemolithotrophic mesophilic culture. [A = reservoir of inorganic growth medium, B = peristaltic pump set at a flow rate of 1ml/min , C= column 1 containing kimberlite mixed with S^0 (w/w) as the energy source, D = Column 2 containing kimberlite with no energy source].

The weathering test was carried out for 8 weeks at ambient temperature. At days 7, 14, 28, 35, 42 and 56, leaching samples (5ml) were taken from the effluent outlet of each column for ICP analyses (Section 2.5.1). During this time, the pH was also monitored using a pH meter (Crison micro pH 2000). After 8 weeks, the contents of the columns were washed with sterile distilled water and XRD analyses (Section 2.5.2) were performed on air dried kimberlite particles that were randomly selected from each column.

5.3 Results

Changes in pH that occurred in both columns over the course of the experiment are shown in Figure 5.2.

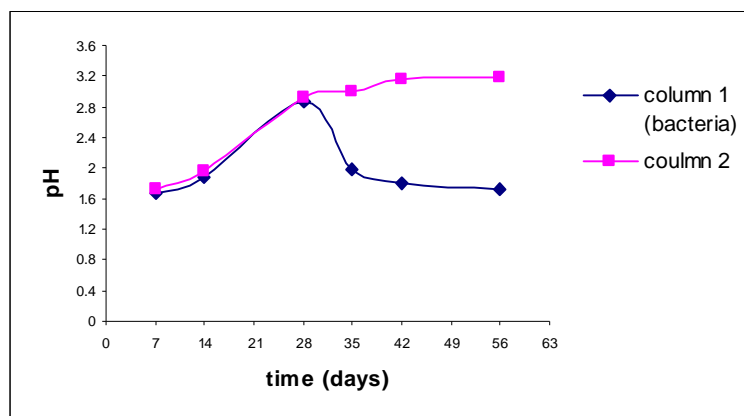


Figure 5.2 Changes in pH observed in two sequential continuous flow leaching columns. (Column 1 contained kimberlite mixed with S^0 (w/w) as the energy source whilst Column 2 contained kimberlite with no energy source.)

From Figure 5.2, it was shown that initially the pH in Column 1 increased until day 28 and thereafter sharply dropped and stabilized around pH 1.6 from day 42 onwards. In the second column, the pH profile was similar to the first column for the first 28 days, but thereafter the pH stabilized between pH 2.9 and 3.19.

5.3.1 ICP results

ICP analyses of the leach solutions from both columns showed that cation dissolution increased over time (Table 5.1) indicating that dissolution of kimberlite minerals occurred. From Table 5.1, it was noticed that Mg was the major cation that solubilized in solution followed by Ca. Relatively small amounts of Si, Fe, and K went into solution. Higher values of solubilized cations were observed in the first column illustrating that weathering of kimberlite via mineral dissolution was accelerated in the presence of the chemolithotrophic culture (Figure 5.3).

Table 5.1 ICP analyses of kimberlite (>5.0mm<6.7mm) from Venetia Diamond Mine after treated in a continuous flow bioleach column system.

	Ca [mg/l]	Si [mg/l]	Fe [mg/l]	Mg [mg/l]	K [mg/l]
Day 7					
column 1	450±7	50±2	50±7	750±10	50±5
column 2	350±3	50±7	0±0	550±8	0±0
Day 14					
column 1	600±9	50±4	100±12	1750±15	50±3
column 2	500±10	50±6	0±0	1050±10	50±1
Day 28					
column 1	700±6	100±11	250±17	2850±12	100±7
column 2	550±5	50±6	50±4	1600±9	50±3
Day 42					
column 1	750±5	150±14	350±9	3250±9	100±9
column 2	550±11	50±5	50±2	2250±14	50±2
Day 56					
column 1	850±7	200±9	450±11	3600±9	150±11
column 2	650±13	100±5	50±3	2500±3	100±8

* Column 1 contained kimberlite mixed with elemental sulfur as the energy source whereas column 2 contained kimberlite but no sulfur.

* Values represented rounded off to the nearest whole number.

* The ICP results are represented as mg/l to reflect the cation concentration present in the leachate of each column.

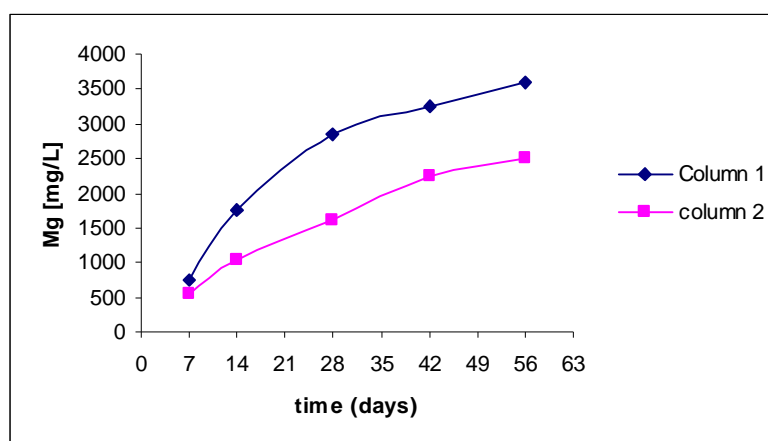


Figure 5.3 Magnesium ion dissolution trends illustrating the effectiveness of continuous leaching on kimberlite. [Column 1 was inoculated with a mixed mesophilic chemolithotrophic culture with elemental sulfur (20% w/w) as the energy source. A fixed continuous flow of growth medium was pumped into Column 1. The leachate from Column 1 percolated through to Column 2 which contained no energy source. Data was obtained from ICP analyses of the leachate solutions of Column 1 and 2 represented in Table 5.1.].

Figure 5.3 represents the dissolution of Mg over an 8 week treatment time (data plotted are represented values of ICP data recorded in Table 5.1). Using Mg as the major soluble cation, the graph was plotted to show the dissolution trends in both columns. Column 1 showed higher concentrations of dissolved Mg than Column 2. This was not expected as the leachate from Column 1 percolated into Column 2, thereby, suggesting if dissolution had occurred in Column 2, then the concentration of dissolved Mg would be expected to be higher in Column 2. However, the dissolution process in both columns seems to follow the same trend, i.e., the dissolution of Mg occurs rapidly initially and then continues to increase slightly resulting in a ‘tailing off.’

5.3.2 XRD results

After the 8 week treatment period, XRD was used to investigate changes in the mineralogical structure of kimberlite. The XRD analyses showed alterations to the serpentine and phlogophite peaks of the treated kimberlite. However, in comparison to the control, more pronounced changes were seen in the peaks of the kimberlite in Column 1 than the kimberlite in Column 2 indicating that more dissolution of the kimberlite minerals occurred in Column 1. No other major changes were seen in the mineralogical structure. There was no evidence of gypsum and jarosite formation in the XRD spectra of the treated kimberlite ores.

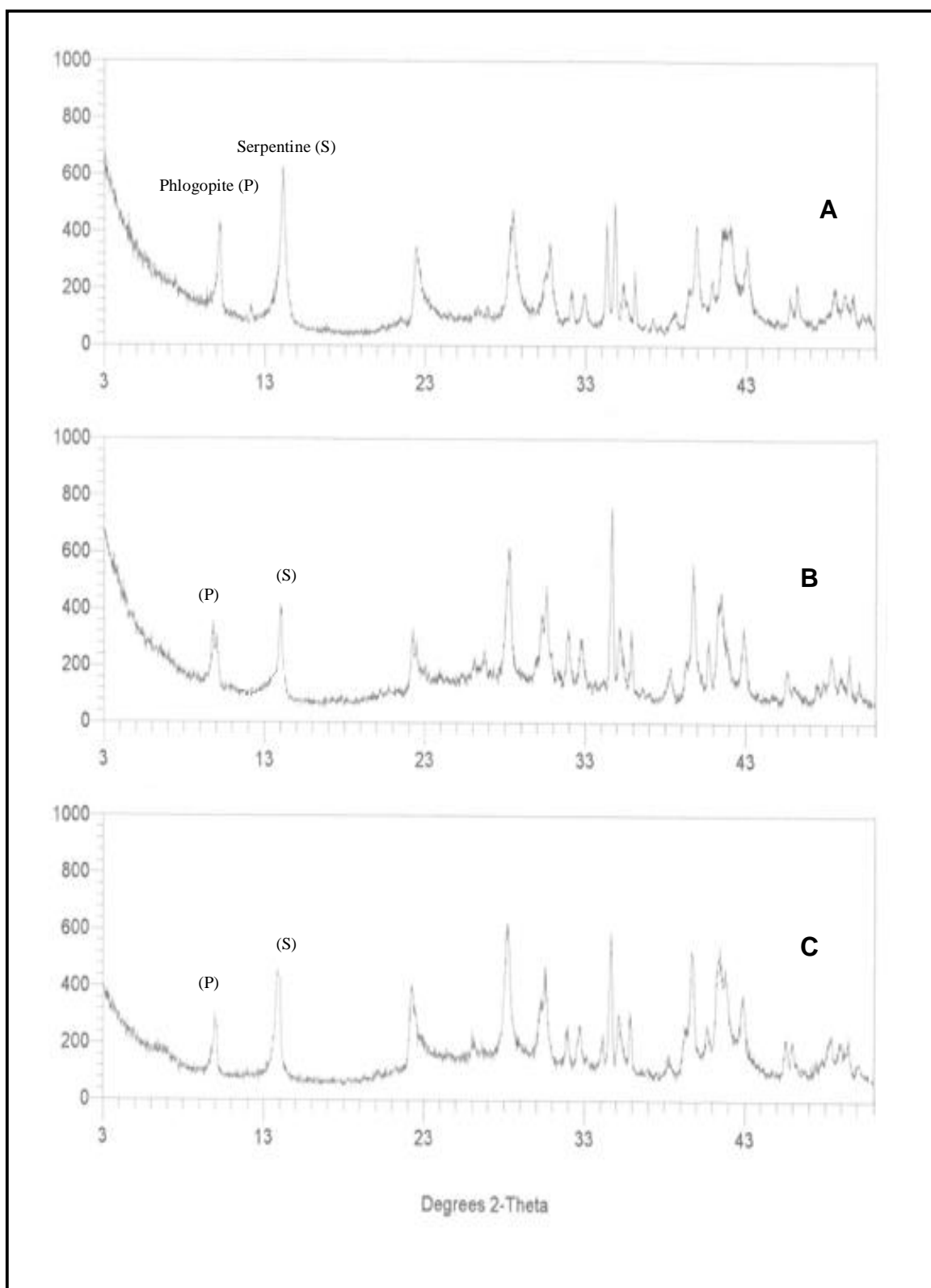


Figure 5.4 XRD analyses of kimberlite from Venetia Diamond Mine after subjected to continuous column leaching. [A (control), B (Column 1 – kimberlite in the presence of a mixed mesophilic chemolithotrophic culture in a continuous flow bioleach system and elemental sulfur as the energy source), C (Column 2 – leaching of kimberlite with the leachate from column 1, no energy source present)].

5.4 Discussion

The success of accelerated kimberlite weathering discussed in previous chapters was restricted to shake flasks tests and the use of batch chemolithotrophic leach cultures. This chapter in contrast investigated the use of continuous cultures with the aid of a mini-column leach setup, which otherwise simulates conditions to be used in dump- or heap-leaching, in accelerating kimberlite weathering. Similarly to the batch culture weathering shake flask tests, a combination of ICP and XRD data yielded promising results in the preliminary investigation of kimberlite weathering in continuous systems. Even more promising was the fact that the effect was seen on larger kimberlite particles from the Venetia mine sample, a relatively less susceptible kimberlite ore to weathering.

ICP data (Table 5.1) showed that cations Mg, Fe, Ca, K and Si were solubilized in solution indicating that mineral dissolution had been initiated. This was further emphasized by the XRD data (Figure 5.4) in which the alteration of the major minerals, namely phlogophite and serpentine, were observed. The higher amounts of Mg dissolved in solution as seen in Table 5.1 was therefore attributed to the active removal of Mg from these minerals and their breakdown. Ca dissolution is also an indication of the breakdown of minor minerals calcite and dolomite present in the kimberlite ores from Venetia mine (Table 2.1).

Figure 5.2 showed that as the dissolution process initially occurred, the pH of both columns increased. This illustrated the consumption of protons by the kimberlitic minerals during the acid attack of phlogophite and serpentine and indicated that the levels of acid produced were rapidly neutralized by the buffering effect of the kimberlite ore (Mousavi *et al.*, 2006). The ICP and pH data indicated that dissolution correlated with pH. As the pH increases, dissolution decreases.

Figure 5.3 and Table 5.1 also showed that the concentration of dissolved Mg and Ca was higher in Column 1 suggesting that the Mg and Ca were probably precipitating to gypsum ($\text{CaSO}_4 \cdot 2\text{H}_2\text{O}$) or magnesium sulfate (MgSO_4) in trace amounts (not detected in XRD analyses) in Column 2. This would also account for the moderate increase in pH in Column 2. Similar observations were made by Platonova *et al.*, (1994).

After 28 days, the pH decreased in Column 1 indicating that the amount of sulfuric acid produced overcame the buffering effect. In Column 2, where there was no S^0 present, the pH remained higher than Column 1 (pH 2.9-3.2) for the remainder of the experiment. This again highlighted the alkaline nature of the kimberlite ore and its ability to neutralize the acid present. This is an important factor that would be need to be addressed and taken into consideration when establishing dump- or heap-leaching technology for these kimberlite ores.

Usually, in theory, when continuous cultures are used, growth occurs exponentially until a steady state is reached, i.e., the rate of microbial growth equals the rate at which the cells are displaced from the reaction vessel. Because microbial growth is dependent on the availability of the rate-limiting nutrient, microbial growth of continuous cultures is therefore dependent on the rate of flow of fresh growth medium into the reaction vessel. This relationship is represented by the dilution rate (D). At steady state, the rate of growth is equal to rate of loss, therefore the dilution rate is equal to the specific growth rate of the microorganism (μ) at steady state (Waites *et al.*, 2001; Middelbeek and Jenkins, 1992). However, in this investigation this did not occur. This was because a high dilution rate of $0.25h^{-1}$ was used, which meant that at this dilution rate, the bacteria would have been completely washed out of the system, as chemolithotrophic bacteria grow relatively slowly. This led to the assumption that this continuous system was growth rate independent and that the bacteria were able to attach themselves on substrates present in the system which prevented them from being washed out. Scanning electron microscope data (not represented) showed no biofilm development on kimberlite surfaces, which therefore allowed for the assumption that the chemolithotrophs were strongly attracted to their energy source and probably attached themselves to the sulfur particles which led to them being able to resist being washed out and to attain 'steady state' conditions.

From Figure 5.2, using pH as an indicator, it is believed that 'steady state' was achieved from day 42 onwards where the pH stabilized. In Column 1, the pH only decreased after day 28. This delay in pH decrease was attributed to the slow establishment of a stable population of growth-rate independent chemolithotrophs. From day 42 onwards, it is believed that the bacterial population achieved equilibrium and remained in a 'steady-state' condition.

Overall, the column leach study produced lower weathering rates and fewer changes to the kimberlite mineralogical structure than the shake flask weathering tests (Table 4.3), which was expected due to the difference in particle size. ICP and XRD data did however show that weathering did occur and that the leaching process was governed by the presence and amount of acid produced by the chemolithotrophic consortia and the buffering effect of kimberlite may impact on the overall effectiveness of the leaching process.

This study did not investigate the microbial population dynamics. This is something that needs to be looked at in future studies. According to Bouffard and Dixon (2002), optimizing the dilution rate and determining the optimal yet feasible substrate concentration (not all sulfur particles were consumed) could possibly increase the leaching efficiency in the column. Higher retention times also increase leaching efficiency and play an important role in maintaining the temperature in the column so that the leaching cultures operate at optimal growth temperature in order to achieve maximum microbial leaching activity. Therefore an optimal HRT is required so that the microbial growth is not adversely affected (Mousavi *et al.*, 2006).

Finally, it was evident that chemolithotrophic cultures in continuous systems have the potential to accelerate kimberlite weathering and hence weaken kimberlite mineralogical structures. However, this study did not investigate the relationship between changes in process operating conditions and process efficiency. From an economic point of view and increasing the viability of applying this technology on a larger scale, it is important that operating conditions such as flow rate, energy source utilization, effects of temperature and other operating parameters that affect the leaching efficiency be investigated.

CHAPTER 6

*Susceptibility of kimberlite ores to heterotrophic microbial leaching using *Aspergillus niger**

6.1 Introduction

Much of the research in the bioleaching of silicates has focused on the use of heterotrophic bacteria and fungi that are able to promote dissolution of silicate minerals and weathering through the production of organic acids (mainly oxalic and citric acid) and metabolites (Gómez-Alarcón *et al.*, 1995; Castro *et al.*, 2000; Gericke *et al.*, 2007). Oxalic and citric acids are leaching agents that solubilize cations from silicate minerals or they assist, together with other organic metabolites, in the complexation and chelation of the cations present in silicate minerals (Gómez-Alarcón *et al.*, 1995; Castro *et al.*, 2000). Therefore, in this chapter the effectiveness and efficiency of heterotrophic leaching on kimberlite ores using the fungus *Aspergillus niger* in shake flask weathering tests was investigated. *Aspergillus niger* was used because it can grow under high pH conditions and it has the ability to produce many organic acid metabolites (including citric and oxalic acid) concurrently which can accelerate the dissolution of silicate minerals. It is also one of the most extensively studied fungus for its use and application in bioleaching technology (Santhiya and Ting, 2005).

Furthermore, comparisons between leaching of kimberlite in the presence of *A. niger* and leaching of kimberlite using the supernatant of *A. niger* containing organic acids and metabolites (collected after growth) as the leaching agent, were also investigated.

6.2 Experimental Procedure

6.2.1 Kimberlite

Two kimberlite samples, namely from Premier and Venetia diamond mine (Section 2.1) were used. They were finely ground and sieved to a particle size of less than a 100µm. These were subjected to shake flask weathering tests (Section 6.2.3).

6.2.2 Microorganisms

Aspergillus niger (Section 2.2.2) was used as the test fungus in weathering tests. Culturing, maintenance and storage of *A. niger* is described in Section 2.3.2 (Chapter 2).

6.2.3 Shake flask weathering tests

Heterotrophic leaching experiments for the two kimberlite samples were carried out in Erlenmeyer shake flasks (250ml) containing a standard growth medium (Section 2.4.2) (75ml) and kimberlite (3.75g, 5% w/v). Prior to weathering tests, the growth media and ore samples in shake flasks were autoclaved at 120°C for 15 minutes. The shake flasks were then subjected to 6 different treatments.

The first treatment served as an uninoculated control to ensure that the growth medium had no effect on the dissolution process. Therefore the flasks consisted only of the growth medium and kimberlite.

In treatment 2, the flasks containing growth medium and kimberlite were inoculated with spores of 7-day-old *A. niger* (2.3.2) (10^8 spores/ml) (10ml) and referred to as the 'biotic' leaching process. In treatment 3, prior to leaching tests, *A. niger* was grown as described in treatment 2 except kimberlite ores were not added. Subsequently, the supernatant liquor (75ml) after cellular growth was collected and filtered through a membrane filter (0.45µm pore size) and added to the test flasks containing the kimberlite ores. This treatment was referred to as the 'abiotic' leaching process.

Preliminary investigations into the amount of citric and oxalic acid produced by *A. niger* in the absence of kimberlite were conducted using High-performance Liquid chromatography (HPLC) (Spectra System: Thermo Separation Product). Separation of organic acids was carried out in a C₁₈ cation exchange column (Phenomenex Luna) using a H₂SO₄ (0.005M) mobile phase with a flow rate of 1.0ml/min. The temperature was set at 25°C whilst the detector was set at 210nm (UV6000LP Diode Array Detector). Thereafter, chemical controls using similar concentrations (0.01M) to the fungal produced citric and oxalic acids were setup in treatments 4 and 5, respectively. In treatment 6, a mixture of both organic acids of same concentration was also used for chemical weathering tests of kimberlite.

All treatment flasks were incubated at 30°C in a shake incubator set at 120rpm for 6 weeks. All treatments were performed in duplicates for each kimberlite sample. For each treatment flask, the initial weight of the flask and its contents were recorded. During treatment time, the flasks were periodically (day 7, 14, 28 and 35) monitored for weight loss due to evaporation. Weight losses due to evaporation were compensated by addition of sterile distilled water (1g \approx 1ml). The pH of the flasks was also monitored on those respective days using a pH meter (Crison micro pH 2000).

During days 7, 14, 28 and 42 of the treatment time ICP analyses (Section 2.5.1) were performed on the leachate sample solutions. These samples were also filtered through membrane filters (0.45 μ m pore size) and quantitatively analyzed for citric and oxalic acid production using HPLC (same conditions as described above). After 6 weeks, the contents of the flasks were centrifuged and XRD analyses (Section 2.5.2) were performed on the final remaining pellets that were air dried.

6.2.4 Statistical analyses

Statistical analysis was carried out using SAS software (Version 6.12) (SAS, 1987). A general linear model (GLM) was used to run an analysis of variance (ANOVA) for ICP results derived from each set of kimberlite ore treatments. Separations of means was based on the principle of least significant difference (LSD) at $P < 0.05$.

6.3 Results

As the experimental time proceeded, turbidity in the flasks inoculated with *A. niger* increased. A dense white mycelium formed at surface of the liquid media was also observed indicating microbial growth. No notable changes were observed in the other treatment flasks.

The pH readings for the ‘biotic’ leaching process for both kimberlite samples decreased from 7.50 and stabilized in the range of 5.81 to 6.73. For the ‘abiotic’ leaching process, the pH readings for both kimberlite samples increased from 2.44 and continued increasing in the range of 6.90 and 8.04. The pH of the oxalic and citric acid chemical controls increased from the ranges of 4.03-4.10 and 4.17-4.37 to 7.18-

8.08 and 8.01-8.44, respectively. The pH of both the kimberlite samples in the chemical control containing both organic acids increased from the range of 3.82-3.86 to 6.34-8.08. The final lower pH range limits of the treatments noted above, were observed for the kimberlite sample from Venetia Diamond mine.

The HPLC results for the 'biotic' leaching process revealed that the concentration of oxalic and citric acid produced was approximately 9mM and 7mM, respectively. The concentration of oxalic and citric acid produced in the 'abiotic' leaching process was approximately 8mM and 7mM, respectively. The test fungus evidently produced more oxalic acid in the presence of kimberlite whilst the concentration of citric acid remained the same for both fungal leaching processes applied.

6.3.1 ICP results

ICP analyses of the leach solutions showed that all elemental cations investigated were solubilized but in relatively small amounts (Table 6.1). It was assumed that weathering due to dissolution had occurred but clearly at low leaching rates. Again, from the ICP results, it was noticed that the susceptibility of weathering of kimberlite differed between the two samples. Comparing the dissolution of the cations in both kimberlite samples, the sample from Premier mine had relatively higher cation dissolution rates.

From Table 6.1, it was seen that Mg followed by Ca were the major cations that solubilized. Negligible dissolution of Si and K occurred for both kimberlite sample types. Negligible dissolution of Fe also occurred except in the 'biotic' leaching of kimberlite from Premier mine. Based on the two major cations that solubilized, it was deduced that the 'biotic' leaching process produced superior results to all other treatments and controls tested on both kimberlite samples (Figure 6.1).

Table 6.1 ICP analyses of heterotrophically leached kimberlite ores (< 100mm) using *Aspergillus niger*. (All treatment flasks were incubated at 30°C in a shake incubator set at 120rpm for 6 weeks.)*

Sample	[Ca][mg/l]					[Si][mg/l]				[Fe][mg/l]				[Mg][mg/l]				[K][mg/l]				
	Day 7	Day 14	Day 28	Day 42	Day 7	Day 14	Day 28	Day 42	Day 7	Day 14	Day 28	Day 42	Day 7	Day 14	Day 28	Day 42	Day 7	Day 14	Day 28	Day 42		
Premier Diamond Mine																						
Kimberlite + growth medium - control	9e	9e	10f	15e	2d	2e	2e	3d	1d	1e	1e	1e	12e	13e	24f	53f	5d	6d	7d	7c		
Kimberlite + <i>A. niger</i> - 'biotic' leaching	96d	218a	384a	417a	33a	45a	46a	54a	31a	34a	38a	40a	139d	325a	511a	701a	29a	31a	33a	34a		
Kimberlite + <i>A. niger</i> - 'abiotic' leaching	147a	163b	205b	271b	32ab	36b	37b	39b	29a	30b	32b	33b	191a	253b	488b	601b	16c	21b	26b	27a		
Kimberlite + oxalic acid	107cb	138d	175c	193d	29b	31c	32c	34b	26b	27c	28c	29c	164c	175d	392d	494d	15c	17c	22cb	26b		
Kimberlite + citric acid	105c	132d	138e	142d	15c	18d	25d	27c	21c	24d	25d	26d	156c	179d	272e	363e	15c	16c	16c	21b		
Kimberlite + oxalic & citric acid	110b	151c	163d	203c	31ab	35b	36b	37b	28ab	29cb	30cb	31bc	176b	205c	454c	560c	19b	20cb	22cb	24b		
F Ratio	2.E+03	5.E+02	2.E+03	1.E+03	3.E+02	4.E+02	4.E+02	2.E+02	1.E+02	2.E+02	3.E+02	4.E+02	4.E+02	5.E+02	1.E+03	1.E+03	1.E+02	6.E+01	3.E+01	6.E+01		
P value	<1.E-04	<1.E-04	<1.E-04	<1.E-04	<1.E-04	<1.E-04	<1.E-04	<1.E-04	<1.E-04	<1.E-04	<1.E-04	<1.E-04	<1.E-04	<1.E-04	<1.E-04	<1.E-04	<1.E-04	<1.E-04	<1.E-04	<1.E-04		
LSD	3.59	7.64	5.35	3.91	1.69	1.56	1.80	2.41	3.20	0.77	0.53	0.56	10.67	12.21	11.34	10.64	2.39	3.14	2.64	3.09		
Venetia Diamond Mine																						
Kimberlite + growth medium - control	6e	7e	8e	8e	1c	1c	1c	1c	2c	2e	3e	3d	5e	12e	24e	43e	4d	4d	5c	5d		
Kimberlite + <i>A. niger</i> - 'biotic' leaching	64d	158a	172a	226a	29a	30a	33a	37a	17a	28a	36a	54a	84d	198a	366a	441a	24a	25a	25a	26a		
Kimberlite + <i>A. niger</i> - 'abiotic' leaching	118a	147b	149b	206b	28a	29a	32a	33a	7bc	22b	25b	39b	131a	181b	313b	380b	22ab	22a	23a	23b		
Kimberlite + oxalic acid	104b	122c	132c	174c	26a	28a	29a	30a	11ba	16d	19cd	24c	97c	160c	251c	311c	12c	16c	19b	20c		
Kimberlite + citric acid	78c	96d	104d	136d	17b	19b	22b	22b	9b	12d	15c	20c	84d	132d	164d	269d	20b	21a	22a	22b		
Kimberlite + oxalic & citric acid	125a	137c	146b	175c	27a	28a	28a	30a	11ba	20b	23b	36b	109b	173b	181d	359b	22ab	22a	22a	23b		
F Ratio	2.E+02	3.E+02	8.E+02	2.E+02	9.E+01	5.E+01	1.E+01	3.E+01	8.E+00	4.E+01	1.E+02	9.E+01	2.E+02	7.E+02	4.E+02	2.E+02	1.E+02	7.E+01	4.E+01	1.E+02		
P value	<1.E-04	<1.E-04	<1.E-04	<1.E-04	<1.E-04	<1.E-04	<1.E-04	<1.E-04	<1.E-04	<1.E-04	<1.E-04	<1.E-04	<1.E-04	<1.E-04	<1.E-04	<1.E-04	<1.E-04	<1.E-04	<1.E-04	<1.E-04		
LSD	1.23	2.95	2.37	6.79	0.85	0.31	1.01	2.34	5.77	5.03	3.12	1.34	4.65	5.67	12.90	9.89	0.59	0.95	3.02	2.69		

* ICP values represented rounded off to the nearest whole number * Mean values from duplicate samples represented. Means with the same letter within a column for each kimberlite ore type are not significantly different (P=0.05)

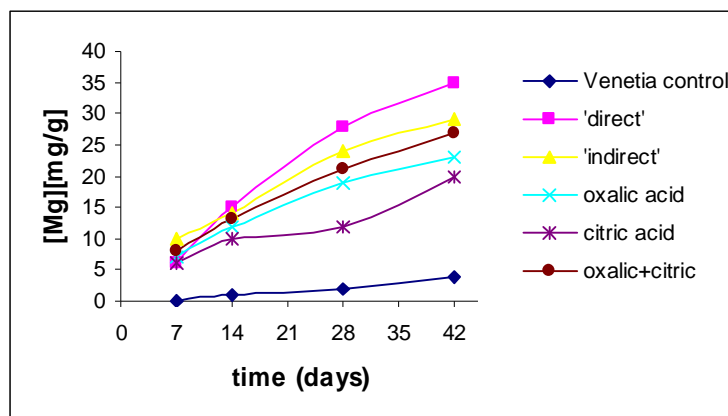


Figure 6.1 Magnesium ion dissolution trends illustrating the effectiveness of the heterotrophic leaching treatments used in the weathering tests of kimberlite from Venetia Diamond Mine. (Data was obtained from ICP analyses of the leachate solutions.)

Figure 6.1 represents the dissolution of Mg from kimberlite over a 6 week period (data plotted are represented values of ICP data of Venetia mine recorded in Table 6.1). Similar results were also seen for the kimberlite sample from Premier mine. Using Mg as the major soluble cation, the graph was plotted to show the effectiveness of the fungal leaching treatments used to accelerate the dissolution process of kimberlite. The treatment in which the *A. niger* was allowed to grow in the presence of kimberlite ('biotic' leaching process) produced the best results followed by the 'abiotic' leaching process. Both processes produced superior results to their chemical control counterparts. In the chemical controls, the mixture of oxalic and citric acid produced better dissolution rates of the cations followed by the oxalic acid control. Calcium ions showed similar results over the course of the investigation. No definite trend could be seen for the other cations investigated.

6.3.2 XRD results

Typical XRD results obtained for both kimberlite samples (but only discussed for the kimberlite sample from Venetia mine) showed only slight alterations to the serpentine and phlogopite peaks indicating slight breakdown of these minerals. The 'biotic' leaching process showed the most pronounced changes in these peaks. Changes seen in the XRD analyses of 'abiotic' leaching process were similar to that of the 'biotic' leaching process except the degree of transformation of the peaks was slightly less. Comparing both acids, it seems that the oxalic acid treatment showed slightly more alterations to the phlogopite and serpentine peaks (Figure 6.2).

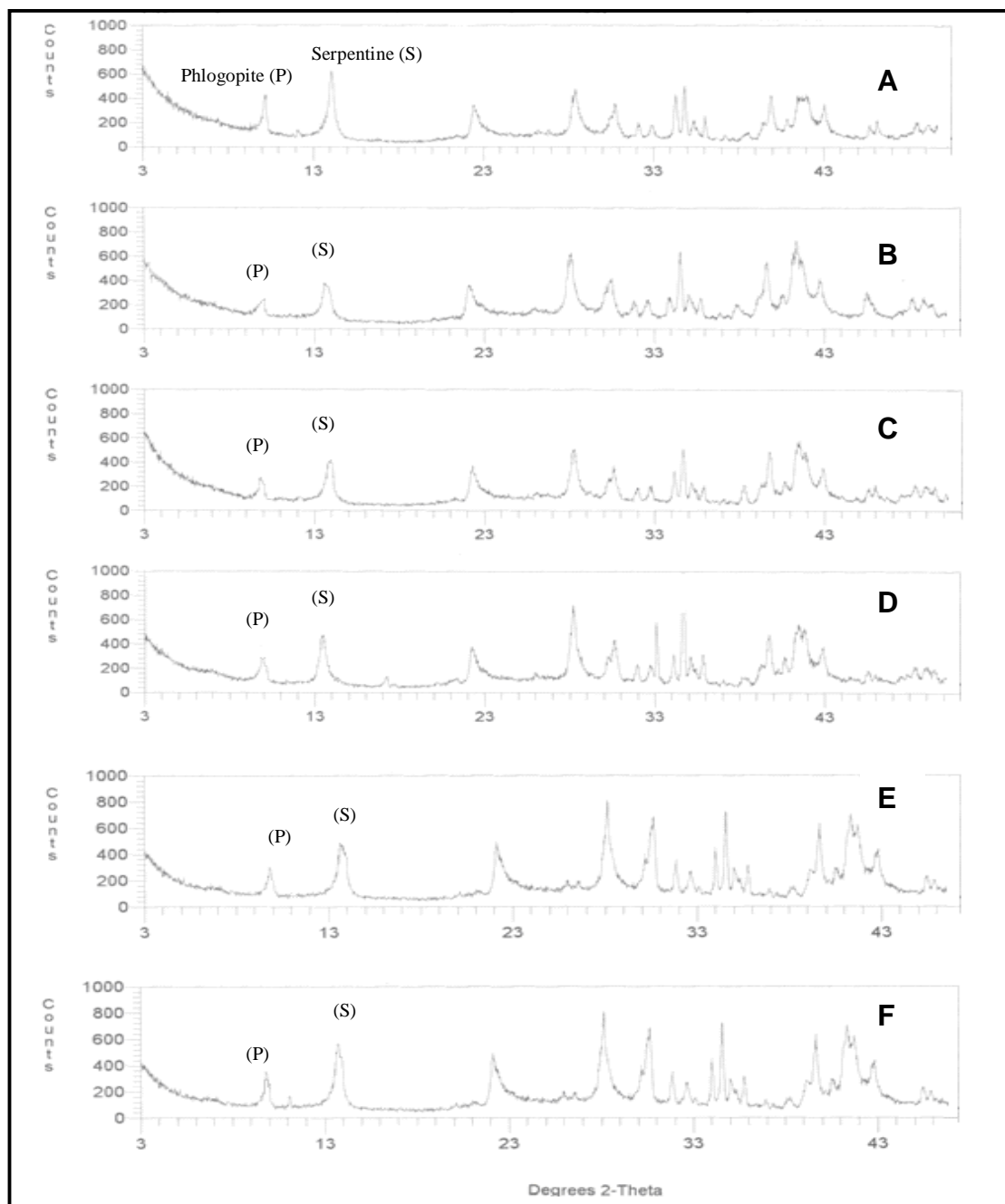


Figure 6.2 XRD analyses of kimberlite from Venetia Mine after being subjected to heterotrophic leaching treatments using *Aspergillus niger*. [A (negative control), B (kimberlite in the presence of *A. niger* - 'biotic' leaching process), C (kimberlite in the presence of *A. niger* after growth metabolites but no fungal cells present - 'abiotic' leaching process), D (kimberlite in the presence of oxalic acid - chemical control), E (kimberlite in the presence of citric acid - chemical control), F (kimberlite in the presence of oxalic acid & citric acid - chemical control)].

6.4 Discussion

The results of the heterotrophic leaching treatments used in this investigation have shown that *A. niger* was capable of altering the kimberlite mineralogical structure via dissolution of kimberlite cations.

ICP data in Table 6.1 showed that Mg and Ca cations leached into solution in the greatest concentrations. Belkanova *et al.* (1987) who performed experiments on kimberlite using organic acid-producing *Bacillus stearothermophilus* and *Bacillus mucilaginosus* attributed this to the selective dissolution of magnesium-rich serpentine and calcium containing dolomite and calcite. Thus, the leaching of Mg and Ca in comparatively higher amounts was attributed to the breakdown of minerals such as serpentine, phlogopite, dolomite and calcite which are rich in Mg and Ca. However, the amount of Mg and Ca that passed into solution was comparatively lower than the values obtained by Belkanova *et al.* (1987) indicating that no drastic changes were made to the kimberlite mineralogical structure. This was also evident in the representative XRD analyses of the kimberlite from Venetia mine (Figure 6.2) where only minor changes in the major mineral peaks were observed. This was probably due to the fact that the strain of *A. niger* used was not capable of producing high amounts of organic acids. In order to achieve efficient and effective fungal leaching of minerals, high levels of organic acids need to be produced and maintained (Gadd, 1999).

Effective kimberlite leaching is attained at low pHs, usually at pHs less than 3 (Ivanov and Karavaiko, 2004). None of the leaching treatments maintained such a pH range, therefore, as expected, no major changes were seen in the XRD spectra of the treated kimberlite. However, literature does document the ability of *A. niger* to obtain low pH ranges that fall between 1.5 and 2.0 when oxalic and citric is being produced (Gadd, 1999). If growth conditions are adequately optimized, high levels of acids can be produced. Depending on the carbon substrate, concentrations greater than 100mM may be obtained for oxalic and citric acid (Ruitjer *et al.*, 1999; Santhiya and Ting, 2005). The concentrations of oxalic and citric obtained in the present study were relatively low in comparison thereby providing a possible reason for the less intense leaching of kimberlite minerals seen in the ICP and XRD data.

Initially, it was observed in Figure 6.1 that the ‘abiotic’ leaching process had higher dissolution values than the ‘biotic’ leaching process. This initial increase in dissolution was possibly due the initial low pH of the supernatant. The presence of all the organic acids and metabolites after fungal growth lowered the pH of the supernatant from 7.67 to 2.44. However, as dissolution continued to occur, the pH of the ‘abiotic’ leaching process increased. Dissolution rates are inversely proportional to pH (Wilson, 2004), therefore as the pH increased for the ‘abiotic’ process, dissolution decreased as there was no counter action to decrease the pH after the protons were consumed and Mg and Ca solubilized into solution. In comparison, the pH of the ‘biotic’ process decreased suggesting that excreted metabolites such as organic acids, lipids and phospholipids were actively being produced throughout the growth stages of *A. niger*. According to Castro *et al.* (2000), the leaching efficiency of heterotrophs depends on both the pH and the amount of organic metabolites secreted in solution that enhance mineral dissolution process. HPLC results revealed that slightly more oxalic acid was produced in the ‘biotic’ process while the production of citric acid remained the same for both fungal leaching treatments. Therefore, this would explain why ‘superior’ results in the ICP and XRD analyses were observed in the ‘biotic’ leaching process. This result is also significant as it indicates that kimberlite did not appear to inhibit metabolite production and did not have possible negative effects on the growth of *A. niger*.

Castro *et al.* (2000) who performed similar experiments on the bioleaching of zinc and nickel from silicates using *A. niger* also found that the ‘biotic’ leaching process improved the leaching results compared to the ‘abiotic’ process. However, in contrast, they stated that citric acid was the important leaching agent in the dissolution of the silicates. In this investigation, the oxalic acid control caused slightly more changes to the serpentine and phlogopite peaks in the XRD analyses of the treated kimberlite when compared to the citric acid control (Figures 6.1 and 6.2) suggesting that oxalic acid played to some extent a higher leaching role than citric acid in the dissolution and mineral transformations of kimberlite. Whilst oxalic and citric acid and other organic acids dissolve many minerals via protonolysis, oxalic acid is able to cause dissolution at neutral and basic pHs, which probably occurred in this instance (Formina *et al.*, 2005). *Aspergillus niger* in a growth medium with a pH close or above neutrality results in the accumulation of oxalic acid (Strasser *et al.*, 1994), which would also

explain the slightly higher concentration of oxalic acid seen in the HPLC results. The optimal pH for citric acid production is below 3.5 (Gadd, 1999).

Although oxalic and citric acid were recognized as the key leaching agents, it is possible that the other fungal metabolites were also involved in the leaching process as both heterotrophic leaching processes produced superior results than the chemical controls. This was also emphasized by the initial pH of 2.44 observed in the supernatant after cellular growth of *A. niger*, which was lower than the initial pH of the mixture of oxalic and citric acid recorded at 3.86, indicating that other organic acids were secreted in solution by the fungus thus lowering the pH. *Aspergillus niger* produces many organic metabolites and acids via the tricarboxylic acid (TCA) cycle. This cycle is one of *A. niger*'s major pathways for energy production (Hatch and Hardy, 1989). The organic metabolites produced in this cycle can dissolve silicate minerals by providing hydrogen ions that help in breaking Si-O bonds via protonation and/or catalysis (Ehrlich, 1996). They may also promote the formation of soluble complexes and chelates whilst some of the acids may act as ligands and pull cations from the structural framework of silicate ores which leads to the further weakening of bonds and their mineralogical structures (Ehrlich, 1996; Rezza *et al.*, 2001).

Overall, this investigation indicated that *A. niger* and its metabolites caused higher dissolution rates of kimberlite when compared to abiotic controls. However, the degree of transformation of kimberlite was slight and dependant on the susceptibility of the mineralogical structure to weathering. Further test work would be required on improving organic acid production of the fungus in order to achieve higher dissolution and weathering rates.

CHAPTER 7

Concluding remarks

The ultimate aim of this study was to evaluate the effectiveness and efficiency of harnessing microbial leaching processes to accelerate the weathering and weakening of diamond-bearing-kimberlite. Kimberlite is a silicate ore consisting of many silicate minerals that are known to be susceptible to microbial leaching. However, little biohydrometallurgical research has been performed on kimberlite and therefore two microbial leaching processes were exploited for this purpose: one aimed at directly using chemolithotrophic organisms (viz., a mixed mesophilic culture of *A. caldus*, *L. ferrooxidans* and *Sulfobacillus spp.*) and another aimed at using heterotrophic organisms, namely, *A. niger* to enhance mineralization of kimberlite. The potential advantages of harnessing microbial leaching processes to pre-treat kimberlite include improved diamond recoveries, reduction in power usage as well as an overall reduction in operating costs. Consequently, microbial leaching processes represent a matter of innovative technologies showing an improved market gap in the mining industry (Krebs *et al.*, 1997).

Preliminary investigations using chemolithotrophic and heterotrophic leaching organisms in shake flask weathering tests showed that kimberlite weathering can be accelerated in the presence of microbial leaching agents but the degree of susceptibility and transformation of the kimberlite particles depended on their mineralogical structure. Kimberlite with clay minerals such as smectite weathered readily when compared to other kimberlite types where minerals such as serpentine and phlogopite were present as major components. It was concluded that the mineral composition and their vulnerability to mineralization determined the degree of transformation and hence, overall weakening of the kimberlite structure. Of the four kimberlite types investigated, kimberlite from Victor diamond mine, which had significant amounts smectite present, appeared to be more prone to weathering than the kimberlite samples sourced from Premier, Venetia and Gahcho Kue diamond mines, which all had increased proportions of phlogopite and serpentine.

Although both chemolithotrophic and heterotrophic leaching processes influenced the weathering and weakening of kimberlite positively, a general comparison made

between both processes showed that more promising results were obtained in the chemolithotrophic leaching process. The weathering rates (using the ICP data as an indication of weathering rates) of the heterotrophic leaching process were relatively lower (Table 6.1) when compared to weathering rates of the same kimberlite samples in the chemolithotrophic leaching process (Table 3.3). The effect caused by the chemolithotrophs was brought about in the presence of 20% (w/w) S^0 and 35% (w/w) Fe^{2+} as the energy source, whereas the effect caused by the heterotrophic organisms required 300% (w/w) sucrose as the energy source, to metabolically grow and produce organic acids that enhance mineral leaching. Considering the high costs of organic carbon sources and the amount required to maintain high levels of organic acids so that efficient leaching may be obtained makes heterotrophic leaching unattractive. Furthermore, contamination by undesirable microbes, which slowed/inhibited the growth of *A. niger*, was observed during the initial kimberlite weathering tests. If the degree of contamination on a laboratory scale is high, prevention of contamination by other unwanted microbes seems unlikely on a large commercial scale and is in keeping with observations reported in the literature (Gericke *et al.*, 2007).

The preliminary investigations of chemolithotrophic leaching of kimberlite showed that kimberlite of particle size of less than 100 μ m was successfully weathered over the 6 week treatment period and showed a significant amount of change in their mineralogical structure. This encouraging outcome led to optimization and continuous plug-flow studies being initiated. In general, from these it was deduced that although the weathering rates of larger kimberlite particles were lower than that of the finer particles, changes in the mineralogical structure were apparent. The influence of time was also noted whereby the extent of the microbial weathering process can be increased by extending treatment times. This suggests that if larger particles were treated for longer periods more profound changes in the mineralogical structure may be seen. Comparisons made between S^0 and Fe^{2+} as energy sources showed that sulfur produced superior leaching results. This was attributed to sulfuric acid generation which lowered pH leading to increased mineralization of kimberlite. Overall, it was concluded that weathering of kimberlite and potential weakening of the mineral structure depended on particle size, treatment times, pH and physico-chemical conditions that influence microbial growth.

The results obtained from using the continuous flow bioleach column system showed that there is a promising base from which chemolithotrophic leaching processes and technologies can be applied on a larger scale for the pre-treatment of kimberlite ores. However, prior to implementation of such technology further research is required. For example, the physico-chemical parameters influencing microbial activity involved in the leaching process needs further elucidation and optimization. Additionally, characterization of naturally enriched microbial populations best suited to the leaching conditions also warrants further investigation. The alkaline nature of kimberlite, which adversely affects leaching of kimberlite was highlighted throughout this study and this needs to be taken into consideration when establishing a dump- or heap-leaching technology for these kimberlite ores.

In conclusion, the findings in this study will ultimately guide in the modeling and development of the microbial leaching technology to be used in accelerating the weathering and weakening of kimberlite. These findings may also assist in formulating recommendations for further and future column microbial leach tests.

References

- Berry, L.G. 1974. Selected powder diffraction data for minerals: Data book and search manual. Joint committee on powder diffraction standards, Pennsylvania, USA.
- Belkanova, N.P., Eroshchev-Shak, V.A., Lebedeva, E.V., and Karavaiko, G.I. 1987. Dissolution of kimberlite minerals by heterotrophic microorganisms. Microbiology (Translated from Mikrobiologiya) **56**, 613-620.
- Bennett, P.C., Rogers, J.R., and Choi, W.J. 2001. Silicates, silicate weathering and microbial ecology. Geomicrobiology Journal **18**, 3-19.
- Bigham, J.M., Bhatti, T.M., Vuorinen, A., and Tuovinen, O.H. 2001. Dissolution and structural alteration of phlogopite mediated by proton attack and bacterial oxidation of ferrous iron. Hydrometallurgy **59**, 301-309.
- Bosecker, K. 1989. Microbial leaching. In: Fundamentals of biotechnology. Eds. Präve, P., Fraust, U., Sittig, W., and Sukatsch, D.A. VCH, New York, USA, pp. 662-680.
- Brandl, H. 2001. Microbial leaching of metals. In: Biotechnology, 2nd edition. Ed. Rehm, H.J. Wiley-vch, Germany, pp. 192-206.
- Brandl, H., and Faramarzi, M. 2006. Microbe–metal-interactions for the biotechnological treatment of metal-containing solid waste. China Particuology **4**, 93-97.
- Brierley, C.L. 1982. Microbiological Mining. Scientific American **247**, 42-50.
- Brierley, J.A., and Brierley, C.L. 2001. Present and future commercial applications of biohydrometallurgy. Hydrometallurgy **59**, 233-239.
- Boshoff, E.T., Morkel, J., and Vermaak, M.K.G. 2005. Accelerated kimberlite weathering – the role of cation type on the settling behaviour of fines. The Journal of South African Institute of Mining and Metallurgy **105**, 163-166.

Bouffard, S.C., and Dixon, D.G. 2002. On the rate-limiting steps of pyrite refractory gold ore heap leaching: Results from small and large column tests. *Minerals Engineering* **15**, 859-870.

Burgstaller, W., and Schinner, F. 1993. Leaching of metals with fungi. *Journal of Biotechnology* **27**, 91-116.

Castro, I.M., Fietto, J.L.R., Vieira, R.X., Trópia, M.J.M., Campos, L.M.M., Paniago, E.B., and Brandão, R.L. 2000. Bioleaching of zinc and nickel from silicates using *Aspergillus niger* cultures. *Hydrometallurgy* **57**, 39-49.

Dopson, M., Lövgren, L., and Böstrom, D. 2009. Silicate mineral dissolution in the presence of acidophilic microorganisms: Implications for heap bioleaching. *Hydrometallurgy* **96**, 288-293.

Edwards, K.J., Bond, L.P., and Banfield, J.F. 2000. Characteristics of attachment and growth of *Thiobacillus caldus* on sulfide minerals: a chemotactic response to sulfur minerals? *Environmental Microbiology* **2**, 324-332.

Ehrlich, H.L. 1981. *Geomicrobiology*. Marcel Dekker Inc., New York, USA, pp. 21-32.

Ehrlich, H.L. 1996. How microbes influence mineral growth and dissolution. *Chemical Geology* **132**, 5-9.

Ehrlich, H.L. 1998. Geomicrobiology: Its significance for geology. *Earth-Science Reviews* **45**, 45-60.

Ehrlich, H.L. 2001. Past, present and future of biohydrometallurgy. *Hydrometallurgy* **59**, 127-134.

Fomina, M., Hillier, S., Charnock, J.M., Melville, K., Alexander, I.J., and Gadd, G.M. 2005. Role of oxalic acid overexcretion in transformations of toxic metal minerals by *Beauveria caledonica*. *Applied and Environmental Microbiology* **71**, 371-381.

Gadd, G.M. 1999. Fungal production of citric and oxalic acid: Importance in metal speciation, physiology and biogeochemical processes. *Advances in Microbial Physiology* **41**, 47-83.

Gadd, G.M. 2007. Geomycology: Biogeochemical transformations of rocks, minerals, metals and radionuclides by fungi, bioweathering and bioremediation. *Mycological Research* **111**, 3-49.

Gericke, M., Benvie, B., and Krüger, L. 2007. Biological transformation of kimberlite ores. *Advanced Materials Research* **20-21**, 75-78.

Gómez-Alarcón, G., Cilleros, B., Flores, M., and Lorenzo, J. 1995. Microbial communities and alteration processes in monuments at Alcala de Henares, Spain. *The Science of the Total Environment* **167**, 231-239.

Hakkou, R., Benzaazoua, M., and Bussière, B. 2008. Acid mine drainage at the abandoned Kettara mine (Morocco): Mine waste geochemical behavior. *Mineral Water and the Environment* **27**, 160-170.

Hossain, S.M., Das, M., Begum, K.M.M.S., and Anantharaman, N. 2004. Bioleaching of zinc sulfide (ZnS) using *Thiobacillus ferrooxidans*. *The Institution of Engineers (India), IE (I) Journal* **85**, 7-11.

Ivanov, M.V., and Karavaiko, G.I. 2004. Geological Microbiology. *Microbiology (Translated from Mikrobiologiya)* **73**, 581-597.

Jain, N., and Sharma, D.K. 2004. Biohydrometallurgy for nonsulfidic minerals – A review. *Geomicrobiology Journal* **21**, 135-144.

Jonckbloedt, R.C.L. 1998. Olivine dissolution in sulfuric acid at elevated temperatures-implications for the olivine process, an alternative waste acid neutralizing process. *Journal of Geochemical Exploration* **62**, 337-346.

Krebs, W., Brombacher, C., Bosshard, P.P., Bachofen, R., and Brandl, H. 1997. Microbial recovery of metals from solids. *FEMS Microbiology Reviews* **20**, 605-617.

Liermann, J.L., Kalinowski, B.E., Brantley, S.L. and Ferry, J.G. 2000. Role of bacterial siderophores in dissolution of hornblende. *Geochimica et Cosmochimica Acta* **64**, 587-602.

Lizama, H.M. 2004. A kinetic description of percolation bioleaching. *Minerals Engineering* **17**, 23-32.

Middelbeek, E.J., and Jenkins, R.O. 1992. Growth in continuous culture. In: *In vitro* cultivation of micro-organisms. Ed. Cartledge, T.G. Butterworth-Heinemann Ltd, Oxford, pp. 107-141.

Morkel, J., 2007. Kimberlite weathering: Mineralogy and mechanism. PHD thesis, Faculty of Engineering, Built Environment and Information Technology, University of Pretoria, Pretoria, RSA.

Mousavi, S.M., Jafari, A., Yaghmaei, S., Vossoughi, M., and Roostaazad, R. 2006. Bioleaching of low-grade sphalerite using a column reactor. *Hydrometallurgy* **82**, 75-82.

Okibe, N., Gericke, M., Hallberg, K.B., and Johnson, D.B. 2003. Enumeration and characterization of acidophilic microorganisms isolated from a pilot plant stirred-tank bioleaching operation. *Applied and Environmental Microbiology* **69**, 1936-1943.

Platonova, N.P., Eroshchev-Shak, V.A., Lebedeva, E.V., and Karavaiko, G.I. 1989. Formation of mixed-layer serpentine-smectite phase in kimberlite under the effect of *Thiobacillus thiooxidans*. *Microbiology (Translated from Mikrobiologiya)* **58**, 271-275.

Platonova, N.P., Karavaiko, G.I., Lebedeva, E.V., and Zherdev, P.Yu. 1994. Transformation of kimberlites by autotrophic bacteria. *Microbiology (Translated from Mikrobiologiya)* **63**, 473-483.

Rawlings, D.E. 2002. Heavy metal mining using microbes. *Annual Review Microbiology* **56**, 65-91.

Rawlings, D.E., Dew, D., and du Plessis, C. 2003. Biomineralization of metal-containing ores and concentrates. *Trends in Biotechnology* **21**, 38-44.

Rawlings, D.E. 2004. Microbially assisted dissolution of minerals and its use in the mining industry. *Pure Applied Chemistry* **76**, 847-859.

Rawlings, D.E. 2005. Characteristics and adaptability of iron- and sulfur-oxidizing microorganisms used for the recovery of metals from minerals and their concentrates. *Microbial Cell Factories* **4**, doi: 10.1186/1475-2859-4-13.

Rawlings, D.E., and Johnson, D.B. 2007. The microbiology of biomining: development and optimization of mineral-oxidizing microbial consortia. *Microbiology* **153**, 315-324.

Rezza, I., Salinas, E., Elorza, M., Sanz de Tosetti, M., and Donati, E. 2001. Mechanisms involved in bioleaching of an aluminosilicate by heterotrophic microorganisms. *Process Biochemistry* **36**, 495-500.

Rohwerder, T., Gehrke, T., Kinzler, K., and Sand, W. 2003. Bioleaching - Review part A: Fundamentals and mechanisms of bacterial metal sulfide oxidation. *Applied Microbiology and Biotechnology* **63**, 239-248.

Ruitjer, G.J.G., van de Vondervoort, P.J.I., and Visser, J. 1999. Oxalic acid production by *Aspergillus niger*: An oxalate-non-producing mutant produces citric acid at pH 5 and in the presence of manganese. *Microbiology* **145**, 2569-2576.

Santhiya, D., and Ting, Y. 2005. Bioleaching of spent refinery processing catalyst using *Aspergillus niger* with high-yield oxalic acid. *Journal of Biotechnology* **116**, 171-184.

Silverman, M.P., and Lundgren, D.G. 1959. Studies on the chemoautrophic iron bacterium *Ferrobacillus ferrooxidans*. I. An improved medium and a harvesting procedure for securing high cell yields. *Journal of Bacteriology* **77**, 642-647.

Strasser, H., Burgstaller, W., and Schinner, F. 1994. High-yield production of oxalic acid for metal leaching processes by *Aspergillus niger*. *FEMS Microbiology Letters* **119**, 365-370.

Štyriaková, I., Bhatti, T.M., Bigham, J.M., Štyriak, I., Vuorinen, A., and Tuovinen, O.H. 2004. Weathering of phlogopite by *Bacillus cereus* and *Acidithiobacillus ferrooxidans*. Canadian Journal of Microbiology **50**, 213-219.

Torma, A.E. and Bosecker, K. 1982. Bacterial leaching. In: Progress in industrial microbiology. Ed. Bull, M.J. Elsevier Scientific Publishing Company, Amsterdam, Netherlands, pp 77-95.

Waites, M.J., Morgan, N.L., Rockey, J.S., and Higton, G. 2001. Industrial Microbiology: An introduction. Blackwell Science Ltd, London, pp. 28-29.

Watling, H.R. 2006. The bioleaching of sulfide minerals with emphasis on copper sulfides – A review. Hydrometallurgy **84**, 81-108.

Welch, S.A., and Banfield, J.F. 2002. Modification of olivine surface morphology and reactivity by microbial activity during chemical weathering. Geochimica et Cosmochimica Acta **66**, 213-221.

White, A.F., and Brantley, S.L. 2003. The effect of time on weathering of silicate minerals: Why do weathering rates differ in the laboratory and field? Chemical Geology **202**, 479-506.

Wilson, M.J. 2004. Weathering of the primary rock-forming minerals: Processes, products and rates. Clay Minerals **39**, 233-266.

www.guilford.edu/geology/imagelibrary/MVC-061F.JPG.

Yatsu, E. 1988. The nature of weathering: An introduction. Sozosha, Tokyo, Japan, pp. 285-358, 420-424.